THE SURFACE ENERGY BUDGET OF A SUMMER CONVECTIVE PERIOD

THE SURFACE ENERGY BUDGET

OF A SUMMER CONVECTIVE PERIOD

by

R. M. Rabin

A thesis submitted to the Faculty of Graduate
Studies and Research in partial fulfilment of the
requirements for the degree of Master of Science.

Department of Meteorology
McGill University   March, 1977
Montreal, Canada

ABSTRACT

An existing numerical model is used to compare
evaporation and sensible heat flux from surfaces of variable
albedo, vegetation density, and soil moisture. Conditions
are found for which differences in soil moisture can account
for significant air mass differences. The surface energy
and water budget is calculated over an area where these
differences exist. The difference in air mass over the
region is found to affect the time of convective precipitation
development when large scale vertical motion is weak. It is
shown that only the average precipitation and land conditions
of an area must be accounted for when using the energy budget
at a single point to represent that for an area. Finally,
significantly higher evaporation during dry summer weather is
shown to occur from areas after experiencing a decrease in
farmland.

i

RESUME

        Un modèle numérique est utilisé pour comparer l'évap-
oration et le flux de chaleur sensible provenant de surfaces
dont on fait varier l'albedo, la couverture végétale et
l'humidité du sol. On a trouvé les conditions nécessaires pour
que des différences d'humidité du sol puissent affecter une masse
d'air. Les équations d'énergie et d'eau sont appliquées à
une surface où existent de telles différences d'humidité.
On constate que les différences de masse d'air qui en résultent
affectent le temps requis pour développer des précipitations
convectives si le mouvement vertical à grande échelle est
faible. On montre aussi que seules la précipitation moyenne et
les conditions du sol sont significatives lorsqu'on utilise
un point pour représenter une surface. Enfin on voit qu'une
évaporation significativement plus élevée a lieu lors d'étés
secs s'il y a diminution de la surface cultivée.

ACKNOWLEDGMENTS

TABLE OF CONTENTS

LIST OF FIGURES

LIST OF TABLES

LIST OF SYMBOLS USED

Ac	Altocumulus clouds
ALB	Albedo
As	Altostratus clouds
ASL	Above sea level
BLA	Leaf area index
BW	Maximum amount of moisture available for evaporation from layer of soil
Cal	Unit of energy in calories
Cb	Cumulonimbus clouds
Cc	Cirrocumulus clouds
CCL	Convective condensation level
Ci	Cirrus clouds
CLOE	Subprogram which incorporates turbulent fluxes into the atmosphere
cm	Centimeter
Cs	Cirrostratus clouds
Cu	Cumulus Humilis clouds
DFL	Downward longwave radiative flux from atmosphere received at surface
EBBA	Computer program which calculates heat and water budget of earth's surface
EST	Eastern standard time
FA	Fraction of potential evaporation possible from layer of soil
FG	Flux of heat from lower soil layer
GW	Present amount of moisture available for evaporation from layer of soil
GW/BW	Saturation of soil layer in terms of moisture available for evaporation (Available soil water saturation)

hr	Hour
in.	Inch
km	Kilometer
kt	Knot = nautical mile hr^{-1}
m	Meter
mb	Millibar (Unit of pressure) = 10^3 dyne cm^{-2}
N	Real number greater than 1
Ns	Nimbostratus clouds
P	Pressure
QE	Latent heat flux (evaporation rate) from surface to air
QS	Sensible heat flux from surface to air
RLOSS	Fraction of air from inside vegetation canopy which mixes with ambient air above, each time step
Sc	Stratocumulus clouds
SG	Shortwave radiative flux incident on ground
SGA	Shortwave radiative flux absorbed by surface
SGC	Shortwave radiative flux incident on surface if sky is cloudless
St	Stratus clouds
T	Temperature of air
Tc	Towering cumulus clouds
TS	Temperature of ground or vegetative surface
UFL	Flux of longwave energy emitted upward to atmosphere from surface
X	Total amount of moisture available for evaporation from all soil layers
Y	Minimum available soil water saturation, GW/BW, at which potential evaporation is possible (Critical available soil water saturation)

$^\circ$C   Measure of temperature in degrees Celsius

θ Potential temperature of air which is conserved
when air parcel moves vertically with no
condensation. The line, an adiabat, parallel
to that marked θ on the figures of atmospheric
soundings and equal to the temperature at 1000
mb, represents the condition of the mixing layer.

CHAPTER I

INTRODUCTION

Large scale weather systems are generally weakest in summer. However, the most intense precipitation rates usually occur during this time of year, because of the larger moisture holding capacity of the atmosphere. The nature of most summertime precipitation is referred to as convective. That is, the extent of precipitation areas is small compared to the normal distance between meteorological observing stations. (Also, the life cycle of such areas is very short compared to one day.) The variability of precipitation patterns observed in summer leads one to believe that convective elements develop randomly. Can these seemingly random patterns be explained?

Since differences of the earth's surface exist on the convective scale, it seems logical to consider their effect on the atmosphere. The air will attain a different temperature and moisture content from place to place over regions containing diverse land types. Much research has been concerned with urban heat island phenomena (Changnon, 1976; Harnick and Landsberg, 1973). The effect on precipitation has been of special interest. However, relatively little attention has been given to meteorological effects of other variations of the earth's surface removed from urban areas. Such regions are likely to contain areas characterized by different vegetation types in summer. It is conceivable that the differences in air masses generated over such areas are at least as marked as those between an urban

environment and its surrounding area. The present investigation
determines the differences in the air masses over a rural region,
containing varied vegetation. The effect of these differences
on the development of convective precipitation is studied.

Changes in albedo and vegetation density from place to
place may be suspected to account for most of the differences
in air mass over a rural landscape. However, the effects of
soil moisture cannot be ignored. Extreme changes in temperature
have been observed when air traverses from saturated to dry
soil areas. Holmes (1969) observed variations up to $5^{\circ}C$ in
near surface air temperature, and up to $2^{\circ}C$ at 1 km height
within a horizontal distance of 10 kms, containing irrigated
and non-irrigated land, in Alberta. Of course, variations in
soil moisture are not only the result of irrigation practices.
They can appear also due to differences in vegetation, soil, or
the scattered nature of summertime precipitation. The conditions
of vegetation, soil, and precipitation necessary to affect
differences in soil moisture and air mass over a region is
studied.

The effect of land use on climate is of general interest
and concern. For example, there has been much speculation about
the effect of poor land management on the drought of the Great
Plains in the early 1930's. More recently, there has been a
decrease in farmland in parts of Canada and the United States.
In this case, the abandoned land continued to support vegetative
growth, with the gradual return of forest vegetation in some
areas. Another object of this study is to assess the effect
of this recent change in land use on the atmosphere during a

summer period. In doing so, the evaporation and sensible heat flux from the earth's surface is calculated over a land area. Numerous previous studies required such calculations over yet larger regions. These include Vowinckel (1965), Ninomiya (1968), and Morin (1973). In most cases it has only been feasible to make calculations at widely spaced points, where meteorological conditions are observed. The values of evaporation and sensible heat flux are then assumed to exist for the area surrounding the points. The validity of this assumption is tested, considering the local variation in air mass within a land area containing diverse vegetation types.

CHAPTER II

THE EFFECT OF THE EARTH'S SURFACE ON THE ENERGY BUDGET

The differences in air mass which can develop in a region containing diverse land surfaces are obtained by first calculating the differences in evaporation and sensible heat flux (turbulent fluxes) from those surfaces. Specifically, the effects of variations in albedo and vegetation on the turbulent fluxes will be compared to those of variations in soil moisture. The turbulent fluxes are obtained as partial results from an existing numerical model. This model simulates the energy and water budgets at the interface between earth and atmosphere (hereafter referred to as an energy budget model). The choice and limitations of such a model must first be considered.

IIA.   Choice of Model

For all energy budget programmes which do not use observed ground surface temperature, the basis of calculation is the same. It is assumed that for each time step there is no change in energy storage of an infinitesimally thin surface layer of the ground. That is, the incoming energy to this top layer is assumed exactly equal to the outgoing quantity of energy. These types of models all solve for the surface ground temperature at which the incoming and outgoing energy are equal. This requires an iteration scheme where the individual energy transfer terms, to be discussed below, must be recalculated several times for each time step. This involves considerable calculation time. The incoming energy is considered to be made

up of absorbed shortwave solar radiation incident to the ground, downward longwave energy from the atmosphere, and heat flux received from soil layers below the top surface. The outgoing energy must then be comprised of upward longwave radiation from the surface, sensible heat flux to the air, and latent heat flux, or evaporation, to the air. The ground flux, latent and sensible heat fluxes are considered negative if they appear in the opposite category. The differences in the models lie in the method of obtaining these elements. The shortwave and long-wave downward fluxes are either derived or measured, depending on the model. The two turbulent fluxes and ground flux are also derived. The complexity of each of these calculations also varies from model to model, while the upward longwave radi-ation is always a simple known function of the surface ground temperature. The method of obtaining each of these other terms will determine the parameters required for their calculation. For example, if the downward fluxes of short and longwave radiation are obtained directly from measurements, no knowledge of the vertical temperature and moisture structure of the atmo-sphere is necessary. However, such measurements are not common, so most models will calculate the downward radiation terms, using the upper air soundings readily available every 12 hours from points some 350 kms apart. Also, the calculation of sensible and latent heat flux requires the knowledge of the air tempera-ture, dew point, and wind speed near the ground. These para-meters can be obtained from the usual surface weather reports available each hour from stations some 200 kms apart, or they

can be calculated based on an initial troposphere and the input of turbulent fluxes from the previous time step. Myrop (1969) derives the turbulent terms by generating winds and temperatures at various heights from the level of measurement. Thomas (1975) derives the parameters of temperature and dew point within a vegetation canopy. Vowinckel and Orvig (1972) make the calculations directly from the usual measurement of temperature, dew point, and wind.

In the present investigation, the main concern is with the differences caused by surface variations in soil moisture available for evaporation. Hence, it is desirable to choose a programme which has the most detailed consideration of the surface and subsurface water budget. It is felt that the EBBA model (Vowinckel and Orvig, 1972) meets this qualification. Also, the calculations of the individual incoming and outgoing energy terms are not overly complex. This is desirable for an experiment such as the present, requiring calculations for a great number of points. These were the major reasons for choosing the EBBA model for use in this project.

IIB.   The Model

The results of energy budget calculations over an area can be verified by considering the evaporation. This calculated term is checked against that obtained directly from the runoff and rainfall for the area. However, an attempt to determine the runoff from the region under consideration in this study will be difficult, since it is so level that the river flow will have a long response time to rainfall. The runoff for individual

short term rainfalls, such as those studied, are difficult to determine. It is for this reason that no attempt will be made to check the results of the programme in terms of runoff. However, the purposes of this study do not require the model to simulate an absolutely real situation. Hence, the model utilises real data for input parameters to test the hypotheses posed in the introduction for a possible set of circumstances in nature. It is assumed that the chosen model will give realistic results. However, the input parameters and assumptions inherent in the calculations must be clearly stated in order to determine accurately this set of conditions created and to answer the questions of this project. This will be done in the following sections, where the different parameters are discussed. The details of the entire program will not be reviewed here. The reader is referred to EBBA, An Energy Budget Programme - Vowinckel and Orvig (1972), for a detailed account of the procedures of this programme. The order of calculations and steps not mentioned in the EBBA publication will now be presented.

First, in Chapters II and III, the calculations are done in the following order. An initial radiosonde is read in, from which is calculated longwave downward radiation, DFL, and the solar radiation absorbed by the ground, SGA, which is calculated each hour from astronomical considerations and absorption by H_2O and CO_2 in the air, as well as albedo of the surface. Next the energy budget is balanced at the surface by determining the ground flux, FG, upward longwave radiation, UFL, latent heat flux to the air, QE, which depends on the available water for evaporation from the surface, the water vapour and temperature

gradient and wind force above the surface, and finally the
sensible heat flux to the air, QS, which depends on the temper-
ature gradient and wind force above the surface. The final step
incorporates QE and QS into the atmosphere to obtain a new radio-
sonde used for the next time step, when the process is repeated.
This is done using the subroutine CLOE, the operation of which
is not described in literature. Therefore, a brief outline
about this method shall be given, after Vowinckel (personal
communication). If QS is positive, the surface temperature is
increased such that a dry adiabatic layer extending upward from
the surface describes a warming equal to QS. The quantity of
water vapour associated with QE is added evenly through the
mixing layer. New dew points in the layer are obtained from
the original specific humidity at a level plus the added quantity.
If QE is negative, the procedure is the same but the quantity
is subtracted. If QS is negative, the height of turbulent mix-
ing is computed as a function of the wind speed. The surface
temperature is decreased such that a constant gradient to the
top of the level of mixing describes a loss of energy in the
radiosonde equal to the sensible heat flux lost to the surface.

In Chapter IV, the energy budget calculations will be
done for a 7 day period at 229 points. It was necessary to avoid
repeating calculations, so SGA was calculated only once and
read in for the calculation at each point. In this case, CLOE
is not used since the surface temperature and dew point are
calculated from observed values each hour, rather than derived
from previous hour's turbulent fluxes. DFL was recalculated at

each point by constructing new soundings with the hourly reports of temperature, dew point, and wind. This procedure will be discussed in more detail in Chapter IV.

IIC.   Energy Partitioning in the Model

For the same air mass and an given distribution of incoming radiation over an area, the spatial variation of the turbulent flux terms can only·be caused by differences in various ground parameters. The resulting variations which can be generated by differences in the less obvious soil moisture factor will be compared to that of albedo and vegetation para-meters. This will be done by changing the various parameters in·the energy budget programme, one at a time, while holding the others constant.

IIC1.   Albedo

Important variations in the turbulent fluxes must of course arise from differences in absorbed shortwave energy from place to place. This can occur from the variability of reflec-tivity (or albedo) of a land area. The albedo can range from .05 for dense coniferous forest and blacktop road to .25 for bare ground and concrete (Sellers, 1965). To get an idea of. the change in turbulent fluxes one can expect from a variation in albedo, the following numerical experiment was performed. A typical morning summer radiosonde, represented by the dotted lines in Figure 1, is placed over a bare surface which can main-tain potential evaporation. The energy budget programme is run, with light winds, for 24 hours. The radiosonde used for each

Figure 1. Temperature and Dew Point with Height   – – –   Original (0400 EST)
                                                   ————   Final   (1700 EST)

Modification Over Wet Ground
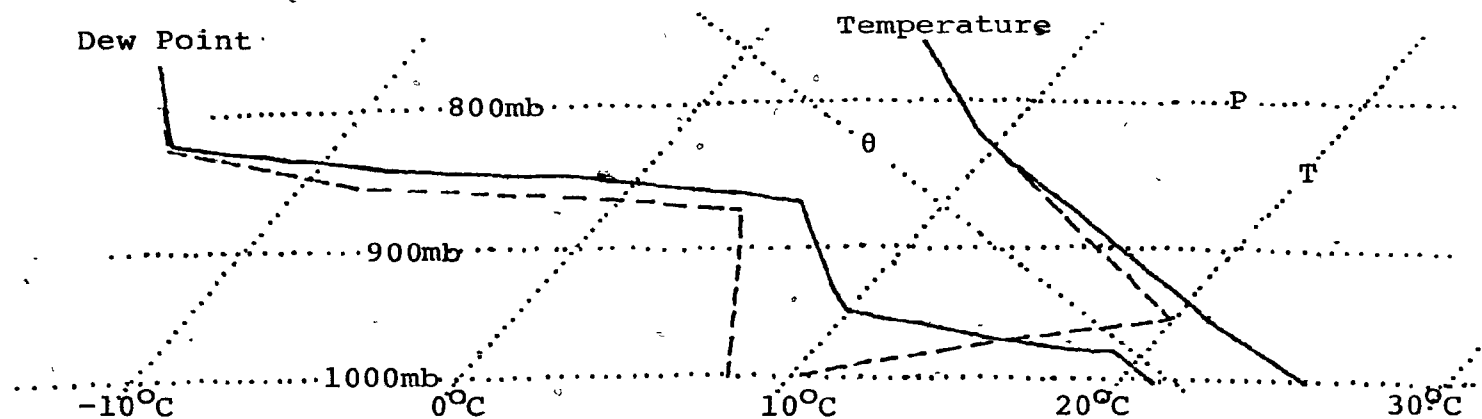
Modification Over Dry Ground
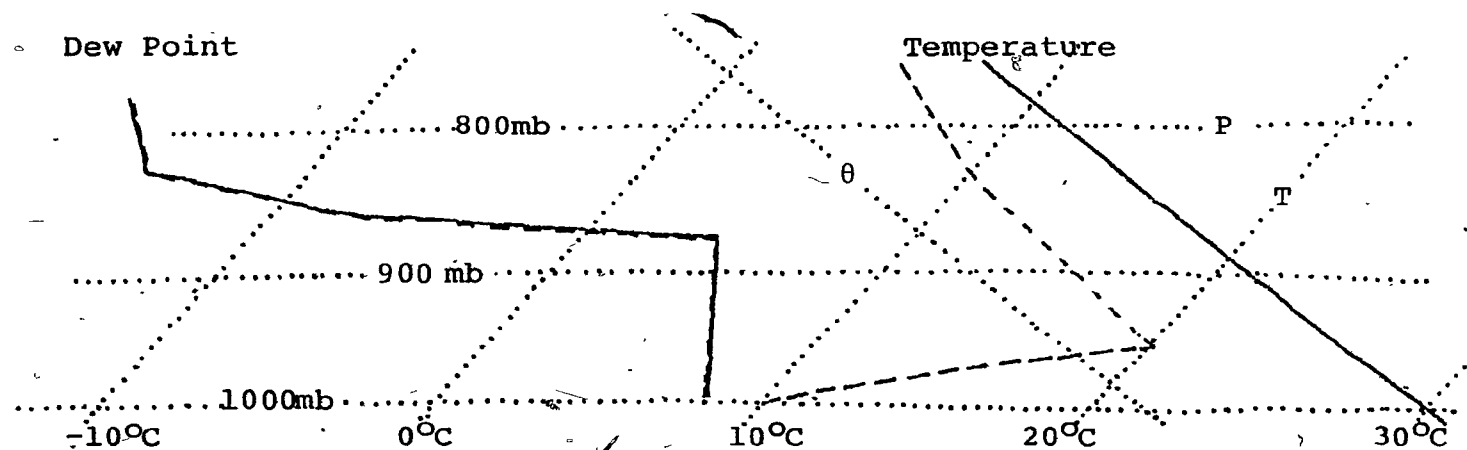
successive hour's calculation is obtained through the subroutine CLOE described in IIB. To get maximum incoming radiation, the case is run near the beginning of summer, July 1, under cloudless skies. The results using two surfaces of different albedos are presented in Table 1.

Table 1. Energy Budget Terms (Calories. cm^{-2} day^{-1}) – Change in Albedo.

ALB	SGA	QS	QE	QS+QE	UFL	FG	DFL
.10	726	121	435	556	901	-23.7	755
.15	685	108	402	510	903	-24.2	753
DIFFERENCES BETWEEN .10 and .15 ALBEDO							
.05	-041	-013	-033	-046	002	0.5	-002
PER CENT CHANGES FROM .10 ALBEDO VALUES							
50	-05.6	-10.7	-07.6	-08.3	00.2	02.1	-00.3

Here it is seen that the decrease in shortwave energy absorbed between the two surfaces is almost entirely accounted for by a decrease in total turbulent fluxes, i.e., QE + QS. Differences in UFL and FG are negligable in comparison. The evaporation term changes by approximately the same amount as the sensible heat flux in terms of percentage. However, the absolute magnitude of the change in evaporation is greater. The comparison of the changes in the two turbulent fluxes depends on the temperature, dew point, and wind speed. This was seen from the results of Lee (1972). He also cited a linear relationship between latent heat flux and albedo. The conclusion here

is that a change in albedo, characteristic of a surface area, will yield a difference in total turbulent fluxes of the same order as the difference in absorbed energy.

The size of areas characterised by different albedos are important when considering local 'air mass' differences which will be generated from the variations in turbulent fluxes over a certain scale. It is felt that the extremes in albedo (.05 to .25) could only be found over areas of a scale smaller than that being considered here. The scale important to this project should be no smaller than that of the convective precipitation cell, in other words, 5 to 10 km. Kung, Bryson, Lenshow (1964) made measurements of the albedo over areas of about this size in Wisconsin. Each such area was characterised by certain combinations of vegetation. The albedos in July ranged between .11 and .17, which included areas with a wide variation in forest cover. Hence, it is believed that the variation in albedo used in the above experiment represents the maximum one can expect in a mixed farmland and woodland area, which is found in eastern North America. It is concluded from the experiment discussed above that the maximum turbulent flux variations from albedo values of the convective scale is about 10 per cent.

IIC2. Vegetation Density

It is observed that areas of dense vegetation, such as forests, are associated with lower temperatures and higher relative humidity than areas of grass or crop nearby (Geiger, 1950). The comparison of the sensible heat flux and evaporation rates from areas of varied vegetation include effects of different

albedo, available soil water for transpiration, as well as total leaf surface per unit area of ground, BLA. The purpose of·this section is to study the effect of BLA alone on the turbulent fluxes. This can be done, using the programme, by holding albedo and soil water constant while changing BLA.

For a land area covered by vegetation, the model considers three levels of surface when calculating the energy budget. The top level represents the first unit of leaf area index which absorbs a large portion of the shortwave energy incident on the surface. The middle level contains the remaining leaf area of the vegetation and absorbs virtually all of the shortwave energy which penetrates the first level. The turbulent fluxes from this layer are enhanced by the additional area from which they eminate. These fluxes are taken to be directly proportional to the unit leaf area index of this layer. The bottom layer is considered to be the ground which receives little shortwave radiation, hence the fluxes are negligible. In the following experiment, ground water is sufficient to maintain potential evaporation at all times and the albedo is constant for all surfaces. The energy budget is calculated for a 24 hour period under clear sky in early summer, using the same radiosonde as in the previous experiment. It is again·modified by incorporation of the turbulent fluxes using the subroutine CLOE at successive hours. The calculations are done over bare ground and over land covered by vegetation with total leaf area index equal to 3. Thus, the middle level will have 2 units of leaf area index, BLA, and the turbulent fluxes as calculated from

the surface temperature, air temperature, dew point, and wind, will be doubled. Table 2 compares the results of the calculations over bare ground and vegetation.

Table 2. Energy Budget Terms (calories cm^{-2} day^{-1}) – Change in Leaf Area Index.

	ALB	SGA	DFL	UFL	QS	QE	QS+QE	FG
Bare Ground, BLA = 0	.15	685.4	753.4	903.4	108.3	402.8	511.1	-24.2
Vegetation, BLA = 3	.15	685.4	746.3	901.8	86.8	435.0	521.8	-08.0

The hourly values of QE and QS are plotted in Figure 2. The ground flux, FG, is reduced by 16 calories when adding vegetation. This is because the vegetation absorbs most of the shortwave energy before it reaches the ground. The daytime ground surface temperature is not as high when covered by vegetation and therefore the temperature gradient just below the surface cannot drive as much heat away via conduction. It is assumed that no conduction of heat takes place through the vegetation itself. The outgoing radiation term, UFL, is slightly higher over bare soil, indicating that the vegetation surface temperature is lower than that of bare ground. This observation is quoted by Geiger (1950). The incoming radiation is smaller over the vegetation surface since there are 7 calories less of downward longwave radiation. This is an outcome of less sensible heat flux calculated from vegetation and will be discussed in detail in the next section. Despite this, the vegetation has 10 more

Figure 2. Turbulent Fluxes from Bare Ground (———) and Vegetation (– – –)
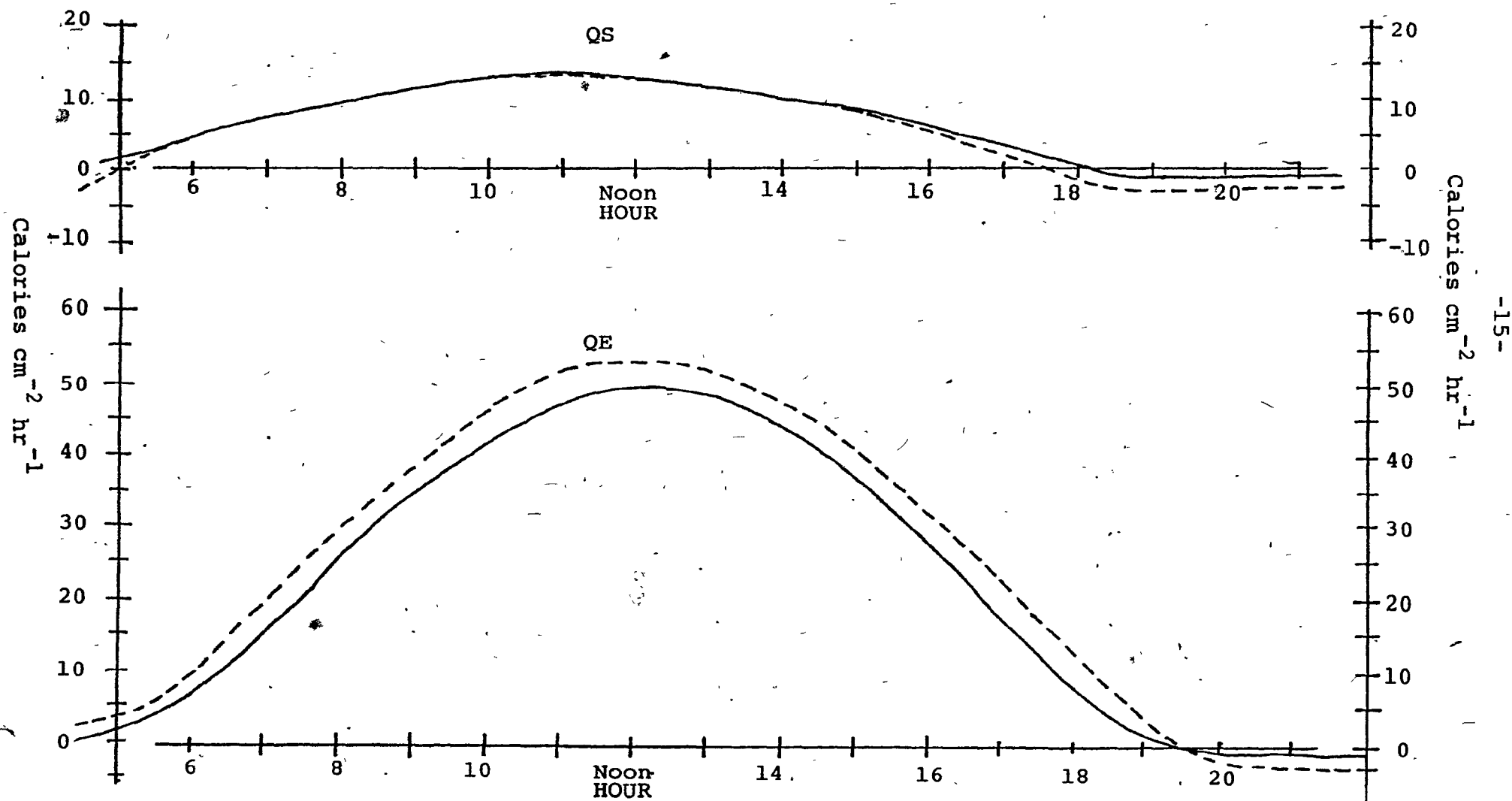
calories to be lost through the turbulent fluxes. Not only is QE + QS higher over vegetation, but there has been a shift of energy from QS to QE. QS is 20 calories lower while QE is about 30 calories higher over vegetation. In order to understand this shift, the formulation of the turbulent fluxes must be considered. Figure 3 contains calculations of QE and QS for given air temperature and dew point as a function of temperature difference between ground and air. The formulation on which the calculations are based is from Malkus (1962). The latent heat flux decreases more rapidly than sensible heat flux when the surface temperature is lowered a given amount. In other words, $(\frac{\Delta QE}{\Delta QS})/\Delta TS > 1$ where TS is the surface temperature. Also, $(\frac{\Delta QE}{\Delta QS})/\Delta TS$ increases as the air temperature and dew point become larger. When BLA is added to a layer, while keeping TS constant, the absolute change of QE compared to that of QS is obtained by comparing the magnitude of QE to that of QS. In other words, $(\frac{\Delta QE}{\Delta QS})/\Delta BLA = \frac{QE}{QS}$. If there is no additional energy available to the total turbulent fluxes, the increase in BLA must be countered by a decrease in TS such that there is no change in QE + QS. The direction of shift of energy between QE and QS depends on the comparison of $(\frac{\Delta QE}{\Delta QS})/\Delta TS$ to $(\frac{\Delta QE}{\Delta QS})/\Delta BLA$. If $(\frac{\Delta QE}{\Delta QS})/\Delta BLA > (\frac{\Delta QE}{\Delta QS})/\Delta TS$, energy will shift from QS to QE, i.e., QE will increase and QS decrease. A schematic diagram of this change is seen in Figure 4. This condition is tested for two atmospheric conditions similar to those of a summer day (Table 3). For most

Figure 3. Turbulent Fluxes

.... 7.5 m sec^{-1}
--- 5.0 m sec^{-1}
—— 2.5 m sec^{-1}

QE
Air temp. = 30°C
Dew Point = 20°C

QE
Air temp. = 20°C
Dew Point = 15°C

QS

Calories cm^{-2} hr^{-1}

Ground Surface Temp. - Air Temp. (°C)

-17-
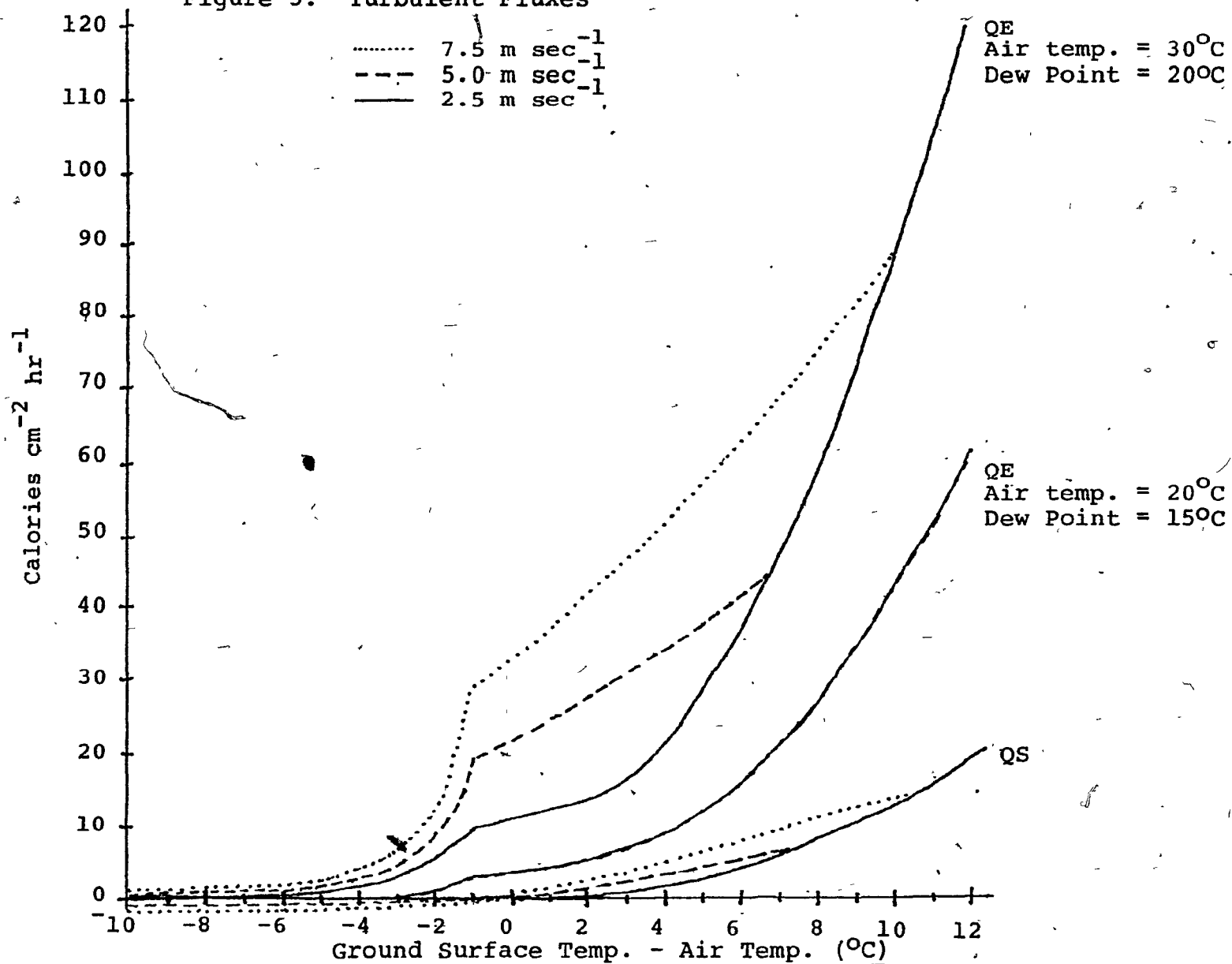
Figure 4. Test for Energy Shift Between QE and QS

$$\frac{\left(\frac{\Delta QE}{\Delta QS}\right)}{\Delta BLA} = X \qquad \frac{\left(\frac{\Delta QE}{\Delta QS}\right)}{\Delta TS} = Y$$

X=3   Y=2

QE_0 QE_1

QS_0 QS_1

Δ BLA $\longrightarrow$ — Δ TS $\longrightarrow$

X>Y
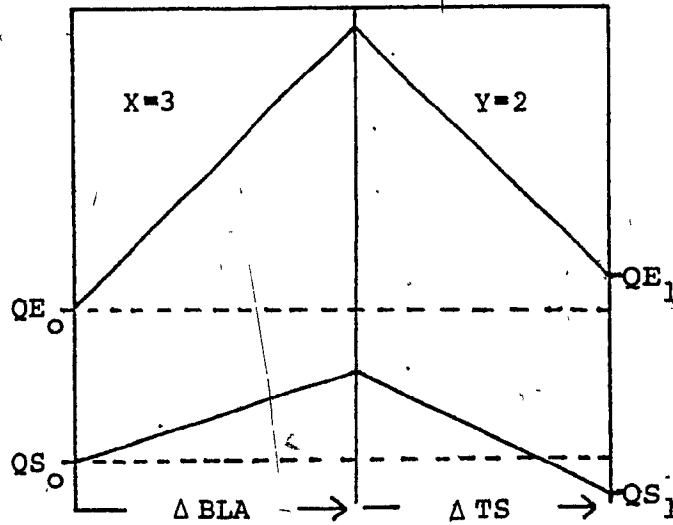
Energy shifted from QS to QE:
QE increases
QS decreases

X=2   Y=3

QE_0 QE_1

QS_0 QS_1

Δ BLA $\longrightarrow$ — Δ TS $\longrightarrow$

X<Y
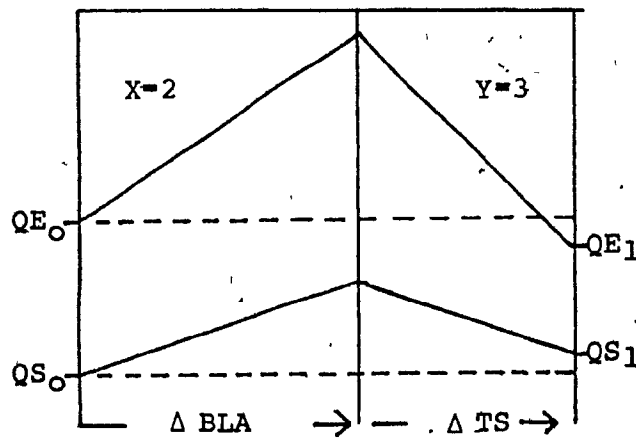
Energy shifted from QE to QS:
QE decreases
QS increases

X=2   Y=2

QE_0 QE_1

QS_0 QS_1

Δ BLA $\longrightarrow$ — Δ TS $\longrightarrow$
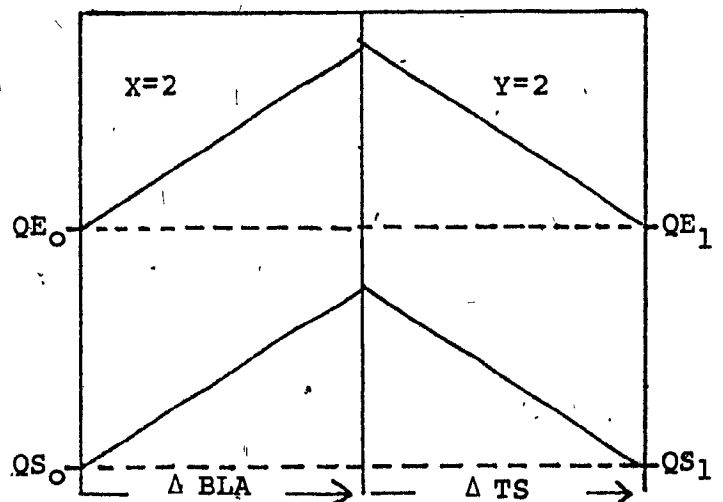
X=Y

No energy shifted:
QE and QS stay the same

Table 3. Response of $(\frac{\Delta QE}{\Delta QS})$ to Change in BLA and TS for Two Air Masses.

Air Temp. (°C)	30	30	30	20	20	20
Air Dew Pt. (°C)	20	20	20	15	15	15
TS-Air Temp. (°C)	14	12	10	14	12	10
$(\frac{\Delta QE}{\Delta QS})/\Delta$BLA	6.4	6.4	6.7	3.3	3.3	3.3
$(\frac{\Delta QE}{\Delta QS})/\Delta$TS	6.1	6.0	5.8	3.4	3.2	3.1

of these conditions, $(\frac{\Delta QE}{\Delta QS})/\Delta$BLA $> (\frac{\Delta QE}{\Delta QS})/\Delta$TS. The difference between the two terms becomes greater as TS is decreased. Hence, the shift of energy from QS to QE can be expected when comparing the turbulent fluxes from bare soil to those from vegetated land. QE increases more than QS decreases since more energy is available to QE + QS with the decrease in ground flux. The result is consistent with the observation of 20 per cent higher evaporation from sod as compared to sand, following rain (Geiger, 1950).

It is necessary to determine the mixing of the air, from inside the canopy of vegetation to the ambient air on the outside, in order to find the contribution of the middle and bottom layer on the turbulent fluxes from the top of the vegetation. Thomas (1975) developed a model which calculates the temperature and dew point inside the canopy and the mixing of the air inside with the ambient air above the vegetation top. He calls the fraction of the air which is mixed, RLOSS. The net loss of

evaporation and sensible heat flux from the vegetation is given by the QE and QS from the top layer, plus that from the middle and lower layers multiplied by RLOSS. In order for the difference between foilage temperature and air temperature to fall within the range of observed values in forests on clear summer afternoons with light winds, RLOSS must be ≥ .9. Here it was felt unnecessary to calculate the modification of the air inside the canopy since the mixing is high when the turbulent fluxes, and hence incoming radiation, are highest. However, this programme has used values of RLOSS which did not vary with thermal stability. The amount of mixing did vary with wind speed and vegetation density. Grass or crop areas are more dense than areas of trees, hence the mixing of internal canopy air was taken to be less for the former. For example, with a 2.5 m sec^{-1} wind, RLOSS for crop was taken equal to .62 while forest was given a value of .88. To study the consequences of these values, the following experiment compares 24-hr energy budget calculations where RLOSS is varied for an area covered with vegetation of BLA = 3 under light winds. The vegetation was again transpirating at potential rate during the period. The results appear in Table 4.

Table 4. Energy Budget Terms (Cal cm^{-2} day^{-1}) - Change in Mixing

RLOSS	ALB	SGA	DFL	UFL	QS	QE	QS+QE	FG
.62	.15	685.4	747.0	903.3	95.0	426.0	521.0	-8.2
1.00	.15	685.4	746.3	901.8	86.8	435.0	521.8	-8.0

As might be expected, QE + QS is unaltered since there is no further reduction in FG. The increased mixing enhances the effect of adding more area from which fluxes can emanate, hence more energy is shifted from QS to QE. If the value of RLOSS chosen for a vegetation area is too small, the effect of adding BLA is diminished.

To summarise, areas covered with sufficient vegetation to shade the underlying surface from significant shortwave energy will have a greater combination of evaporation plus sensible heat loss than others. There will also be a shift of energy from QS to evaporation. The evaporation may be as much as 10 per cent higher from bare ground to crop even if both surfaces have the same available soil moisture and albedo. These differences will be compared to those found from variable available soil moisture in the next section.

IIC3. Soil Moisture

Variations in soil moisture content will affect the turbulent fluxes even if the areas are absorbing the same quantities of incoming radiation. This parameter is usually expressed in terms of soil saturation with respect to water available for evaporation (referred to as available soil water). Here the two extreme values of this parameter will be discussed. That is, soil which is completely saturated with available water for evaporation (i.e., filled to available soil water capacity) and soil dried to the point where no further water can be extracted by evaporation under normal atmospheric conditions (no available soil water). The former condition was that used

for the experiment with albedo in IIC1. The drying of the soil with time will be discussed in the next section, IIC4. There it will be seen how the fluxes behave as the surface wetness parameter changes between the two extremes presented here.

Although dry soil has a higher albedo than saturated soil (Sellers, 1965), most land, where precipitation is not deficient, is virtually completely vegetation covered. Such areas will not exhibit changes in albedo as the soil saturation varies. This was observed by Aase and Id (1975) over mixed prairie rangeland. Thus, the following test was done holding the albedo constant in both cases. As was the case in the albedo experiment, hourly calculations were done for 24 hours using a typical summertime morning radiosonde for the first time step and modifying it each successive hour by inputing the turbulent fluxes into the atmosphere, using CLOE. The results appear in Table 5.

Table 5. Energy Budget Terms (Calories cm^{-2} day^{-1}) – Dry and Wet Soils.

	ALB	SGA	DFL	FG	QE	QS	QE+QS	UFL
Saturated Soil	.15	685.4	753.4	-24.2	402.8	108.3	511.1	903.4
Dry Soil	.15	685.4	768.1	-14.4	0	443.8	443.8	995.5

It is of interest that the DFL term is higher over dry soil. From a closer examination of hourly fluxes, not presented here, it was seen that a more rapid warming of the morning inversion was evident over the dry land, where QS is considerably higher. This accounted for greater amounts of DFL from the air modified over the dry soil than over the saturated soil in the morning, giving a larger 24-hour total. The result of this is that the saturated soil receives less incoming radiation than the dry soil. Also, the wet soil is observed to be a better conducter of heat than dry soil. The programme takes this into account, and it is seen that the saturated soil surface looses more heat to lower soil layers than the dry one. Even though the saturated soil gains 15 less calories from longwave radiation and looses 10 more calories through conduction of heat to the subsurface, it is most significant that the total quantity of turbulent fluxes is 67 calories more than from the dry soil surface. This is because the lack of evaporation over the dry surface requires the energy budget to be balanced at a higher surface temperature. This yields a substantially higher UFL since the upward longwave radiation is proportional to the fourth power of the surface temperature. The same phenomenon modelled here is observed by our bodies as a lower skin temperature when transpiring on a hot day.

Finally, there is no doubt from these results that both the sensible heat flux and evaporation terms are individually greatly different between these two extreme land types. The two extreme soil moisture conditions can exist simultaneously

over an area which becomes very dry from lack of precipitation
and then receives a scattered pattern of rainfall. The variability
in the turbulent flux patterns will be more substantial than
those generally found from differences in albedo or vegetation
density.

IIC4.　The Development of Soil Moisture Variation with Time

First, the evaporation of water from non-vegetated
ground will be considered. Kramer (1949) states that little
evaporation takes place from depths below the first foot of
soil. Veihmeyer (1927) found that in California most evapora-
tion is from the upper 4 in. of soil, much less from the next
4 in.; and very little from below 8 in. However, no precise
values are given. Indeed, the water depletion with depth from
bare soil is highly variable, depending on the type and condi-
tion of the soil. The evaporation vs. depth curve, Fig. 5,
is constructed from these general reports. We next consider a
variety of soils, in terms of texture. Table 6 gives available
water holding capacities for a range of soils (Thornthwaite and
Mather, 1957).

Table 6.　Available Water Holding Capacities (m/m) for Soils
of Variable Texture.

TYPE	TEXTURE NO	AVAILABLE WATER HOLDING CAPACITIES m/m
Fine Sand	1	.10
Fine Sandy Loam	2	.15
Clay Loam	3	.25
Clay	4	.30

Figure 5.   Evaporation vs. Depth
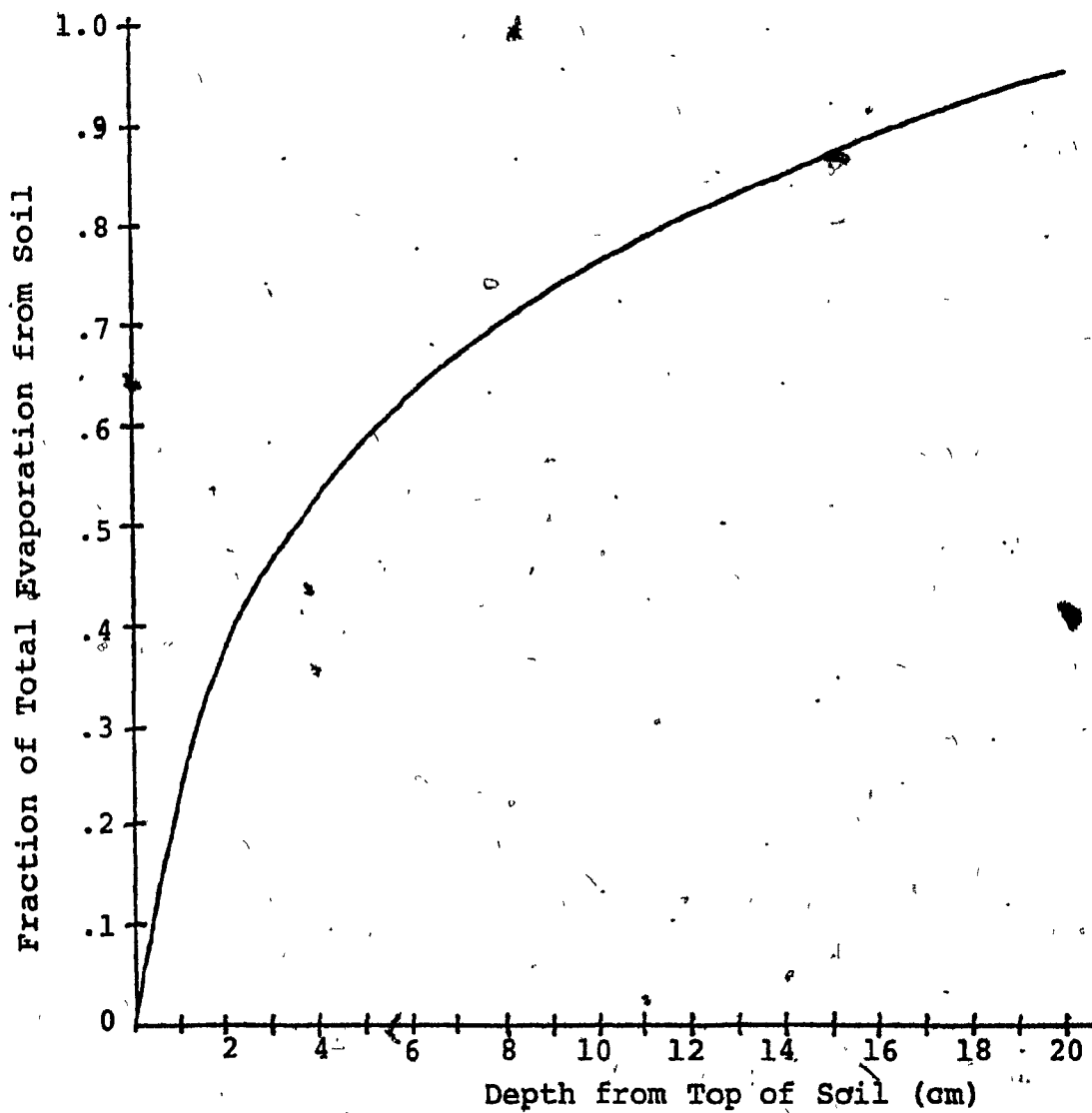
If Figure 5 were constructed for each of these soils, the more coarse types would have evaporation supplied from deeper layers and the more fine texture soils from shallower depths. However, the present model will consider evaporation from 6 layers. Each layer has been defined in terms of water holding capacities rather than actual depth. For a given depth in terms of water holding capacity, the real depth is deeper for the more coarse soil. Thus, the variation of Fig. 5 between soils will be diminished when the evaporation from various depths is considered in terms of water holding capacities. Because of the uncertainity of Fig. 5, the following experiment was carried out only to obtain an idea of how the evaporation from bare ground changes with time. The tendency will be compared to that of vegetated ground later.

The experiment begins with 6 layers of soil, filled to capacity in terms of available soil water. The layers are defined by dividing the total evaporation depth into 6 even parts; i.e., about 17 per cent of the total evaporation will come from each layer. The depths in terms of water holding capacities given to each layer are from Fig. 5 and the water holding capacities, BW, for soil #3 are presented in Table 7.

Table 7. Available Soil Water Capacity of Soil Layers, BW.

Layer	1	2	3	4	5	6
Fraction of Total Evaporation	.17	.17	.17	.17	.17	.15
BW (cm)	.12	.20	.38	.78	1.32	3.20

The force required to extract water from soil by capillary action is known, as a function of saturation. Evaporation can take place at the potential rate when the soil is saturated. As it dries, the necessary force increases and the soil can only evaporate further water at a fraction of potential, FA. Fig. 6 contains graphs of FA as a function of saturation for soils differing in texture. The programme uses the surface temperature, screen level dew point, and wind to calculate the potential evaporation rate from the surface, QE from an open water area. The fractions of this evaporation are applied to each layer from the above table. The actual evaporation possible from each layer is obtained from considering their saturation (GW/BW, where GW is the water held in the layer) and obtaining FA. Clearly, the top layer will maintain evaporation for the shortest time since layer thickness increases with depth. The energy budget programme is run for several days over the soil in a manner identical to that described in the preceeding sections. Daily values of QE and QS are plotted as dashed lines in Figs. 7 and 8, using the water holding capacities from Table 7. The dot-dashed curves are for soil with one half the available soil water capacity per layer. This case also represents a soil with full available soil water capacity, but when the evaporation is limited to occur from one half the depth given in Figure 5. The flux rates are seen to change following smooth curves whose rate of change with time changes only slowly with time. Potential evaporation cannot even be maintained for the first day and decreases steadily through the third day.

Figure 6. Fraction of Potential Evaporation Possible vs. Saturation of Soil

1 – Fine Sand
2 – Sandy Loam
3 – Loam
4 – Clay

Fraction of Potential Evaporation, FA

Saturation of Soil Layer, GW/BW
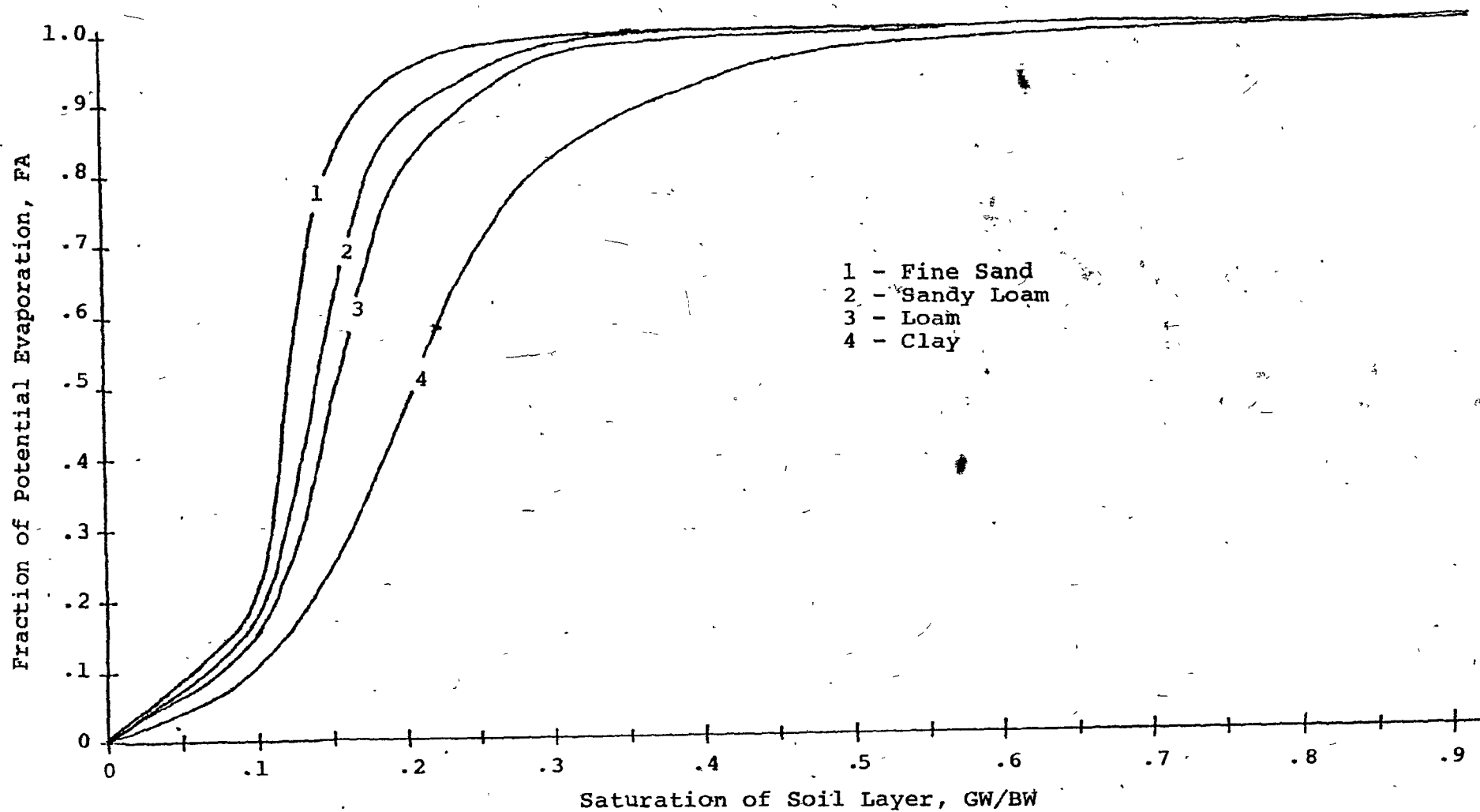
Figure 7.   QS vs. Time Over:

Bare Ground: — — — Normal
                     .—..—.. ½ Storage Capacity
         and
Vegetation: ———— Deep Roots
                    .... Shallow Roots
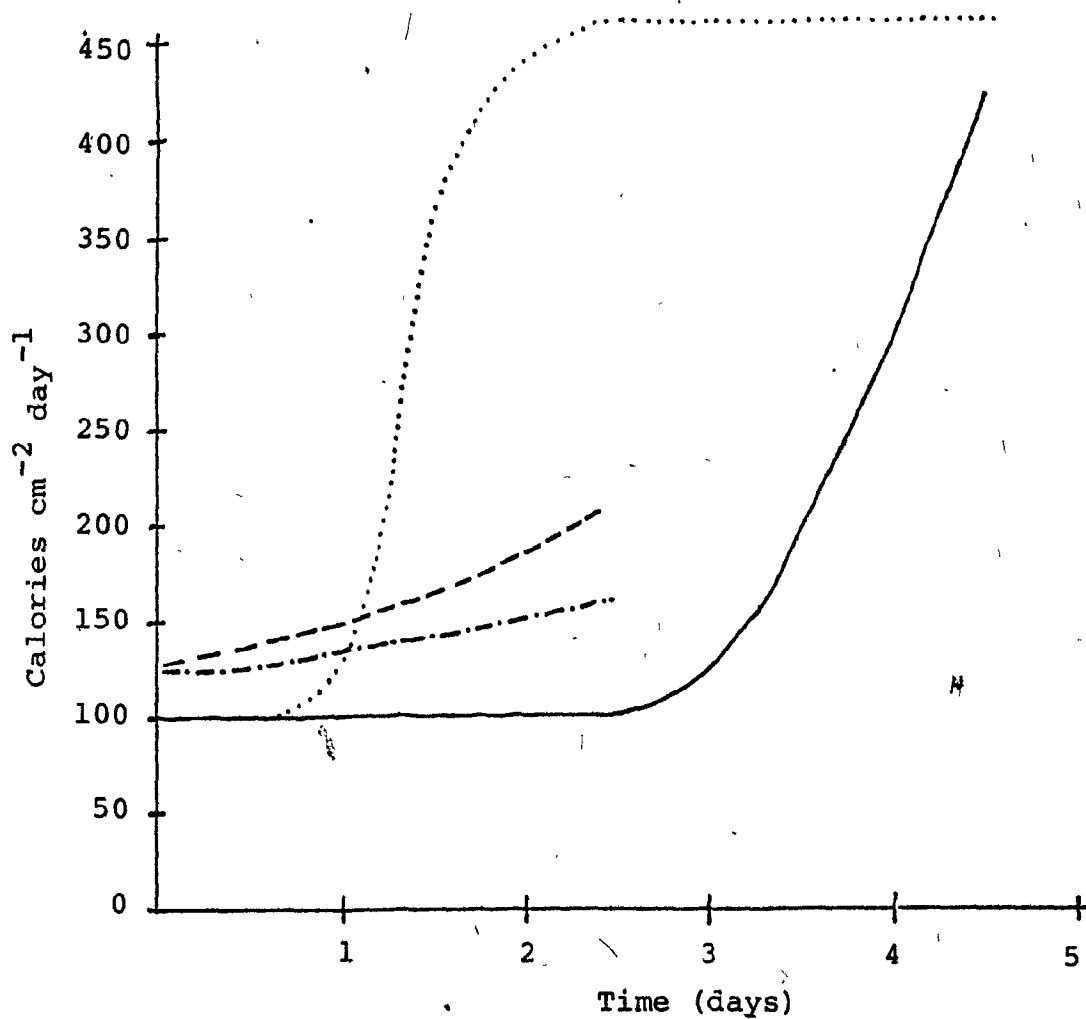
Figure 8. QE vs. Time and QE+QS vs. Time over:
Bare Ground: — — — Normal
                    —·—·— ½ Storage Capacity
        and
Vegetation: ——— Deep Roots
            ····+···· Shallow Roots
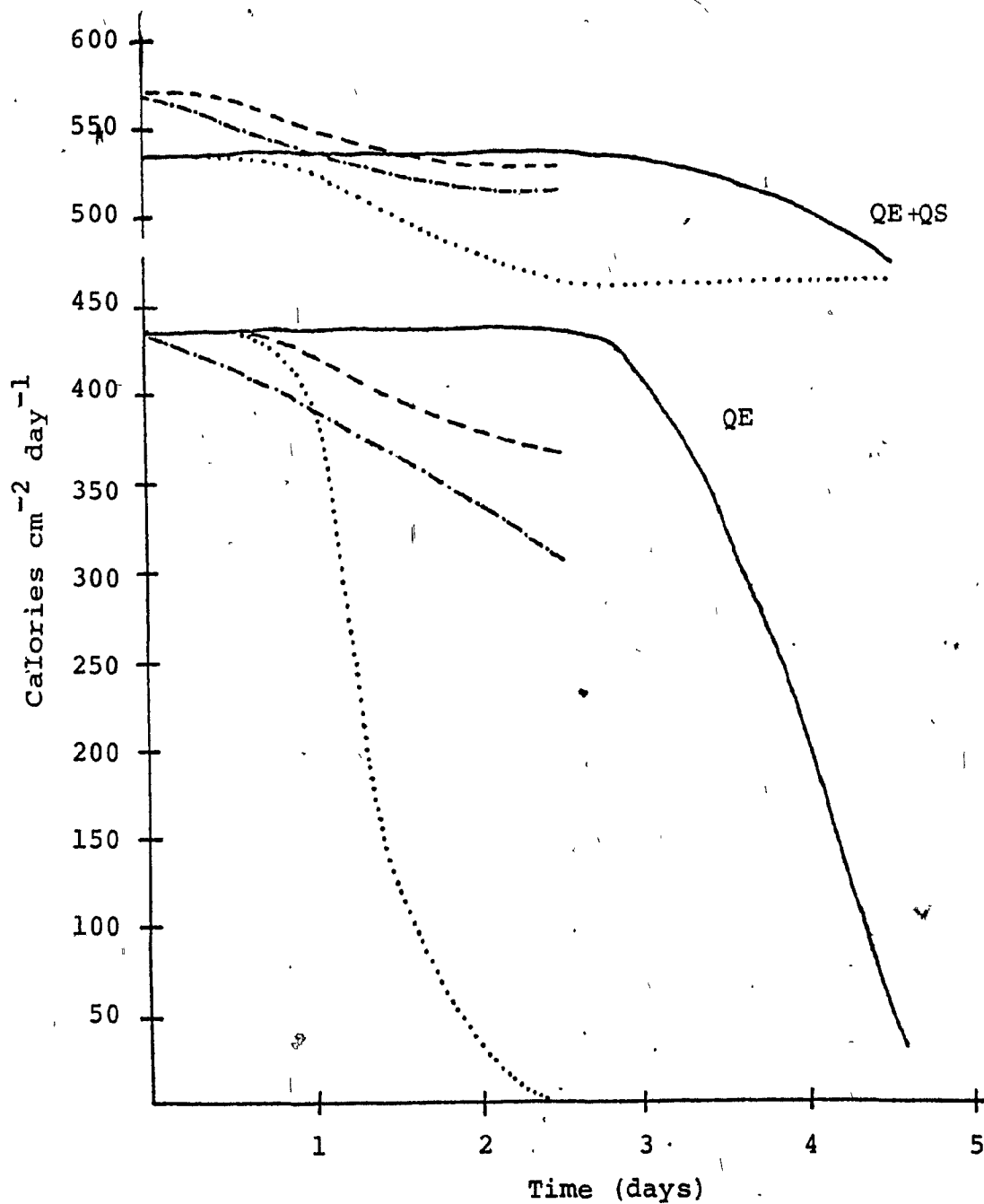
QS increases at a slightly slower rate since the QE + QS total decreases with higher surface temperatures, associated with soil drying as seen in section IIC3.

When a vegetation layer is present, a large portion of the incoming shortwave energy fails to reach the soil surface. This was reflected by the smaller ground fluxes calculated under vegetated surfaces in section IIC2. It is for this reason that the direct evaporation from the soil under vegetation is very small as compared to transpiration from the plants themselves (Kramer, 1949). Water from soil layers is extracted through plant roots from a range of depth defined by the root zone. The roots are capable of extracting water from a layer more efficiently than evaporation of water from the top of a layer via capillary action. When the volume of soil in immediate contact with the root hairs dries up to the extent that removal of further water becomes difficult (FA drops below unity), the roots will grow out through the layer, coming in contact with soil which is more saturated. That is, the capillary action of water drawn through the soil is increased by the plant itself. Let it be assumed that a particular plant can maintain potential transpiration until the saturation of a soil layer drops to a value equal to Y. Also, that the evaporation, through the soil layer via capillary action alone without the aid of roots, can only be maintained at a fraction of the potential rate when the saturation is equal to Y. If this fraction is assumed to be the potential rate divided by N, where N is greater than one, potential transpiration is assumed possible until

$FA < \frac{1}{N}$. For soil number 2, Y is found to be the following saturations for various N (Table 8).

Table 8. Critical Soil Water Saturations

N	1	2	3	4	5	10
Y	.35	.155	.135	.125	.115	.075

For N ≥ 2, the change in these critical saturations becomes small as N is changed. If one could be certain that N ≥ 2, the error in choosing the correct critical saturation becomes small. For soil #2, FA drops below unity at GW/BW ≤ .35. If N = 2 with roots present, potential transpiration is maintained until GW/BW ≤ .155. Twenty per cent more water is made available in changing N from 1 to 2. If this change is equated to the change of surface area of roots from one single vertical strand for N = 1, then N ≥ 2 becomes quite acceptable since the addition of root hairs alone to roots can increase the surface area 1.6 times (Kramer, 1949).

Now, if the root zone soil layer contains X cm of available soil water, then potential transpiration will occur for the depletion of the first $X \cdot (1 - \frac{GW}{BW} \text{ critical})$ cm of water, where GW/BW critical is obtained from the method above. If for example, X = 20 cm (1 metre root zone in silt loam), and N = 3, then $20 \cdot (1-.135) = 17.3$ cm which can be transpired following saturation at the potential rate until the turbulent fluxes will be affected by the drying with the eventual consequences discussed in IIC3. From the results of IIC2, it is

found that the daily potential evaporation on a clear day in July from vegetation with leaf air index of 3 is .78 cm day^{-1} (430 cal). If the 17.3 cm is transpirated at this rate, it will take nearly 3 weeks before transpiration will drop below the potential rate. This then represents the minimum time for potential transpiration from an area of silt loam with vegetation of roots 1 metre deep, starting with saturated soil.

Next, the total time until all evaporation ceases will be considered. This occurs when the supply of available water in the root zone is depleted. The fraction of potential evaporation possible from an area with vegetation is assumed to be governed by the force necessary to extract water from pure soil, a function of GW/BW, and the addition of the root branching, parameterized by N. It must also be considered that, as the potential evaporation is no longer possible, the surface must have a higher equilibrium temperature to dispose of the same incoming energy. However, the potential evaporation at these higher surface temperatures increases. The potential evaporation from a surface which cannot maintain potential evaporation is higher than the potential evaporation from a wet surface. The difference is considered in Fig. 9, which gives the fraction of wet ground potential evaporation as a function of FA, the fraction of potential evaporation possible for given saturation and root systems. The data for this graph is obtained from calculations of the energy budget over surfaces of different saturations on a clear July day. Finally, the fraction of wet potential evaporation possible is graphed as a function

- 34 -

Figure 9. Fraction of Potential Evaporation Possible
from Unsaturated Soil as a Function of that
from a Saturated Soil
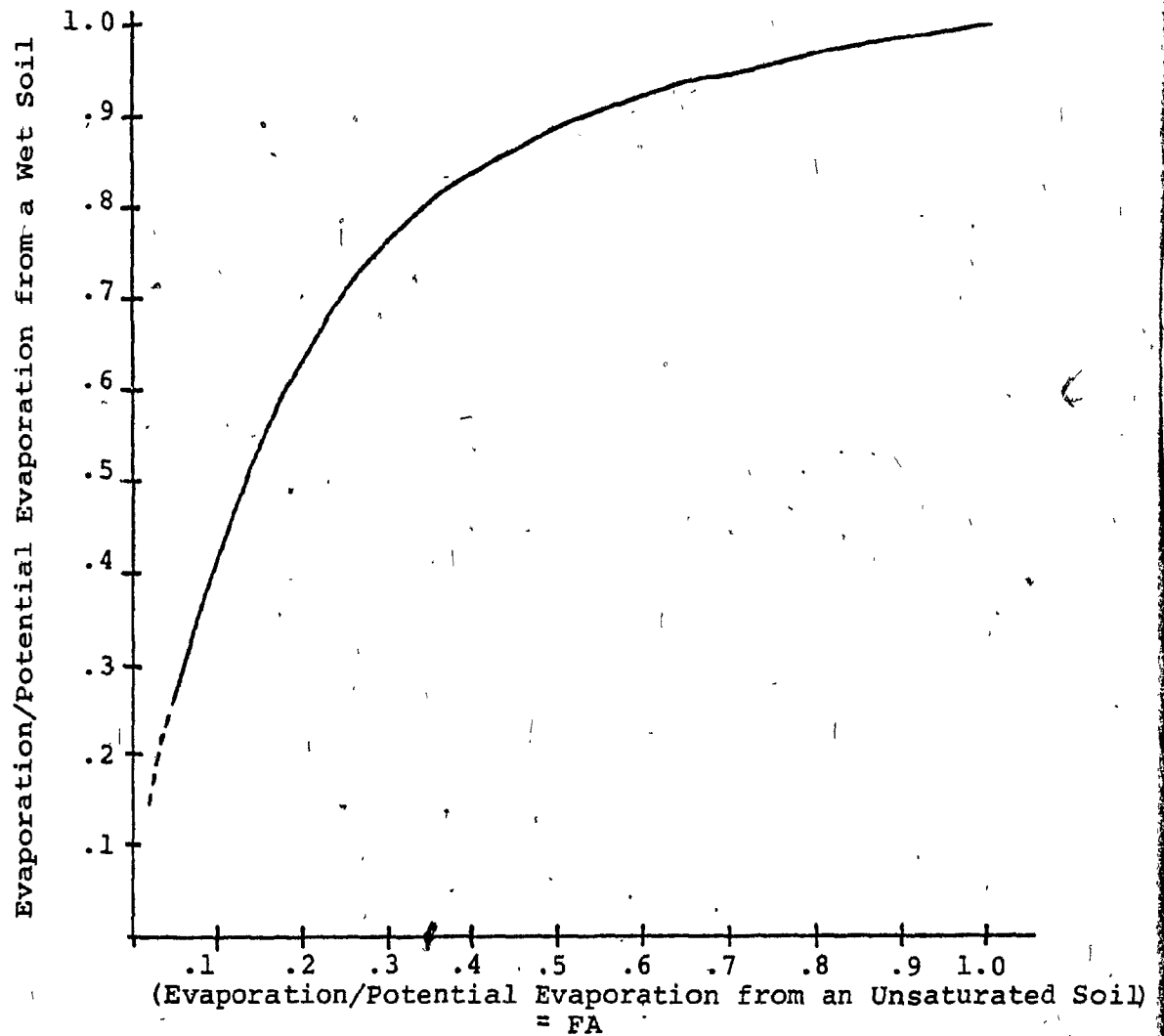
of soil saturation and N in Figure 10. One notes the near
linear dropoff of the fraction of wet evaporation with satur-
ation. The effect of adding root branching (N = 3) to the model
is to prolong potential evaporation to a saturation of .135.
The fraction of wet transpiration decreases linearly from this
point to nearly 0. This curve will now be used to estimate
the time of soil water depletion in the root zone. The fraction
of wet transpiration is integrated over saturation values from
the critical saturation to zero. Since the decrease is linear,
the average fraction, .7 of potential wet evaporation, can be
used as a constant for the range of saturations. If .78 cm day^{-1}
is used again as the wet potential evaporation and X cm of water
was available to the root zone when the soil was saturated, then
X . $\frac{GW}{BW}$ must be evaporated at .7 of the .78 cm day^{-1} rate to be
depleted. This gives: X . $\frac{.135}{.7x.78}$ days = X . .247 days.
If X again equals 20 cm from our other example, 5 days will
elapse from the time of reduced evaporation (3 weeks) until the
available water supply is depleted. Such a sharp and steady
decrease of ground water with time is not observed in nature
because the programme assumes the plant can draw water from
the ground with the same efficiency, even while drying out.
However, the results should be useful to obtain an idea of the
minimum time needed to develop differences in water storage
under clear conditions. Following saturation, these periods of
available soil water depletion are plotted in time as a func-
tion of root depth in Figure 11 and water initially avail-
able to the root zone in Figure 12. This is presented for

Figure 10. Evaporation (as a Fraction of the Potential from Wet Soil) vs. Saturation of Soil
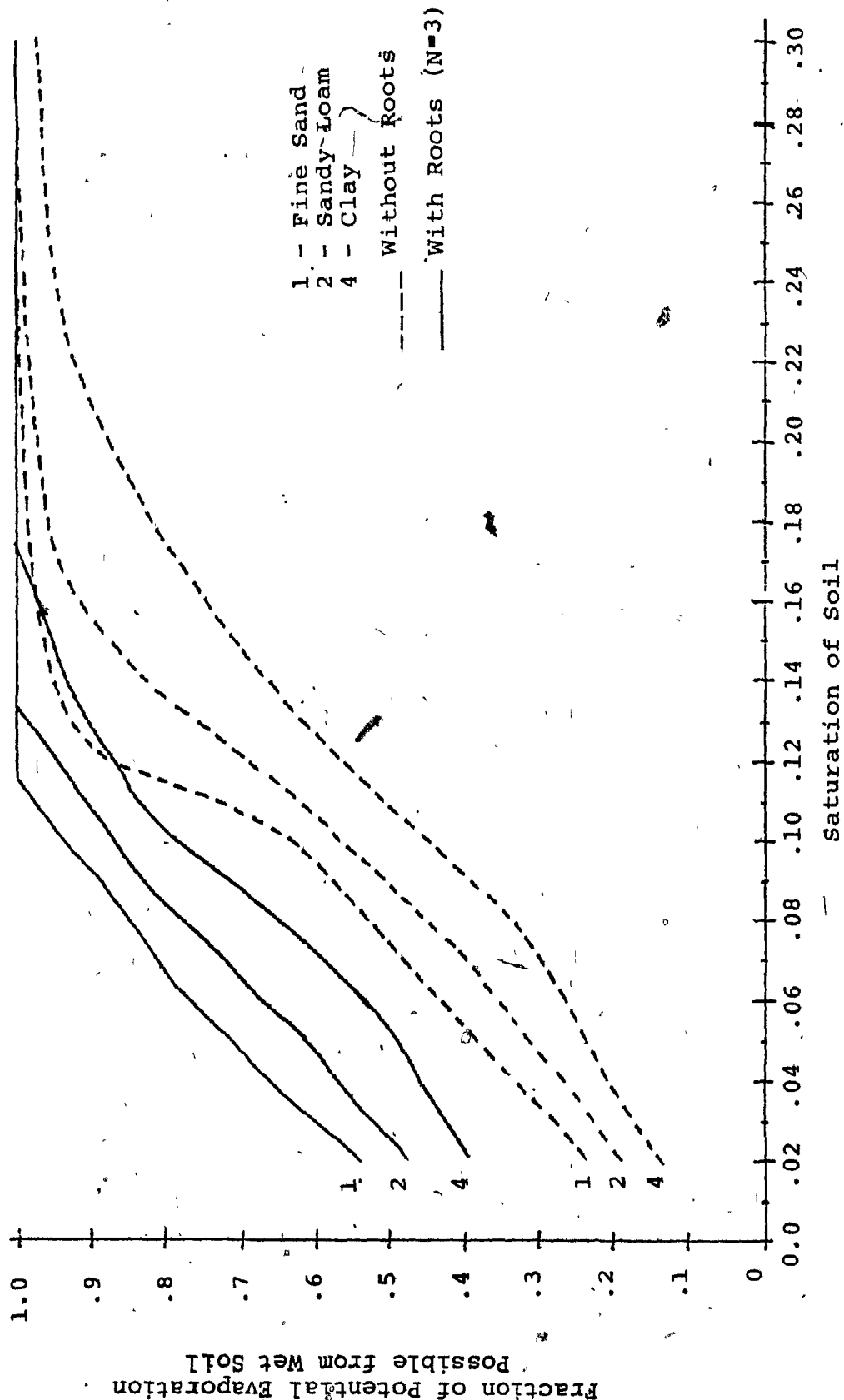
Figure 11. Minimum Time After Soil Saturation Until Evaporation Decreases from Potential Rate (-–-) and Until Evaporation Ceases (——), as a Function of Rooting Depth
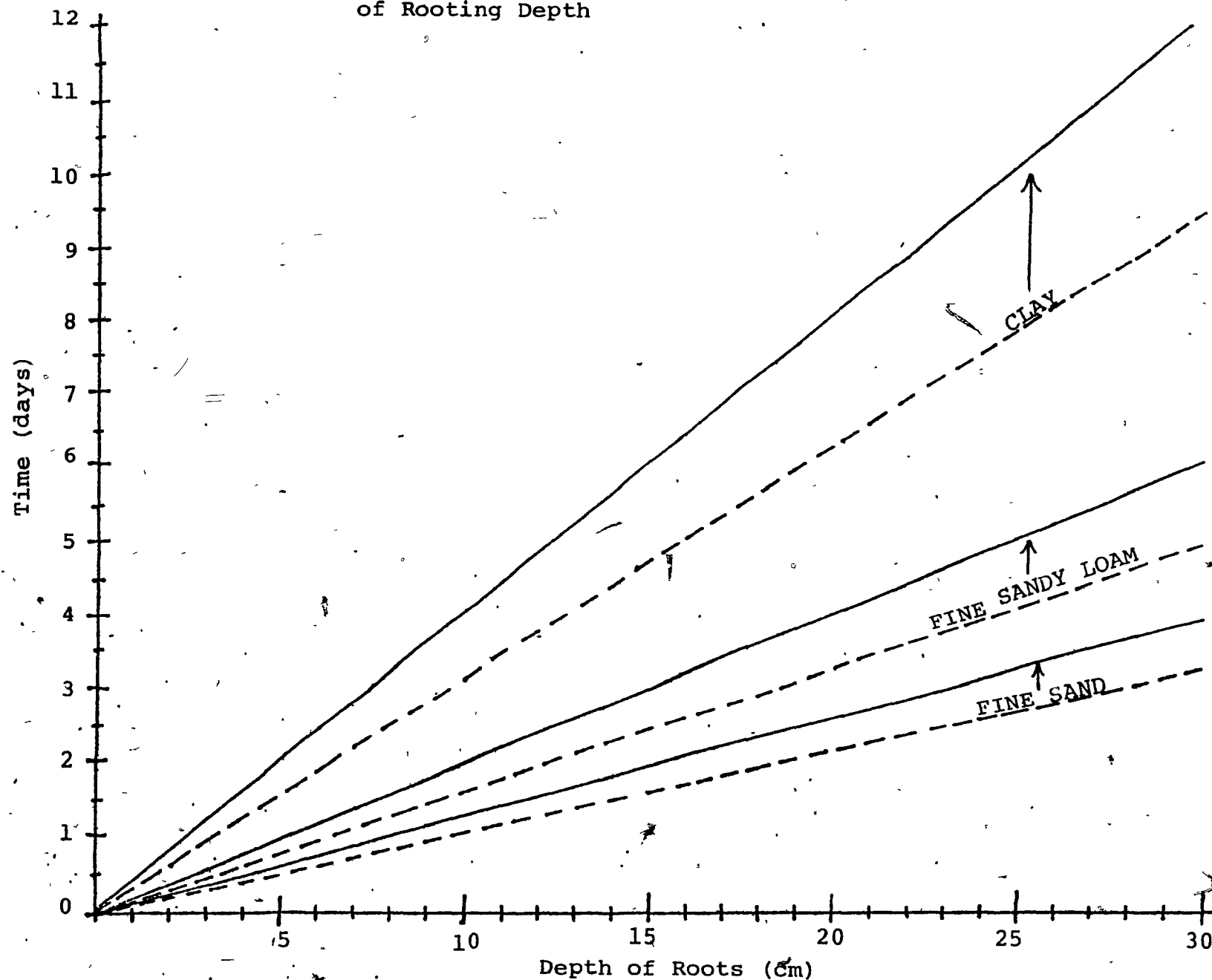
Figure 12. Minimum Time After Soil Saturation Until Evaporation Decreases From Potential
Rate (—–) and Until Evaporation Ceases (——), as a Function of Available
Soil Water

*Water Available to Crop Types

1-Shallow Crops   A-Fine Sand
2-Moderate Crops   B-Fine Sandy Loam
3-Deep Crops   C-Silt Loam
4-Orchards   D-Clay Loam
5-Closed Mature Forest   E-Clay

*(Water Available to Various Crop-Soil
Combinations are obtained from their
position along the abscissa)
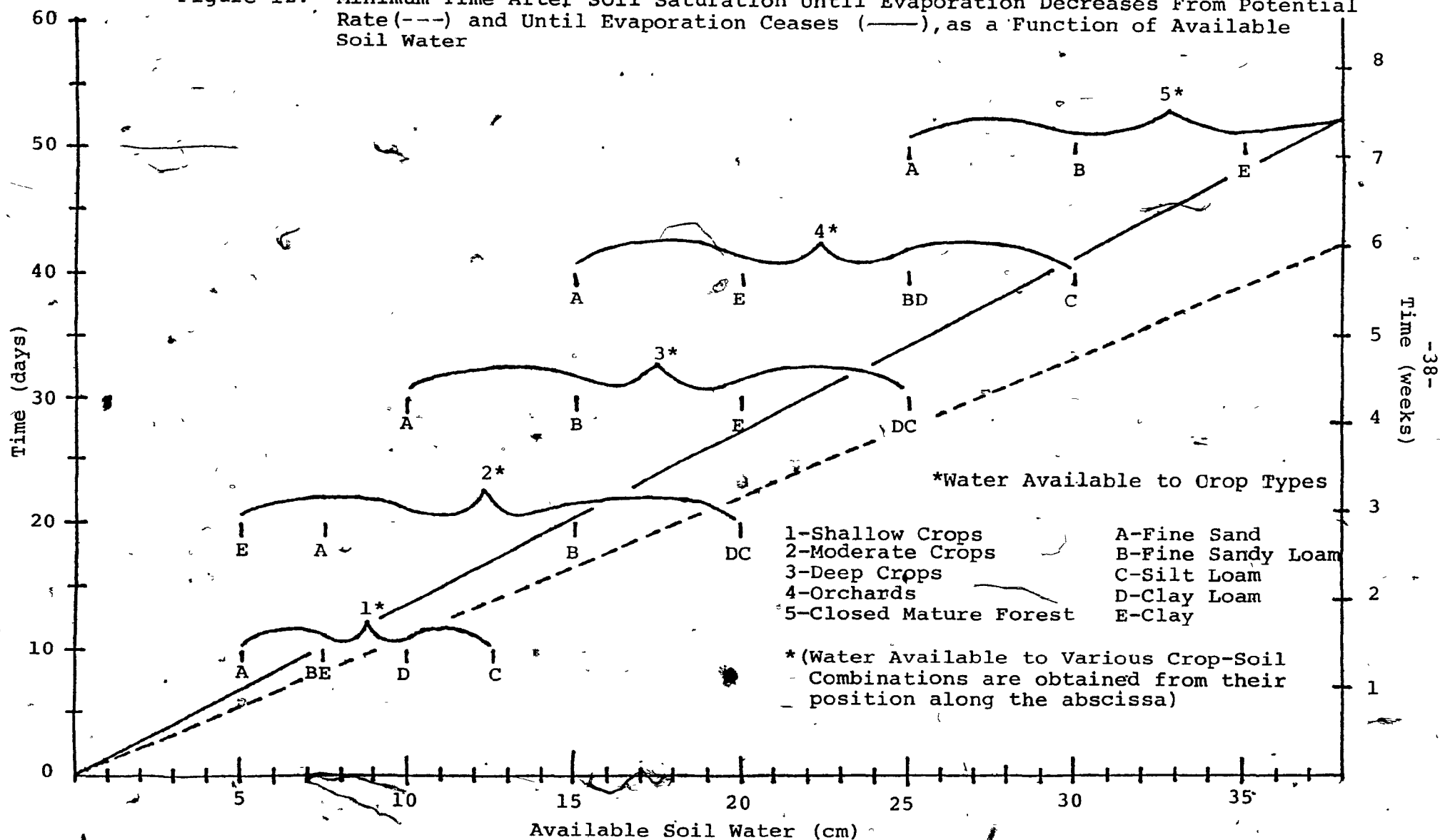
a range of soil textures. The classification of plant types
and their root zones in the various soils was obtained from
Thornthwaite and Mather (1957). From these graphs, one·can
estimate the minimum time necessary between general rains (when
soil layers are saturated) for which the given root systems
will no longer support potential evaporation. Of importance
here are the areas of different turbulent flux characteristics
which can be generated over a region of vegetation of variable
rooting depth.

When vegetation is present, the programme calculates
the potential transpiration from the two layers of leaf area
above the ground. This quantity of water is assumed to be drawn
up through the plant stems without restriction even when maximum
demands of up to .5 cm hour^{-1}occur. The water is taken evenly
with depth in the root zone. This assumes that the density of
roots is assumed constant with depth in this zone. The actual
transpiration from each layer is then calculated separately
from the saturation, BW/GW, with N = 3. In reality, the density
is greater in the more shallow layers of soil. The transpira-
tion will decrease sooner and more gradually than with the assump-
tion used here, since the withdrawal from the lower layers is
more gradual. The times calculated for which a plant can main-
tain potential evaporation are overestimated. Hence, these times
represent upper limits of the time necessary between rains to
affect a change in the turbulent fluxes.

As was done earlier for bare ground, the programme was
run for a few days for two vegetation surfaces in soil which was

saturated with respect to available water. The first type has
shallow roots extending to only 5 cm in silt loam, the roots
have access to 1 cm of available water. The second type has
deep roots extending 3 times deeper. Figures 7 and 8 present
results of daily turbulent flux rates as dotted and solid lines
for these two surfaces. As seen before, the deeper roots can
draw water for a longer period since more storage is available.
It is noted also that evaporation drops to zero from the shallow
plants before bare ground, while the deep roots maintain poten-
tial evaporation through 3 days. Note also that it takes longer
for the evaporation from the deep roots to decrease to zero
once the decrease begins. Hence, the sensible heat flux will
be considerably higher and latent heat flux considerably lower
over the shallow plant areas by the 3rd day after rain, as
compared to the deeper rooted plants. Referring back to Fig. 12
it is seen that the turbulent fluxes will not shift to all
sensible heat before 10 days over shallow rooted plants (such as
spinach, peas, beans, etc.) while 8 weeks is needed for the same
effect over a 'closed mature forest'. Thus, an area containing
portions of forest and crops can develop the large contrast in
turbulent fluxes discussed in IIC3   if more than 10 days of
clear dry weather follow a uniform precipitation pattern over the
area. Of course, if the pattern of rain is nonuniform, differ-
ences can develop sooner.

CHAPTER III

ENERGY BUDGET CALCULATIONS AT POINTS WHERE METEOROLOGICAL PARAMETERS ARE NOT MEASURED

In order to study the spatial variation of turbulent fluxes (and hence air mass) of the scale of convective precipitation, calculations of the energy budget are required at grid points 5 to 10 kms apart. To manufacture a realistic set of meteorological conditions to use for the calculations, it would be advantageous to use the meteorological parameters observed hourly at surface stations, rather than to generate them numerically as was done for temperature and dew point in the experiments of Chapter II. However, meteorological observations are only available from stations about 100 km apart. The consequences of extrapolating the meteorological parameters from these stations to closely spaced points between them will be analysed in this chapter. This will be done by comparing the results of energy budget calculations at a point using the maximum variations of input meteorological parameters found between synoptic stations. Each parameter will be considered separately.

IIIA. Temperature and Dew Point

The CLOE programme will be used to generate the maximum temperature and dew point variations associated with the spatial variations in wetness discussed in Chapter II. The variation in temperature and dew point are related to each other by variations in surface wetness, and thus these two parameters are discussed together. Their effect on the calculation of evaporation is a form of an oasis effect.

IIIA1. Characteristics of Air Over Wet and Dry Areas

To begin, an area is considered consisting of two portions which generate vastly different combinations of QE and QS. The two extremes in surface wetness, as discussed in IIC, will be considered first. In other words, this area consists of a portion of saturated soil and a portion of dry soil. Let it now be assumed that each portion is sufficiently large and the advection of air sufficiently small that a vertical column of the troposphere will remain over each portion for at least one day. That is, the residence time of the air over each portion is at least 24 hours. The air over each area will attain characteristics of the sensible and latent heat fluxes associated with each surface. From the experiments of IIC, the hourly QE and QS quantities and ground temperature were obtained and plotted in solid lines in Figs. 13 and 14 for the two surfaces. It was mentioned that the initial radiosonde used (Fig. 1) was felt to be a typical morning summertime sounding. However, the surface inversion chosen was particularly strong, so that the temperature and dew point were modified most rapidly for a given quantity of sensible and latent heat. In this way, the difference will be greatest between each temperature and each dew point over the two surface types. The hourly screen temperature and dew point obtained from CLOE are plotted on Fig. 15 for the two air masses. It was also mentioned in IIC that the 24-hr DFL   was greater over dry soil than saturated soil. The hourly values of this energy term are plotted in Fig. 16 for the two surfaces. It is seen that the downward

Figure 13. Turbulent Fluxes and Ground Surface Temperature for Saturated Ground.
———— Stationary Air Mass
----- Advection of Air Mass from Dry Ground
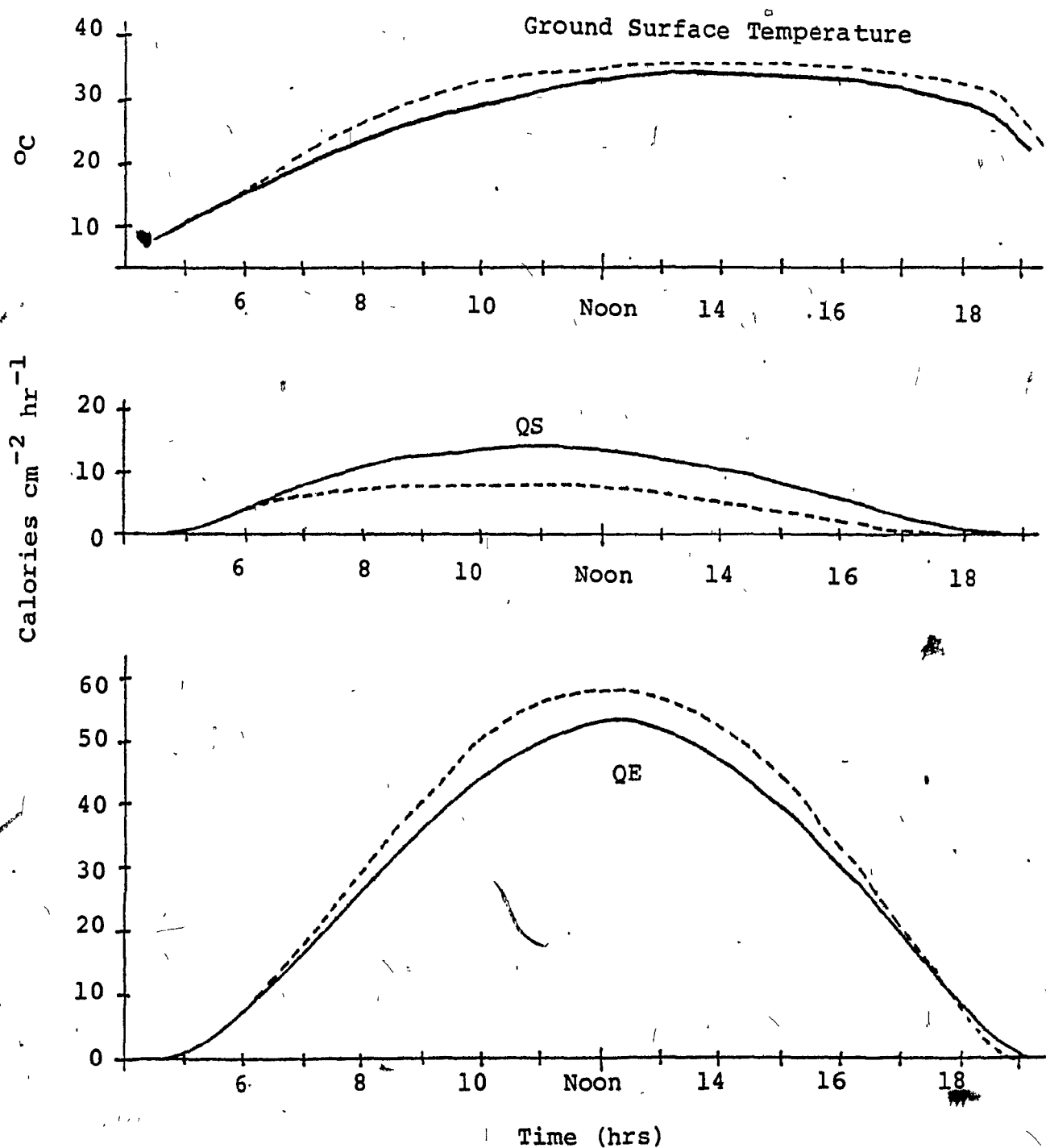
Figure 14. Sensible Heat Flux and Ground Surface Temperature
            for Dry Ground.
            ————— Stationary Air Mass
            - - - - Advection of Air Mass from Saturated Ground

Ground Surface Temperature

QS
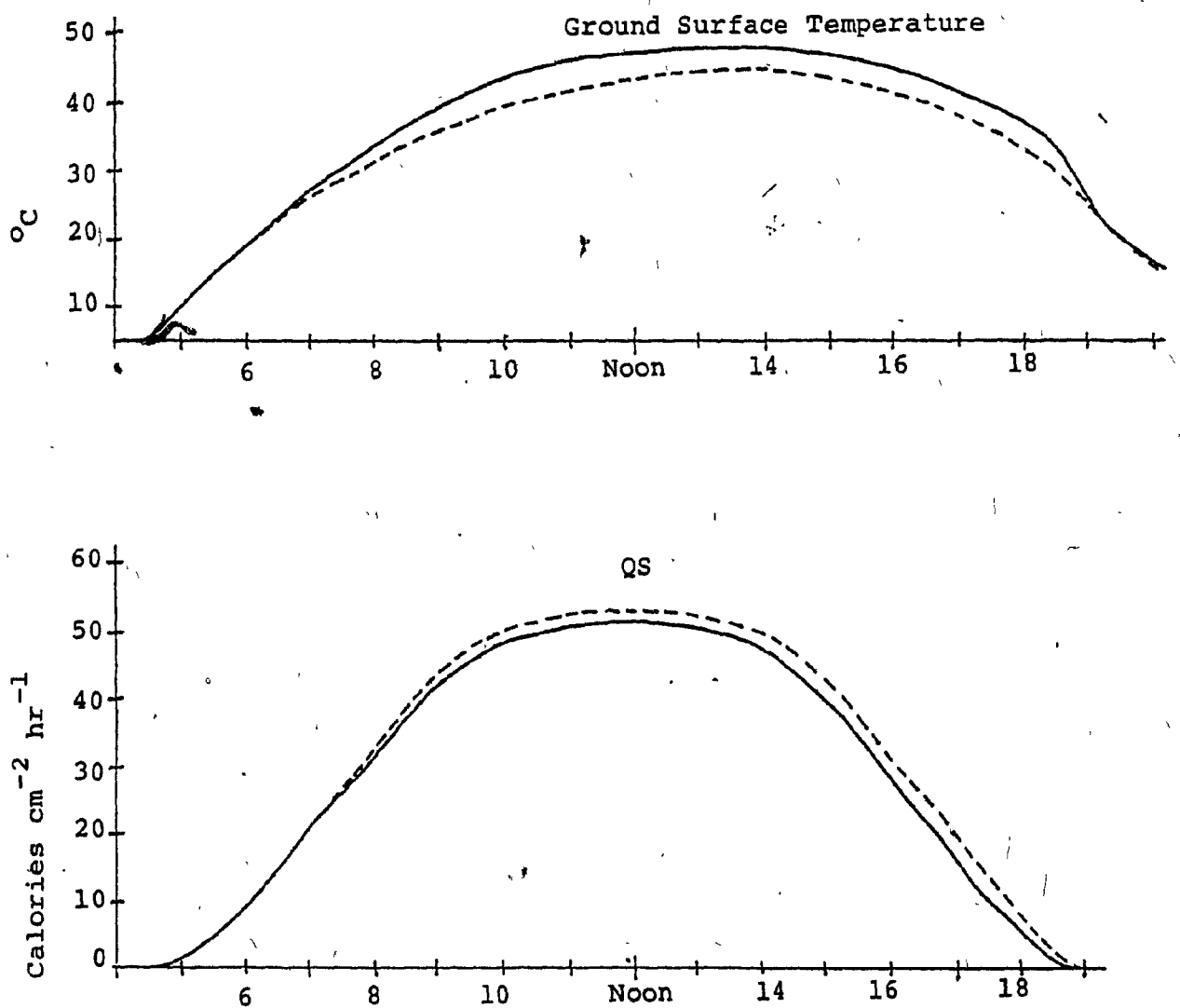
Figure 15. Comparison of Air Temperature and Dew Point over Saturated and Dry Ground

-45-
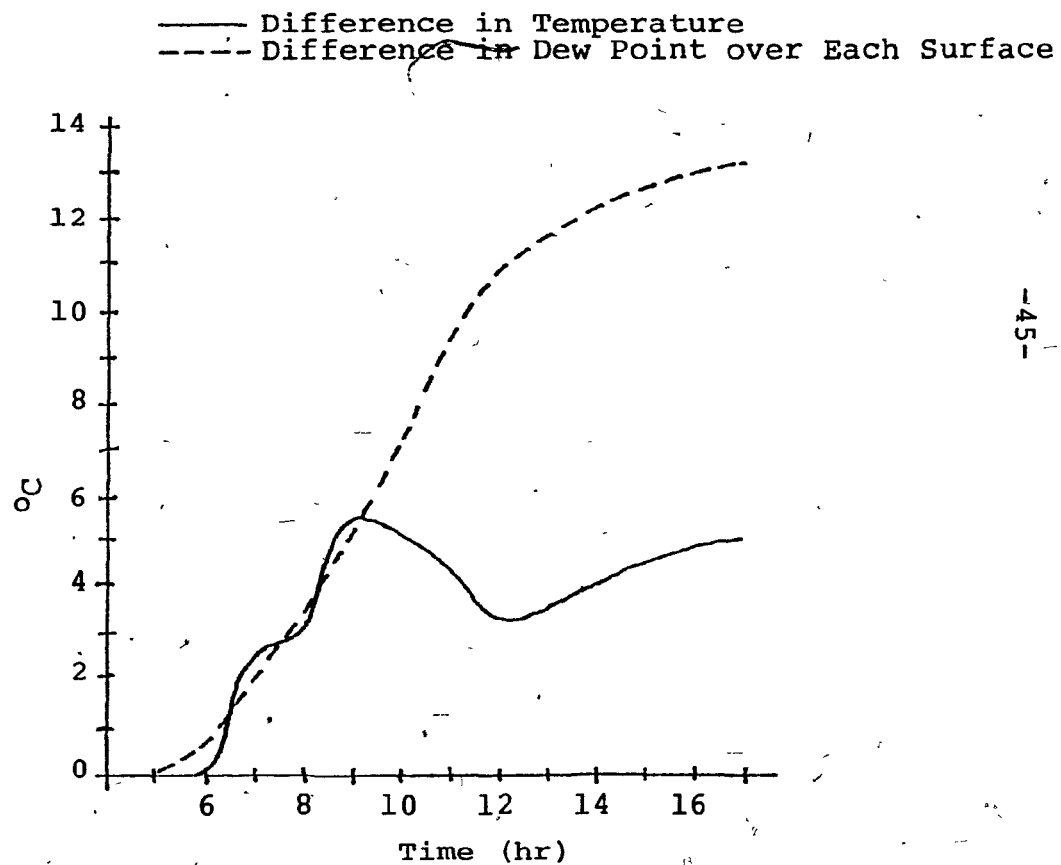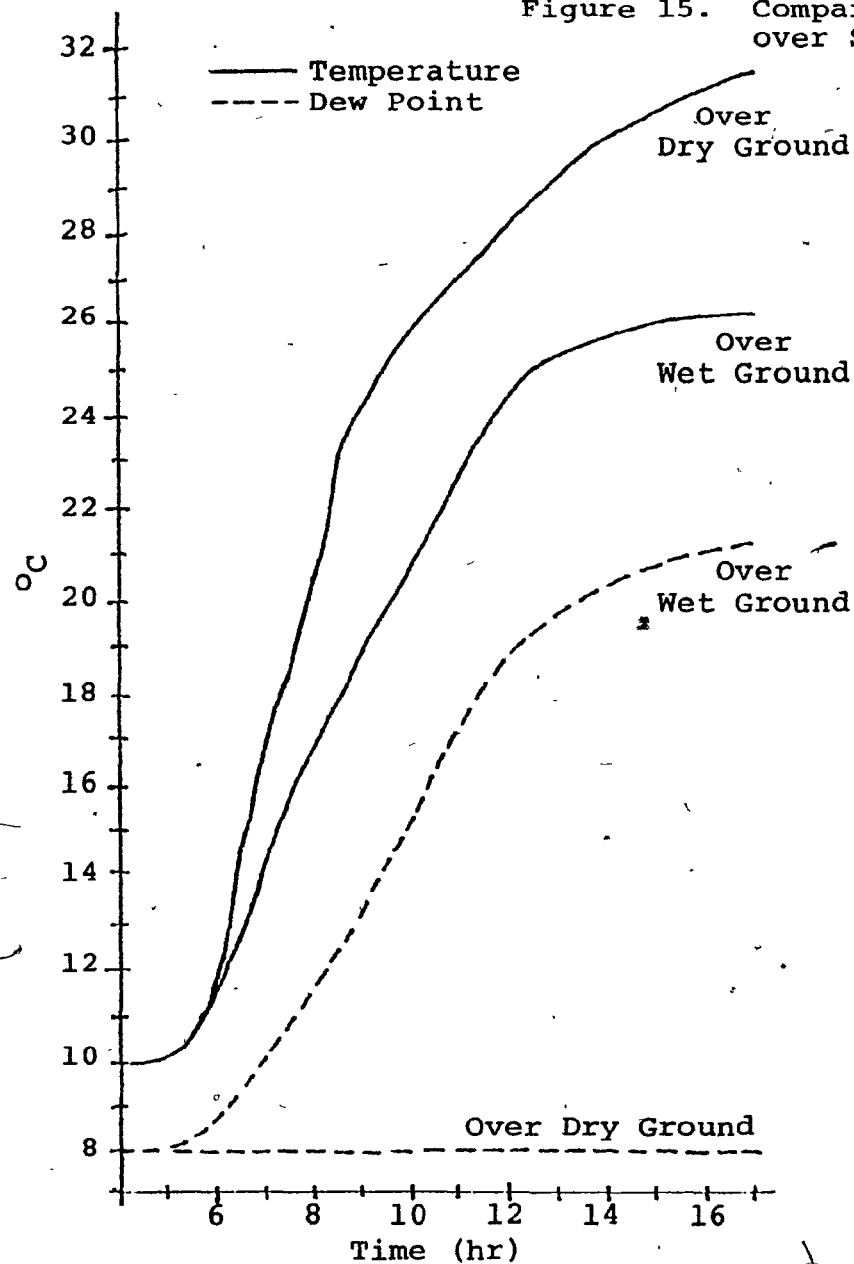
Figure 16. Comparison of DFL Over Saturated and Dry Ground

————— Stationary Air Mass over Dry Ground
– – – – Stationary Air Mass over Wet Ground
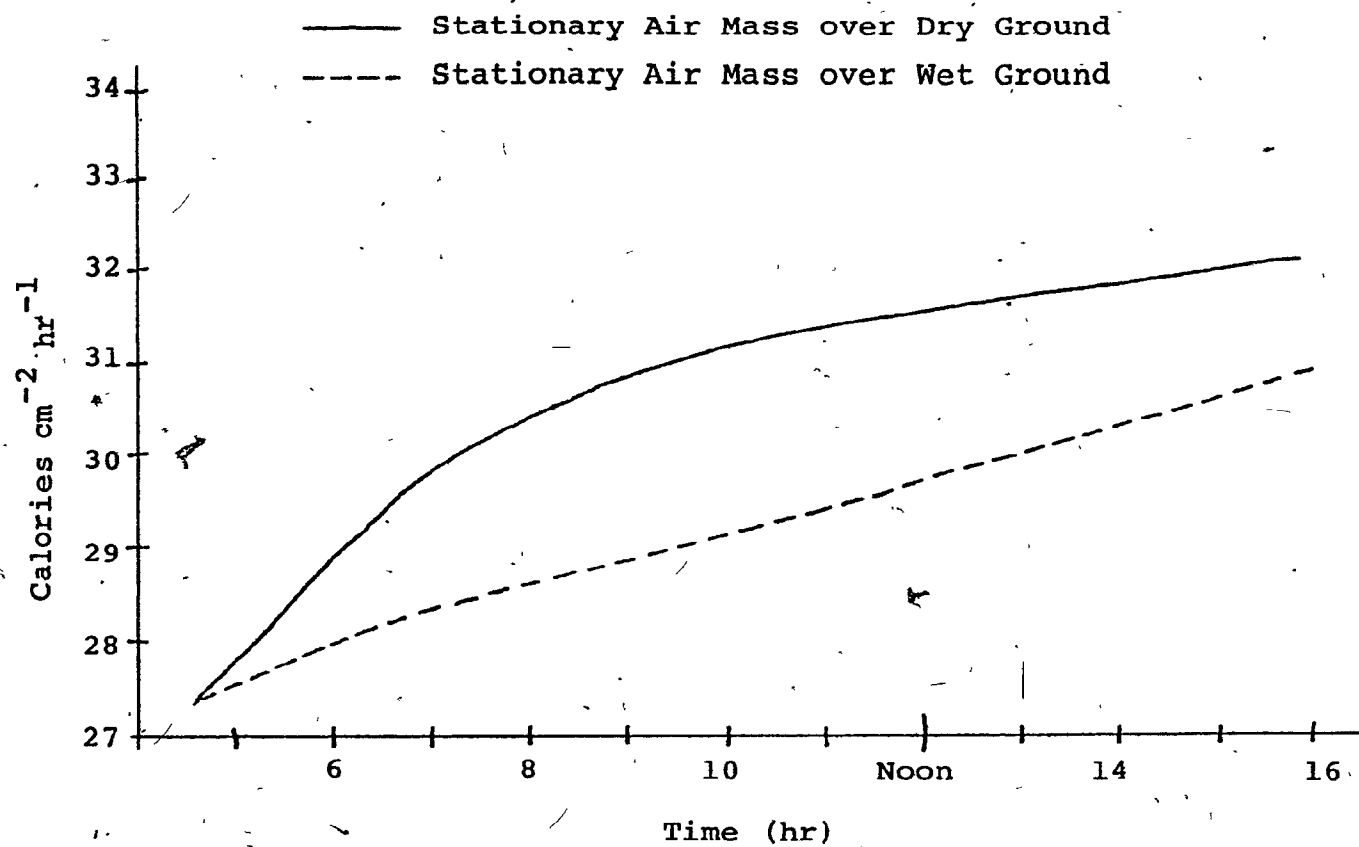
longwave radiation increases more rapidly over dry land,until the inversion is broken at about 0900 hrs (the sounding becomes nearly adiabatic in the lowest 200 mb). Later, the further addition of turbulent fluxes increases DFL almost equally over the 2 surfaces. Thus, the wet surface has less incoming radiation, yet the turbulent flux total is greater than over the dry surface.

IIIA2. Station in Wet Area - Calculation Done Over Dry Area

It is now assumed that a meteorological station is located in the wet land region and must be used to calculate the energy budget over the entire area. There is no problem in calculations at points in the wet area, since the screen temperature and dew point used will be characteristic of the air in that region. However, the temperature used for the calculations over the dry land will be too low, and the dew point too high. Also from the above discussion, the DFL used will be too low. Table 9 compares the daytime energy terms obtained vs. the values calculated with the real air mass, characteristic of the dry area:

Table 9. Energy Budget Terms (Calories cm^{-2} daylight hours^{-1}) Over Dry Land Compared to Those Using Station From Wet Land Area.

	SGA	DFL	UFL	QS	QE	QS+QE	FG
Real Values	685.4	499.5	722.0	449.0	-0.1	449.0	-14.3
Station Over Wet Area	685.4	489.4	693.2	469.8	-0.6	469.8	-12.4

Fig. 14 compares the hourly QS and ground temperature values when
the real known temperature and dew points are used (solid line)
to those obtained when the station is located over the wet
region (dashed line). It is seen that QS can be overestimated by
20.8 calories, an error of 4.6%. Since the screen temperature
used over the dry area is too low, the same surface temperature
as that calculated with the real screen temperature will lead to
a greater daytime temperature gradient and QS. To maintain a
balance of energy, the surface temperature (and hence UFL) must
be underestimated when the screen temperature used is too low.
The overestimate in QS plus the underestimate in UFL must equal
the underestimate in DFL. This implies that the error in QS
will be smaller than that in DFL.

IIIA3. Station in Dry Area - Calculation Done Over Wet Area

The next test will be to assume that the hourly reports
of temperature and dew point are received from a station located
in the dry land region. The calculation of turbulent fluxes
over the dry area will use the air mass characteristic of that
area. However, the screen temperature used for energy budget
calculations over the wet area will be too high and the dew point
value too low,while DFL is too high. Table 10 compares the
energy budget over the wet surface using air from the dry area
against using the air characteristic of the wet surface. All
values are daytime totals using the same initial atmospheric con-
ditions as before with clear skies.

Table 10.   Energy Budget Terms   (Calories cm^{-2} daylight hours^{-1})
Over Wet Land Compared to Those Using Station From
Dry Land Area.

	SGA	DFL	UFL	QS	QE	QS+QE	FG
Real Values	685.4	489.4	631.4	112.3	406.0	518.3	-25.0
Station Over Dry Area	685.4	499.4	643.5	63.2	451.0	514.2	-27.2

Figure 13 compares the QS and QE terms and the ground temperature
calculated with the actual conditions over the wet area (solid
line) to those using the air mass from the station over the dry
section (dashed line). The air temperature from the station is
too high which leads to a smaller gradient of temperature if the
actual ground temperature is used. This leads to an under-
estimate of QS and would have the same tendency for QE. However,
the dew point from the station is too low which leads to a
greater gradient of water vapour if the actual ground tempera-
ture is used. This has the opposite effect on QE, one of over-
estimation. Since the downward longwave radiation calculated
from the sounding at the station is too great, the total of the
outgoing terms, (QE+QS+FG+UFL), must be overestimated. This is
attained by an overestimate of ground temperature. Not only
will this enhance the water vapour gradient and hence QE, but
also it will increase UFL and FG such that a balance occurs.
QS is underestimated by 44%,while QE is overestimated by 11%.
QE + QS is underestimated by only 4%. The errors in the individual
terms can be most serious when the calculation is done over a

wet area, using data from a station in the dry area. This is because the error in temperature and dew point affect the QE calculation in the opposite way from QS. The results of these errors discussed in the above experiment are summed up in Figure 17.

IIIA4. <u>Portions of Different Albedo</u>

Although albedo variations will not be considered in this study, it will now be determined what magnitude of errors could occur if the two portions of land have different albedo rather than wetness.

The area of lower albedo will have greater values of QE and QS simultaneously. The air mass over this region will have both temperature and dew points which will be too high if used over the area of higher albedo. Both QE and QS will be underestimated over the section with higher albedo. Thus, ground temperature, UFL, and FG will be overestimated so that a balance is maintained between incoming and outgoing energy from the surface. When regions of surface wetness were considered and the calculation over the wet region was based on the air mass from the dry region, the error in QE was in the same direction as ground temperature, UFL, and FG, but opposite to that of QS. For regions of different albedo, QE error is in the same direction as QS; both are opposite to the errors in ground temperature, UFL, and FG. Hence, the individual errors of QE and QS will not be as large.

Figure 17. Comparison of Errors in Turbulent Fluxes when Using Unrepresentative Air Mass

Turbulent Fluxes Calculated over Area of Saturated Soil

Sensible Heat Flux Calculated over Area of Dry Soil
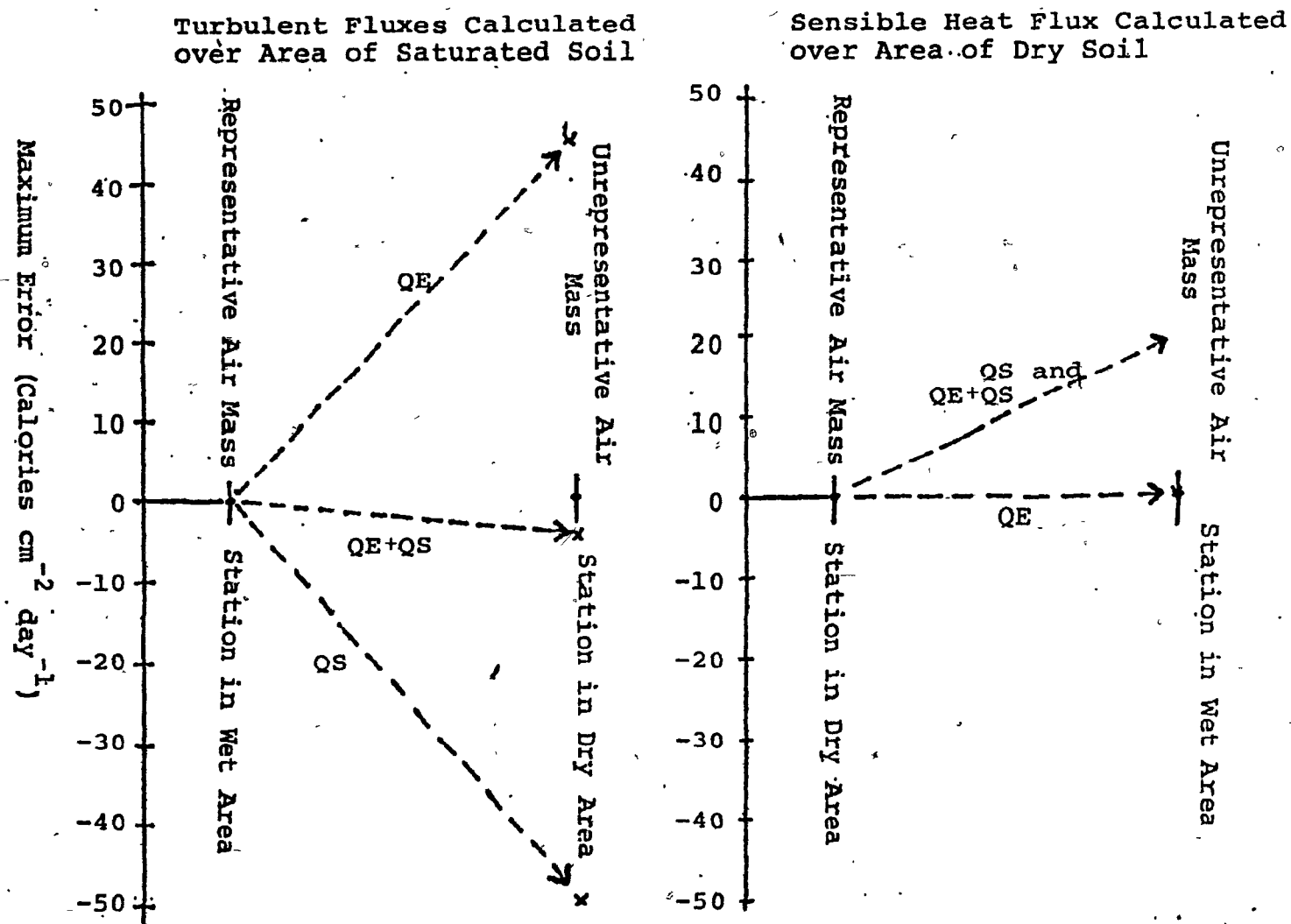
IIIA5. Change in Error When Residence Time of Air Over
        Characteristic Portions is Changed

The above section studied the maximum effect of temperature and dew point variations, due to surface variations, on the calculation of turbulent fluxes. The air masses were considered to remain over the same characteristic land type for at least the daytime (16 hours). In order to satisfy this residence time, each characteristic portion must be about 140 km wide with light winds of 5 kt. In other words, the areas must be of synoptic scale (at least one station will lie in each characteristic area) to produce the air mass differences which lead to the errors discussed above. However, the concern in this project is the air mass differences generated by characteristic areas small enough to lie between observation stations. The effect of air mass differences on the energy budget calculations will now be considered using characteristic areas with smaller residence times.

Calculations of the energy budget are done again at a point over wet ground. However, the area of wet ground is considered to be surrounded by an infinitely large area of dry ground, such that it constantly receives the air mass from the dry area (a wet oasis). Table 11 contains the energy budget terms for various residence times of air over the wet area:

Table 11. Energy Budget Terms (Calories cm^{-2} daylight hours^{-1})
From Wet Land Surrounded by Dry Land

RESIDENCE TIME	LENGTH (5kt wind)	SGA	DFL	UFL	QS	QE	QS+QE	FG
.0 hr	0 km	685.4	499.5	643.5	63.2	451.0	514.2	-27.2
2 hr	18 km	685.4	498.1	641.0	69.7	446.1	515.8	-26.7
3 hr	27 km	685.4	497.0	639.6	72.7	443.6	516.3	-26.4
16 hr	144 km	685.4	489.4	631.4	112.3	406.0	518.3	-25.0

The calculations were done for 16 daylight hours of clear skies, beginning with the same sounding as in previous experiments. The residence time of 0 is equivalent to an infinitely small wet oasis continuously receiving air which is modified by the fluxes from the surrounding dry soil. The terms in this row are exactly those presented in IIIA3 of this chapter. That is, they are the calculations, from wet soil using temperature and dew point observations from a station over dry land. The other rows represent calculations of the surface energy budget considering the modification of the dry air mass as it flows over a larger wet oasis. When compared to the quantities from the first row in the above table, we find the maximum error possible in calculating the energy budget over the wet area if temperature and dew point data are used from a dry area. These are presented in Table 12.

Table 12. Maximum Error in Turbulent Terms From Wet Area

RESIDENCE TIME	0HR	2 HR	3 HR	16 HR
Length (5kt wind) km	0.0	18	27	144
QE - Calories	0.0	4.9 (1.1%)	7.4 (1.7%)	45.0 (11%)
QS - Calories	0.0	-6.5 (-9%)	-9.5 (-13%)	-49.1 (-44%)
(QE+QS) - Calories	0.0	-1.6	-1.9	- 4.1

When the residence time is reduced by 1/8, the maximum possible errors in the turbulent flux terms decreased by about the same proportion.

It is rather unlikely to find only one oasis between meteorological stations. More likely, one expects an arrangement of a number of wet and dry areas. As a final test, the same experiment is run, except that the oasis will be surrounded by an infinite area of interspersed wet and dry sections of the same size. In this way, the air reaching the wet area under consideration is modified by the turbulent fluxes from both land types. The experiment compares the daytime (16 hours) turbulent flux quantities from the oasis for various residence times in Table 13.

Table 13. Turbulent Fluxes (Calories cm^{-2} daylight hours^{-1}) From Wet Land Surrounded by Wet and Dry Areas

RESIDENCE TIME	1 HR	2 HR	3 HR	4 HR	6 HR	8 HR	12 HR
Length (5kt wind)	9 km	18 km	27 km	36 km	54 km	72 km	108 km
QE - Calories	470	470	468	466	463	457	439
QS "	85.4	85.5	85.6	89.4	93.2	101	118
QE+QS "	555	555	554	555	556	558	557

These results are also plotted in Fig. 18. Note that the flux totals approach a nearly constant value as the residence time decreases to 1 hour. It is assumed from this that if the residence time would be reduced to zero, the total values will be unchanged from the 1 hr figures. The change from these values to those with 4 hr residence times is only 4 calories, a very small maximum error considering the magnitude of the quantities. It appears from these results that if the residence time is less than 4 hrs, the air does not stay over single characteristic areas long enough to develop differences in temperature and dew point which are great enough to affect the calculation of the energy budget over wet areas when the meteorological station is located over a dry spot. The temperature and dew point over each area are plotted in Fig. 19 for both 1 HR and 12 hr residence times.

Figure 20 gives the residence time as a function of both wind speed and area of characteristic land blocks. To satisfy the residence times of less than 4 hours with light winds of 2.5 m sec^{-1} (5 kts), the areas must be no greater than 36 km in the direction of wind flow.

In using the meteorological stations to provide temperature and dew point for the grid points in between, the wind speed, size and distribution of wet and dry areas should be considered when analysing possible errors in turbulent flux terms at these points.

Figure 18. Turbulent Fluxes From Alternating Areas of Saturated and Dry Soil as a Function of Residence Time of Air Mass over Each Area

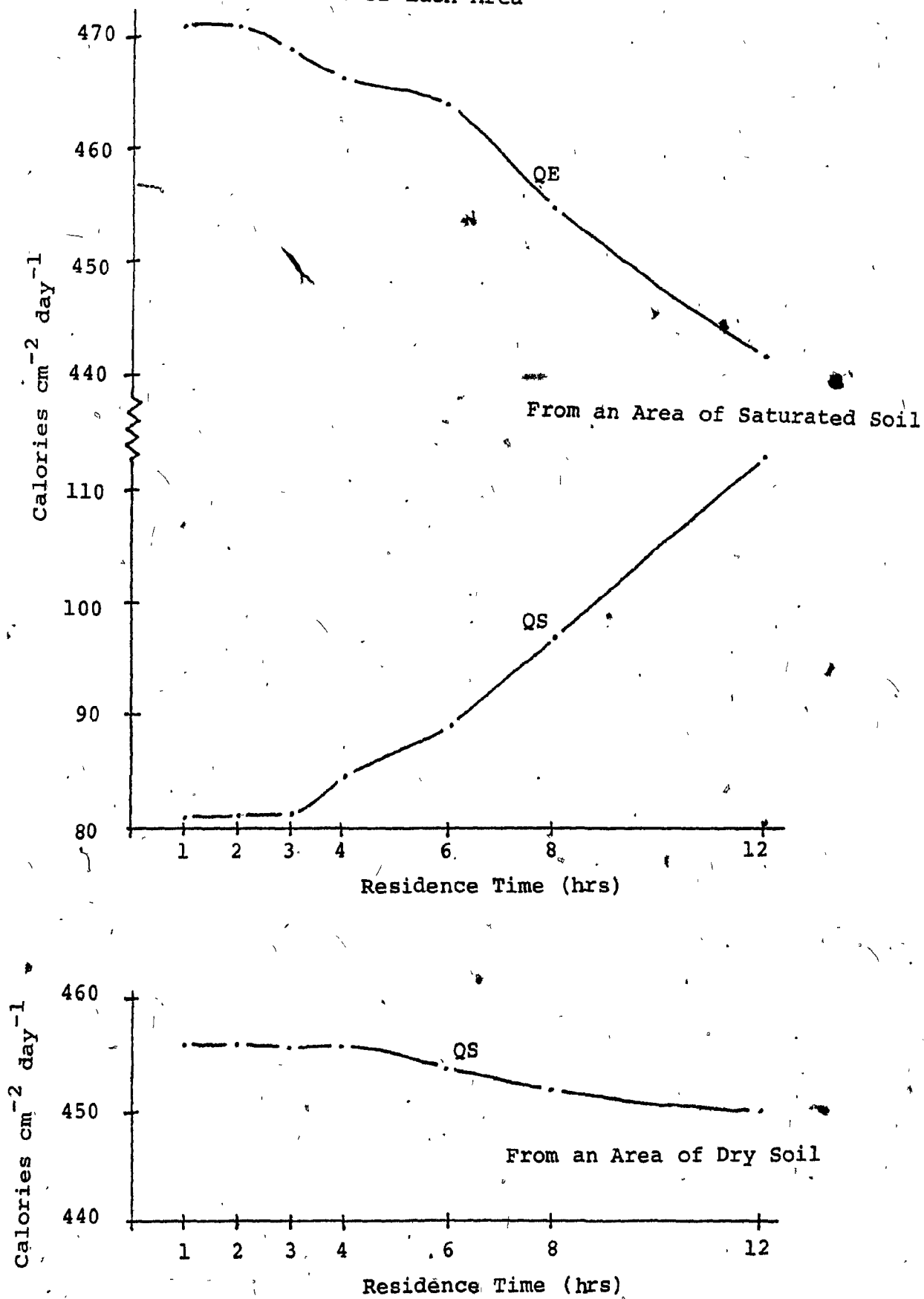From an Area of Saturated Soil

From an Area of Dry Soil

Figure 19. Comparison of Air Mass when Residence Time is Varied Over Alternating Areas of Saturated and Dry Soil: Residence Time   Air Mass 1 – Initially Over Dry Soil
——— 12 Hours   Air Mass 2 – Initially Over
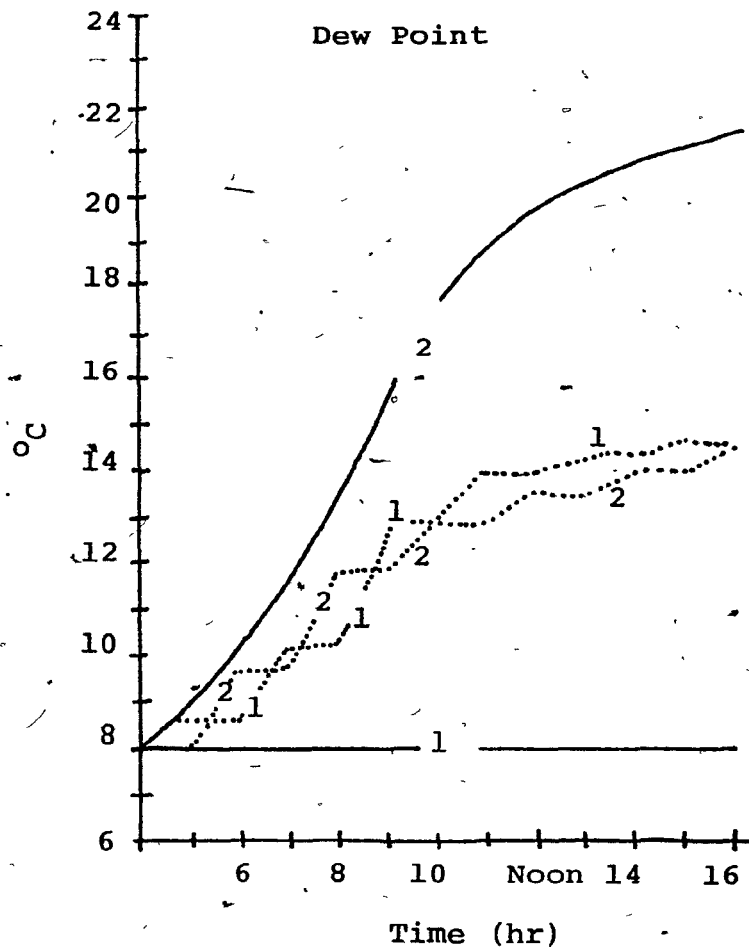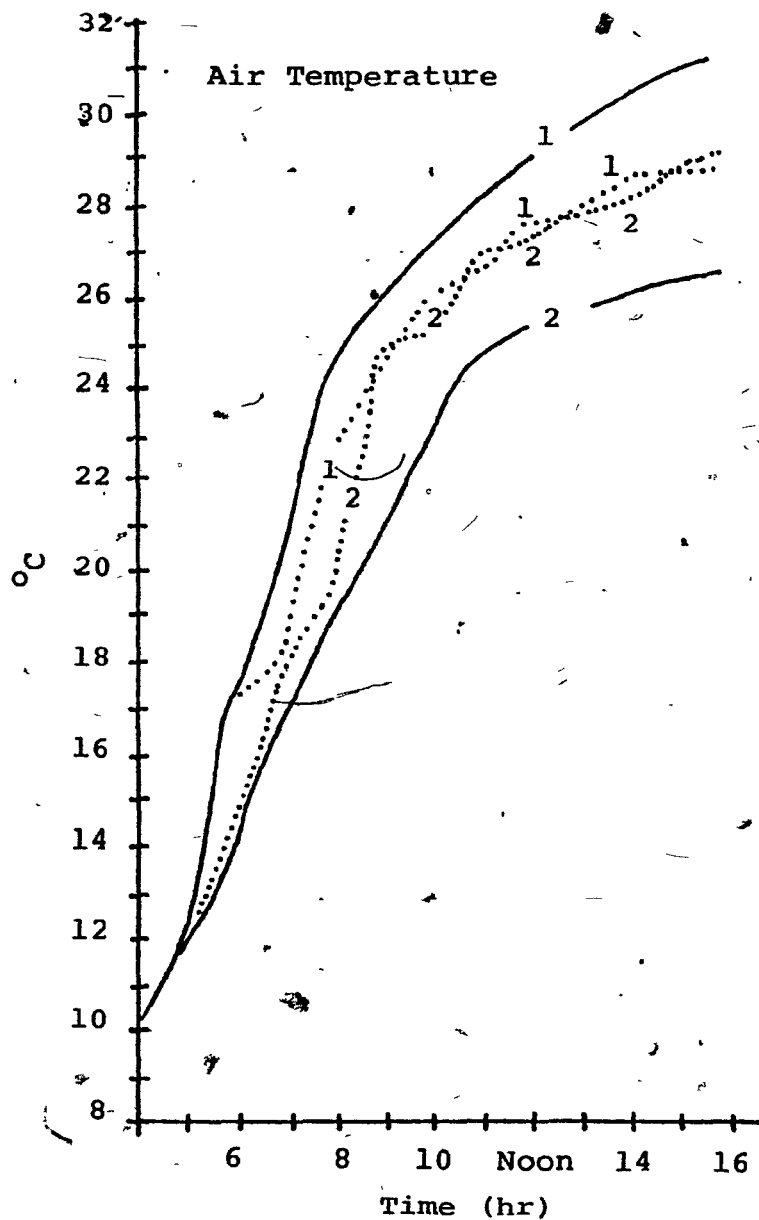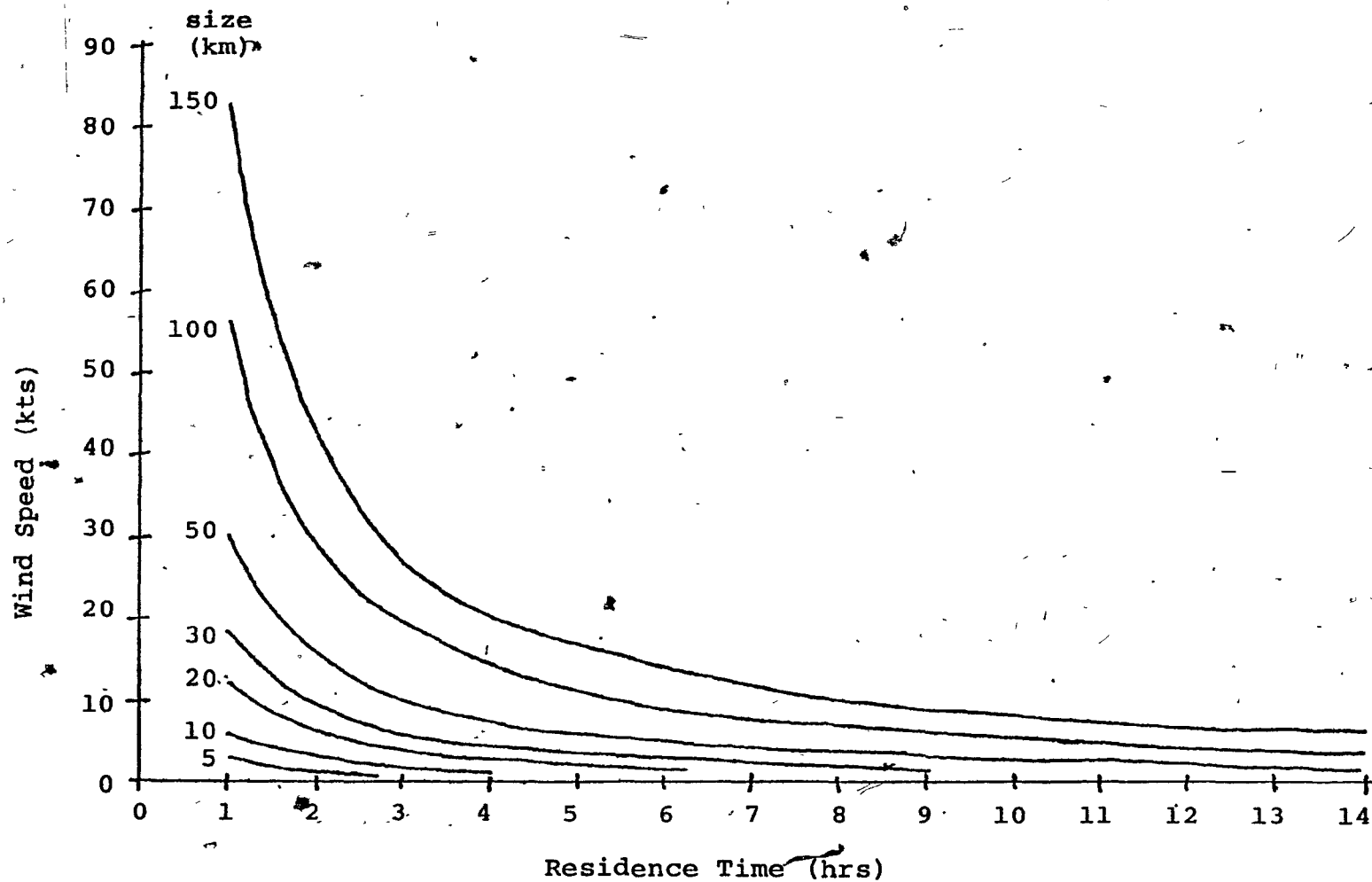·········· 1 Hour   Saturated Soil

Figure 20. Residence Time vs. Wind Speed
For Areas of Variable Size

IIIB. Pressure, Wind, Cloudiness, and Rainfall

IIIB1. Pressure

Pressure variations over areas of subsynoptic extent generally are not very large in magnitude. Violent thunderstorms are attended by pressure fluctuations of several mb over mesoscale areas (Fujita, 1955). However, the systems usually move rapidly for their size, that is, the [diameter/ speed of motion] is smaller than for synoptic systems. Thus, the spatial variation in pressure over a subsynoptic area is smoothed out over a time period of one hour. More important spatial differences can occur from topographical variation. The topography of a region is known, so pressure may be adjusted for height. The area under study is flat so the elevation does not vary by more than 100 m. The maximum adjustment to sea level of a synoptic station pressure measured at 100 meters ASL is about 8 mb. An error of 5°C in determining the temperature at a point (used with elevation to adjust pressure to another height) would result in an error of only .1 mb in the 8 mb adjustment. How these errors in pressure will affect the energy budget calculations will now be examined.

The determination of vapour pressure or absolute humidity for a given temperature and dew point is also dependent on the pressure, thus the sensitivity of a calculation of QE is checked against pressure. For T surface = 40°C, T air = 20°C, dew point = 15°C, the pressure was varied by 10 mb (T = temperature):

P	1000	990
QE	190.1	192.1

Thus, even a violent thunderstorm can only affect the evaporation calculation slightly if synoptic stations are used to determine the pressure in the subsynoptic scale.

IIIB2. Wind

Lee (1972) has demonstrated the effect of changing the wind speed on various energy budget terms while keeping all other input factors constant. This was done for a day with maximum solar energy received. As the wind was increased from zero, little change took place until the wind exceeded 4 m sec^{-1} (8 kts). Until then, convective turbulence was assumed dominate in vertical transfer of the turbulent terms. This range is of course dependent on the magnitude of the temperature gradient, which also depends on the amount of shortwave energy available. When the wind was increased above this range, QE was found to increase and QS decrease steadily. Here, the mechanical mixing by the wind is assumed dominant. The calculations made in this study are based on experimental results of Malkus (1962). The results of varying wind speed and temperature on QE and QS for a given dew point of the air are shown in Fig. 3. For any gradient value, there is a critical wind speed above which the fluxes depend on the wind. For example, the critical wind speeds of 5.0 and 7.0 m sec^{-1} correspond to gradients of approximately 7 and 10°C respectively (obtained from Fig. 3). Clearly, the critical wind speeds are proportional to the gradient. Thus, errors in wind speed will likely be of little consequence on clear days when fluxes are of highest magnitude. On the other hand, when the radiation balance is small and positive, the same

error in wind speed will affect the calculation but the fluxes
will be quite small in such cases so that the total error can
only be small in relation to fluxes on clear days. Note that
when the radiation balance is negative, associated with negative
gradients at night, an error in wind speed can have only a
very small effect on the turbulent fluxes.

IIIB3. Cloudiness

The amount, type, and height of clouds are used to
determine the incoming shortwave radiation at the ground, SG,
and the longwave downward radiation, DFL, which are very critical
in determining the energy available for the turbulent fluxes.
A true representation of the effect of cloudiness on these terms
at a point on the earth's surface is impossible since the exact
position of the clouds in the sky is unknown from cloud reports
at a station. For example, if 5/10 ths of the sky is reported
to be cloud covered, the DFL term will be greatest if the clouds
are near the zenith while SG will be greatest if the sun is
shining through a clear spot in the sky. In all calculations
of SG and DFL, it is assumed that the direct effects of over-
cast conditions will be felt over a portion of an area propor-
tional to the fraction of sky covered by cloud, while the effects
of clear sky will be felt over the remainder of the area. This
is only correct for an area averaged over a certain length of
time, that is, it is only statistically the case. The parameteri-
zation of cloudiness will be discussed in more detail in the
next chapter.

It must also be realised that local variations in cloud amount are present between the reporting stations and in fact can be the result of local variations in the turbulent fluxes. For example, more clouds may form over moist spots on a certain day,and the omission of this fact will cause the solar radiation to be overestimated there . An overestimate of turbulent fluxes will then be made over these moist areas. It was felt that parameterization of cloud formation was too uncertain. However, radar information available over the area will be of some use in determining local areas of cloudiness. The cloudiness at grid points not receiving precipitation will be a statistical average as determined from station reports,and will not give the true quantities of incoming radiation on areas represented by the points.

IIIB4. Rainfall

One must consider the minimum spatial resolution of rainfall data necessary for this study. The resolution chosen need not be finer than the resolution of ground parameters used to determine infiltration of water into the ground. It is this latter quantity which is important to determine soil saturation, of prime importance in this study. Present techniques of determining infiltration are empirical and do not warrant fine resolution since only a few variables are used to give gross approximations of a watershed's capability to infiltrate water. Results from a method by Lee (1972) are used in this study,where infiltration is taken as a function of rainfall rate, runoff length, slope, roughness of the surface, and infiltration

capacity of the soil. However, even if infiltration could be resolved more accurately and over smaller areas, the improvement gained by increased spatial resolution of rainfall will be limited since runoff tends to offset the effect of very small scale rainfall variation in terms of actual infiltration. That is, infiltrated water over a small area will be known directly from spatially averaged rainfall over the area, because of runoff of surface water from areas of heavier rain to areas with less rain.

It is apparent from the reasons discussed above that it is not necessary to obtain radar data with a resolution finer than individual shower cells, the scale of turbulent flux variations with which this study is concerned. The standard 5.85 km diameter squares of averaged precipitation from the McGill Radar in Ste. Anne de Bellevue will be utilised. The average precipitation determined for these squares are based on averaging of smaller areas. Precipitation rates are determined from echo intensity using a correlation between rainfall rates and radar reflectivity, based on raindrop size distributions measured by Marshall and Palmer (1948). The accuracy of such methods are most limited for heavy precipitation rates. This is however not of great concern to the energy budget calculations of the length of time used in this study. First, infiltration rates cannot be determined accurately. Second, areas receiving heavy precipitation will have enough water stored in the ground to maintain potential evaporation for the duration of the period. This will be the case for a large range

of precipitation, such that a large error may not be felt.
Rainfall is the only meteorological parameter available on
the subsynoptic scale.

CHAPTER IV

ENERGY BUDGET CALCULATIONS OVER A SUBSYNOPTIC AREA

The surface energy budget is calculated over an area of about 8×10^3 km^2 southwest of Montreal, lying between the Ottawa and St. Lawrence Rivers. The area was chosen because it has the flatest topography of any area within range of the local radar. It is hoped then, that precipitation will not be influenced by orographic effects since this investigation deals with the influence of turbulent flux variations on precipitation. Individual calculations will be made at points separated by a distance smaller than the diameter of convective precipitation; their spacing will be 5.85 km. The time steps will be one hour long in order to utilise the available observed meteorological data. Calculations are carried out for a one-week period, including 3 days of precipitation. Given the following set of input conditions, the results are analysed for variations in turbulent fluxes.

IVA. Ground Parameters

The period chosen, from 2 to 8 July, 1975, followed a two-week period of clear weather. From the discussion in the previous chapter, areas covered with vegetation of shallow rooting systems will have no available water for evaporation at the beginning of the period, on July 2. The roots must be less than 30 cm (1 foot) deep if the ground was assumed saturated before the two-week drought.

IVA1.   Soil Type

The soil predominant in each area of the grid was deter-
mined from the Soil Capability for Agriculture maps, Canada
Department of Agriculture (1966). From examinations of finer
resolution soil surveys, United States Department of Agriculture
(1958), it is clear that each grid area actually contains many
smaller areas of different soil types. However, most of these fit
into the general soil classification given by the soil capability
maps. Each soil was fit into a range of four soils classified
by texture. The soil types are numbered from the most coarse
(fine sandy loam): 1, to the most fine (clay or loam): 4.

IVA2.   Soil Layers

The soil profile contains 6 layers, each 10 cm deep.
It is assumed that of direct evaporation from the soil top,
75% comes from the first 10 cm, 20% from the second layer, and
5% from the third layer. This distribution is really of little
concern since it was seen in Chapter II that direct evapora-
tion is very small compared to transpiration from plants.

The water holding capacity is defined here as the
available water for evaporation, and is given in Table 14 for
the various soils. Also included is the rooting depth of
shallow rooting crops, defined by Thornthwaite and Mather as
spinach, peas, beets, and carrots. It is assumed here that the
major agricultural crops of the area to be studied, young corn
and grain, will have similar rooting depths in early summer.
The total water available in the root zone is obtained for the
various soils, Thornthwaite and Mather (1957). This information
appears in Table 14.

Table 14. Available Soil Water to Root Zone

NO	SOIL TYPE	WATER HOLDING CAPACITY cm cm^{-1}	ROOTING DEPTH cm	AVAILABLE WATER FOR TRANSPIRATION cm
1	Fine Sandy Loam	.15	50	7.5
2	Sandy Silt Loam	.20	62	12.5
3	Clay Loam	.25	40	10.0
4	Clay	.30	25	7.5

It is noteworthy that the combination of water holding capacity and rooting depth leads the medium texture soils to have the most water available to the root systems of these plants.

Next, the above information is used to determine the water holding capacity of each 10 cm layer, BW, and the proportion of roots in each layer, FP. The roots are considered to be evenly spaced in the vertical, as discussed earlier. BW and FP are presented in Table 15 for the various soils.

Table 15. Appropriation of Root Zone

SOIL NO	Each Layer BW - cm	FP 1st Layer	FP 2nd Layer	FP 3rd Layer	FP 4th Layer	FP 5th Layer	FP 6th Layer
1	1.5	.20	.20	.20	.20	.20	0
2	2.0	.16	.16	.16	.16	.16	.16
3	2.5	.25	.25	.25	.25	0	0
4	3.0	.40	.40	.20	0	0	0

IVA3.   Vegetation Type and Amount

Each grid area was assumed to contain a fraction of the following land types:

a) CROP - These are land areas determined as non-forested from topographical maps, Canada Department of Energy, Mines and Resources (1974). They are chosen to represent the areas of shallow rooted crops with the above available water for transpiration from the various layers, depending on soil type. In order to investigate the extreme variation in turbulent fluxes possible in such a region, it is assumed that these regions will have no water storage in the root zone at the start of the calculation. That is, the saturation level of these layers is set to zero, initially. The parameter of vegetation amount is taken as leaf area index of 2 and the albedo is .20.

b) FOREST - These are delineated by green shading on the topographical maps. They are assumed to have a sufficiently deep rooting system to maintain potential transpiration of water stored deep below the surface. These areas will maintain potential transpiration through the entire one-week period. The leaf area index, BLA, is taken as 6, with an albedo also of .20. The soil below the vegetation stand is considered to be covered by 2 units of leaf area index of dead vegetation matter which can also interrupt water and shortwave energy before reaching the ground.

c) WATER - Only a small area of the entire region is covered by water. Most of it includes the major river systems, although there are a few small lakes. It was not felt

warranted to spend an extra calculation at each grid point on the energy budget of water surface, as it would not differ greatly from the wet land or forest area if the water is sufficiently shallow. Hence, the water areas were included as additional fractions of forest.

Calculations of the energy budget were done separately for crop and forest at each grid point. The turbulent flux terms from each surface are combined in the ratio of the areas comprising each grid point.

IVA4. Elevation, Slope, and Runoff Length

a) ELEVATION - This parameter will be used to adjust temperature and pressure to a common height for all grid points, which will be discussed later. The values are read off the topographical maps of the region at each grid point to an accuracy of about 30 meters. Fig. 21 represents the elevation of the area under consideration.

b) SLOPE - This parameter is used to determine runoff using the method of Lee (1972). The maximum slope from the resolution of the topographic map was determined across each grid square. The slopes are expressed as the fraction of change in elevation divided by horizontal distance. For the area studied, the range of slopes were from .003 to .026 corresponding to 20 to 200 meter change in elevation for a horizontal distance of 5,850 meters. However, for the most part, the slopes were found at the shallow end of this range. Since the area is likely to contain steeper slopes of a scale too small to be resolved on the map used, it is believed that this

Figure 21. Elevation (m)
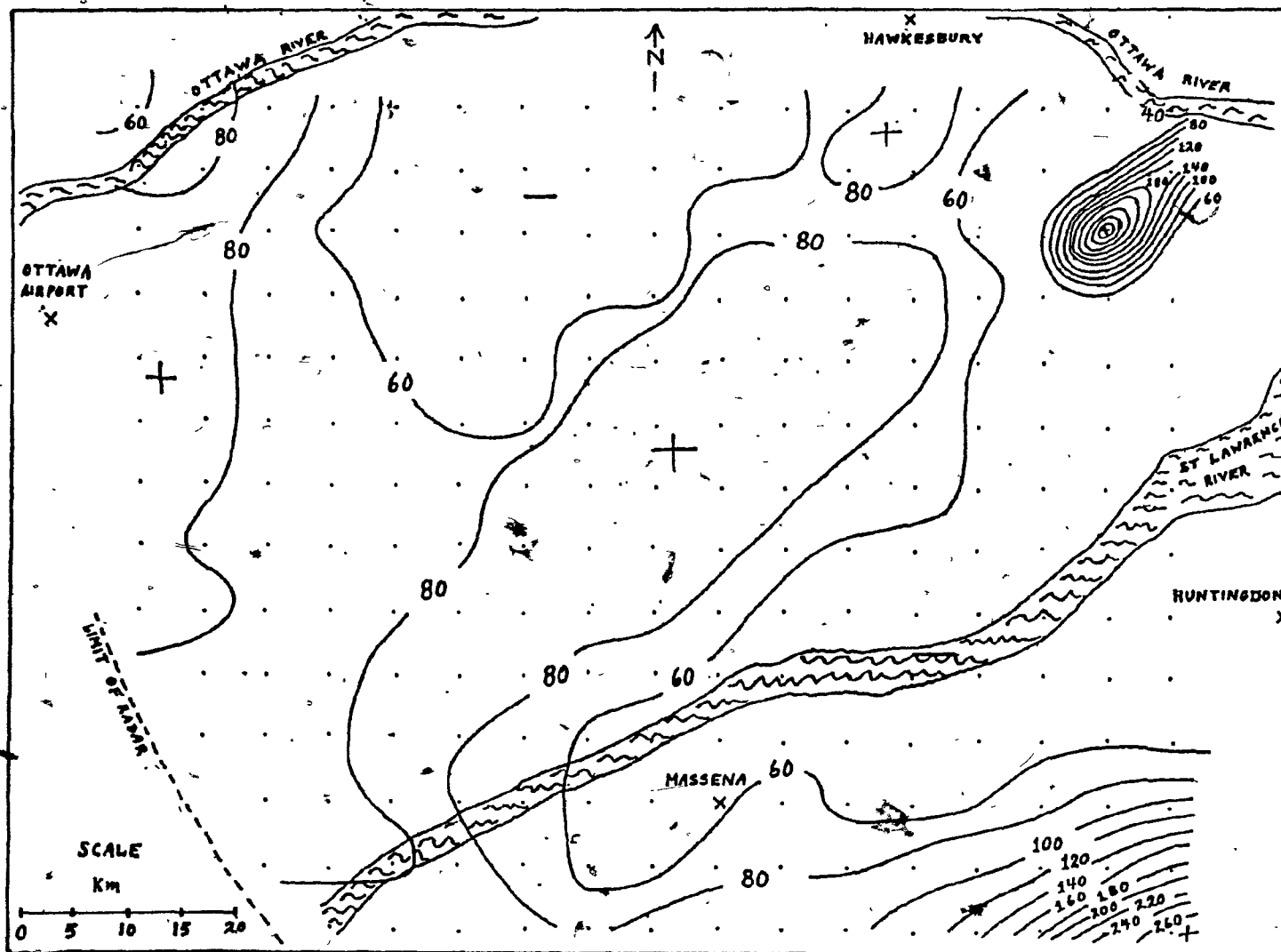
LEGEND

+ Relative Maximum
− Relative Minimum
. Grid Point
X Reference Point

parameter was generally underestimated. The effect will be to underestimate runoff.

c) RUNOFF LENGTH - This is another parameter used to determine runoff and is defined as the distance water can flow along the ground from elevation ridges to troughs. It is the length which water may be infiltrated into the ground before flowing into a channel or stream. It was taken from the map as half the perpendicular distance between adjacent streams. Since all troughs are not resolved, this parameter will also be overestimated. The result of this will as well be to underestimate runoff, because infiltration is overestimated.

IVB.   Meteorological Parameters

The value of each meteorological parameter used at a grid point is obtained in the following manner. There are three meteorological stations which report the parameters on an hourly basis: Montreal, Ottawa, and Massena. The value at a grid point is extrapolated from these three observations, weighing the importance of each by their distance from the point. The method used is taken from Pugsley (1970). The extrapolated value must fall within the limit of the three values observed.

IVB1.   Screen Level Temperature

Also known as surface temperature, their reported values at the stations are first adjusted to sea level using the gradient between this temperature and the 975 mb temperature from the radiosonde. However, the dry adiabatic lapse rate is never exceeded. Next, these adjusted temperatures are extrapo-

lated to the grid point in question, using the method cited above. Finally, this temperature is readjusted to the height of the point.

IVB2. Dew Point

The screen level dew points measured at the three stations are extrapolated to the point in question. No adjustments are made for elevation.

IVB3. Wind

The surface wind reports measured at the three stations are extrapolated directly to the point in question.

IVB4. Station Pressure

The station or surface pressures reported at the three stations are adjusted to sea level using the hydrostatic approximation with the temperature of the 'added layer' of atmosphere equal to the average between the surface and 975 mb level. The sea level pressure is then extrapolated to the point in question. Finally, this pressure is adjusted to the elevation of the point using the same procedure.

IVB5. Sounding

The soundings from Albany, New York and Maniwaki, Quebec are averaged and used as the base radiosondes for the entire grid. Each base radiosonde is used for a 12 hour period, six hours before the observation of the upper air to six after. Shortwave clear sky radiation, SGC, is calculated from such soundings, considering absorption of energy from

space by water vapour and CO_2 based on equations from Bailey (1965). The value of SGC is considered constant over the entire grid for a given time. The maximum variation of SGC at noon over seven days is about 5%. The change in SGC is quite small as the radiosonde varies from day to day, hence it is highly improbable that the spatial variation of SGC is significant for any instant in time.

For purposes of longwave calculations, the sounding is modified from point to point, each hour, in the following manner. After the surface temperature, dew point, wind, and pressure are determined at the point in question, the surface temperature is checked against the base radiosonde surface temperature. If warmer, the higher levels of the radiosonde are warmed such that a dry adiabatic layer is formed to the level of pressure where the dry adiabat becomes less than or equal to the base radiosonde temperature. This level is then taken as the height of thermal mixing. The surface dew point determined at the point is used to calculate the surface mixing ratio. This mixing ratio is considered constant with height up through the layer of thermal mixing. Although such complete mixing does not always appear in evening radiosondes, the findings of Schaefer (1975) show that such is nearly the case during periods of maximum surface heating in Oklahoma. If the surface temperature at the point is lower than the surface temperature from the base radiosonde, then the height of mechanical mixing is determined as a function of wind speed, as in CLOE. The temperatures between the mixing height and the surface are cooled,

such that a constant gradient exists through the mechanical mixing layer. Again, pressure levels within this layer are set to dew points which correspond to the mixing ratio determined from the surface dew point and pressure at the point.

IVB6.   Cloudiness

Hourly information of cloudiness is obtained from surface aviation weather reports. Cloud amount, base height, and cloud type are given for as many as three visible layers, with the exception of Massena which does not report cloud type. Cloud amount is reported to 1/10 accuracy, with the exception of Massena which reports to the nearest 1/4 of sky covered. Cloud type at Massena has been taken as that of the Canadian stations reporting clouds near the same height at the same time.

Cloud bases and amount are determined at a grid point by extrapolating these parameters from stations reporting the same cloud type. The cloud base levels and amounts at these levels are used for longwave calculations. Depletion of shortwave radiation is calculated, using Table 16 of transmission due to various cloud types under overcast conditions. These figures are based on observations taken near Boston by Haurwitz (1945) and are statistical in nature.

Table 16. Transmission Under Overcast Conditions

CLOUD TYPE	LOW					MIDDLE			HIGH		
	St	Sc	Cu	Tc	Cb	As	Ac	Ns	Ci	Cs	Cc
Transmission Under Overcast Conditions	.25	.35	.35	.20	.10	.40	.50	.15	.85	.75	.75

The depletion is taken linearly as a function of cloud amount from zero under clear skies to [1 - Overcast Transmission] when overcast using the following equation:

1-Cloud amount fraction x [1-Overcast Transmission]

The calculation is done separately for each cloud type visible at one of the three stations and averaged in proportion to the fraction covering the celestial dome. The above represents a statistical average over space and time of the effects from cloudiness at each point, rather than the actual distribution for a given time.

If precipitation is reported at a point from the radar, it is assumed overcast with the transmission being a function of rainfall rates in a linear fashion from Table 17.

Table 17. Transmission as a Function of Rainfall Rate

	LIGHT RAIN	MODERATE RAIN	HEAVY RAIN	HEAVIER RAIN
Rainfall Rate (inches hr^{-1})	0 → 0.1	0.1 → 0.3	0.3 → 1.0	1.0 →
Transmission	.25 → .15	.15 → .10	.10 → .05	.05

Fig. 22 depicts the shortwave radiation absorbed by the ground over the area during the 7-day period. It has to be remembered that the incoming radiation is constant, as is the albedo over the area. The absorbed energy is seen to vary by about 10%, with lowest values in the north and highest in the south. This is a result of a difference in cloudiness. Variation in rainfall during daylight hours has some affect on the

Figure 22. Shortwave Energy Absorbed at the Earth's Surface, 2-8 July (Calories cm^{-2} week^{-1})
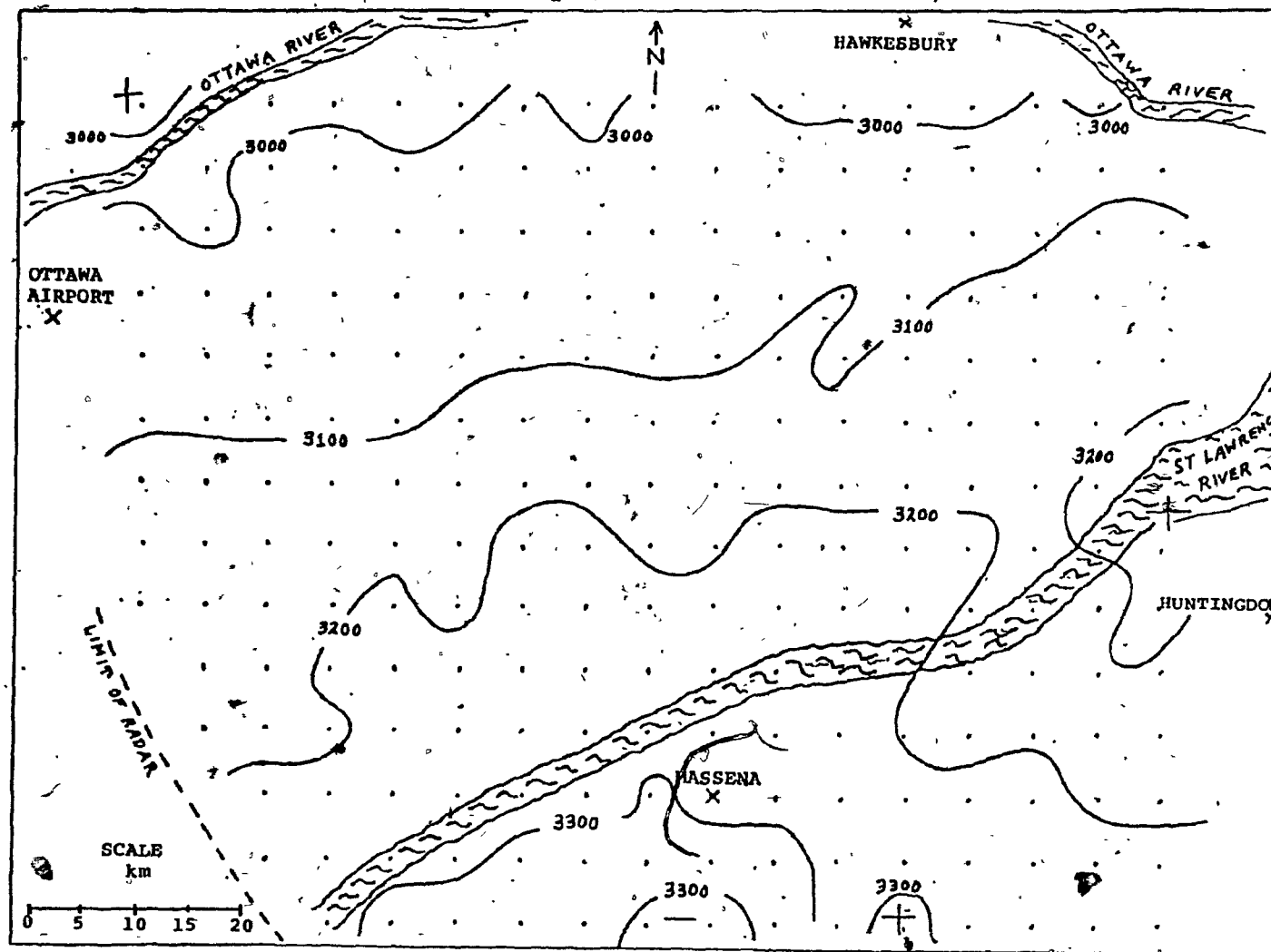
LEGEND

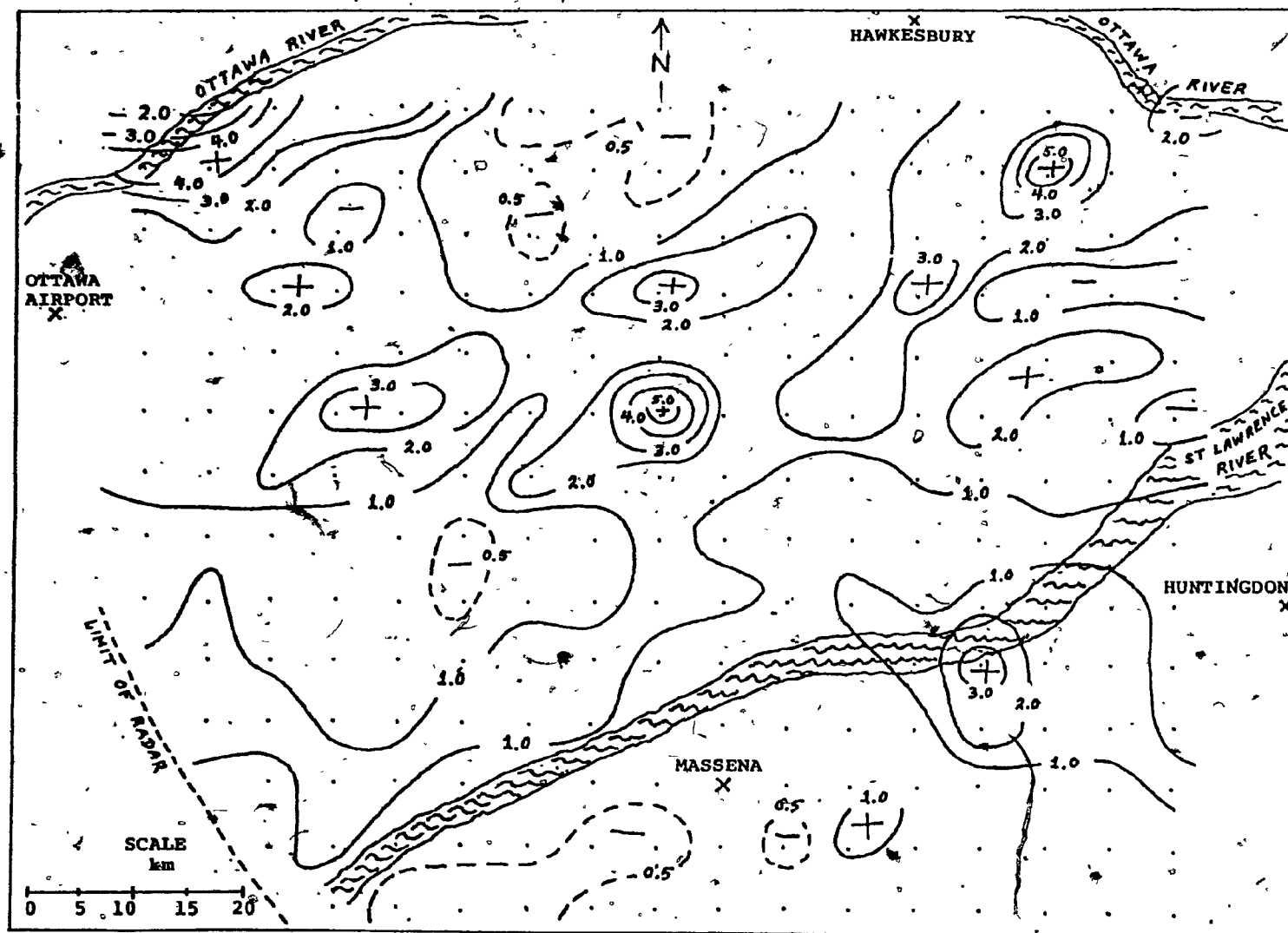+ Relative Maximum
- Relative Minimum
. Grid Point
X Reference Point

cloudiness calculations, and hence causes the small scale varia-
tions in SGA. However, the large scale variation in SGA from
north to south could not be due to the very scattered precipi-
tation pattern (Fig. 23). This must be the result of a con-
sistent minimum cloudiness reported from Massena in comparison
to Ottawa and Montreal, which are on a line to the north. If,
for example, middle clouds are reported (overcast transmission
= .50) and Massena reports .2 less cloud amount than the other
two stations, then the transmission will be .1 or 10% higher
at Massena. Since the cloud cover at Massena was only given
to the nearest .25 in amount, the variation in SGA over the
7-day period, of 10% seen in Fig. 22, is not likely to be real,
but rather due to the inaccuracy of the observations. This error
could present itself in turbulent flux maps to be presented
later as a 10% variation from one end of the map to the other,
but not over small distances.

IVB7. Rainfall

Hourly rainfall rates were gathered from records at
the Ste. Anne de Bellevue radar for grid squares 5.8 km in
diameter, corresponding to the grid points where the energy
budget is calculated. As mentioned earlier, the rainfall rates
are determined from their correlation to radar reflectivity.
The lowest height for which the radar reflectivity can be
obtained increases with distance from the radar. This is because
a horizontally directed radar signal travels in a straight
line, rather than following the curved path of the earth's surface.
This height of the signal above the surface at the grid point

Figure 23. Precipitation, 2-8 July (cm)

LEGEND

+ Relative Maximum
- Relative Minimum
. Grid Point
X Reference Point

furthest from the radar is 3 km. To be consistent for all points, the rainfall rates used are determined from reflectivity intensity at this height.

IVB8. Runoff and Infiltration

The runoff and infiltration rates are taken as a function of slope, runoff length, rainfall rate, infiltration capacity of the soil, and surface roughness, based on results from Lee (1972). The results from this method produced no runoff, even where maximum rainfall rates of up to 2.8 $cm\ hr^{-1}$ (~1 inch hr^{-1}) fell on relatively dry ground. It is believed that the runoff was underestimated since the slope was underestimated and runoff length overestimated. Too little runoff from rainfall on the first day could cause too great a soil moisture content later in the period. The time required for a change in turbulent fluxes due to soil moisture depletion was found to be directly proportional to the initial water available, X. Hence, the overestimation of this time will be directly proportional to the error in X, caused by an underestimation in runoff. The maximum rainfall to occur on a given day was 3 cm. If X is overestimated by 10% because of the neglection of runoff, the time at which QE becomes zero will be overestimated by only .4 days of the actual 4.2 days.

IVC.   Results

IVC1.   Potential Evapotranspiration

The results of the 7-day total of QE from the forest area are presented in Figure 24. Since it was assumed that an unlimited supply of ground water was available, the forest areas represent the potential latent heat flux. As with the SGA map, there is about a 10% variation in total QE over the area, but in this case the pattern is increasing from southwest to northeast instead of from north to south. Referring to Fig. 25, we see nearly the opposite for QS, i.e., it increases from NE to SW . It is unlikely that these patterns are mostly the result of the radiation pattern, because the two turbulent fluxes increase in nearly the opposite direction. From earlier analysis of turbulent flux calculations, it seems likely that the variations are due to the effects of a variation in surface dew point, temperature, or nightime wind.

Table 18 gives the 7-day average temperature, dew point, and wind for Ottawa, Montreal, and Massena.

Table 18. Average Temperature, Dew Point, and Wind for 7-Day
           Period.   (NIGHT = 1700 EST - 0600 EST)
                      (DAY = 0600 EST - 1700 EST)

	OTTAWA	MONTREAL	MASSENA
	Temperature (°C)		
NIGHT	21.5	20.4	19.4
DAY	25.6	25.0	26.9
	Dew Point (°C)		
NIGHT	13.9	16.4	14.8
DAY	14.7	16.4	14.1
	Wind (kt)		
NIGHT	3.2	6.2	2.8

Figure 24.   Latent Heat Flux From Forest, 2-8 July
(Calories cm^{-2} week^{-1})
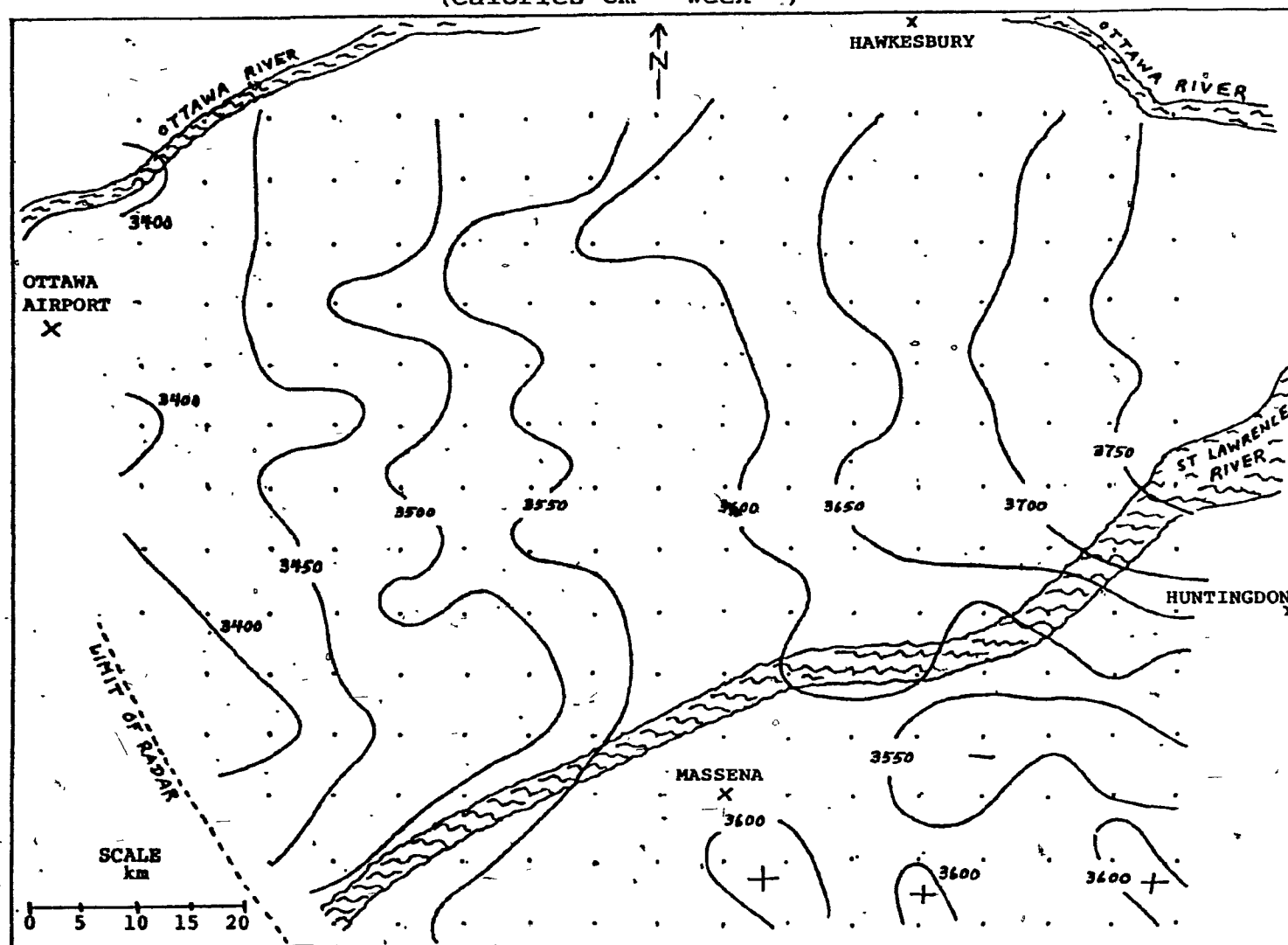
Figure 25.   Sensible Heat Flux From Forest, 2-8 July
(Calories cm^{-2} $week^{-1}$)
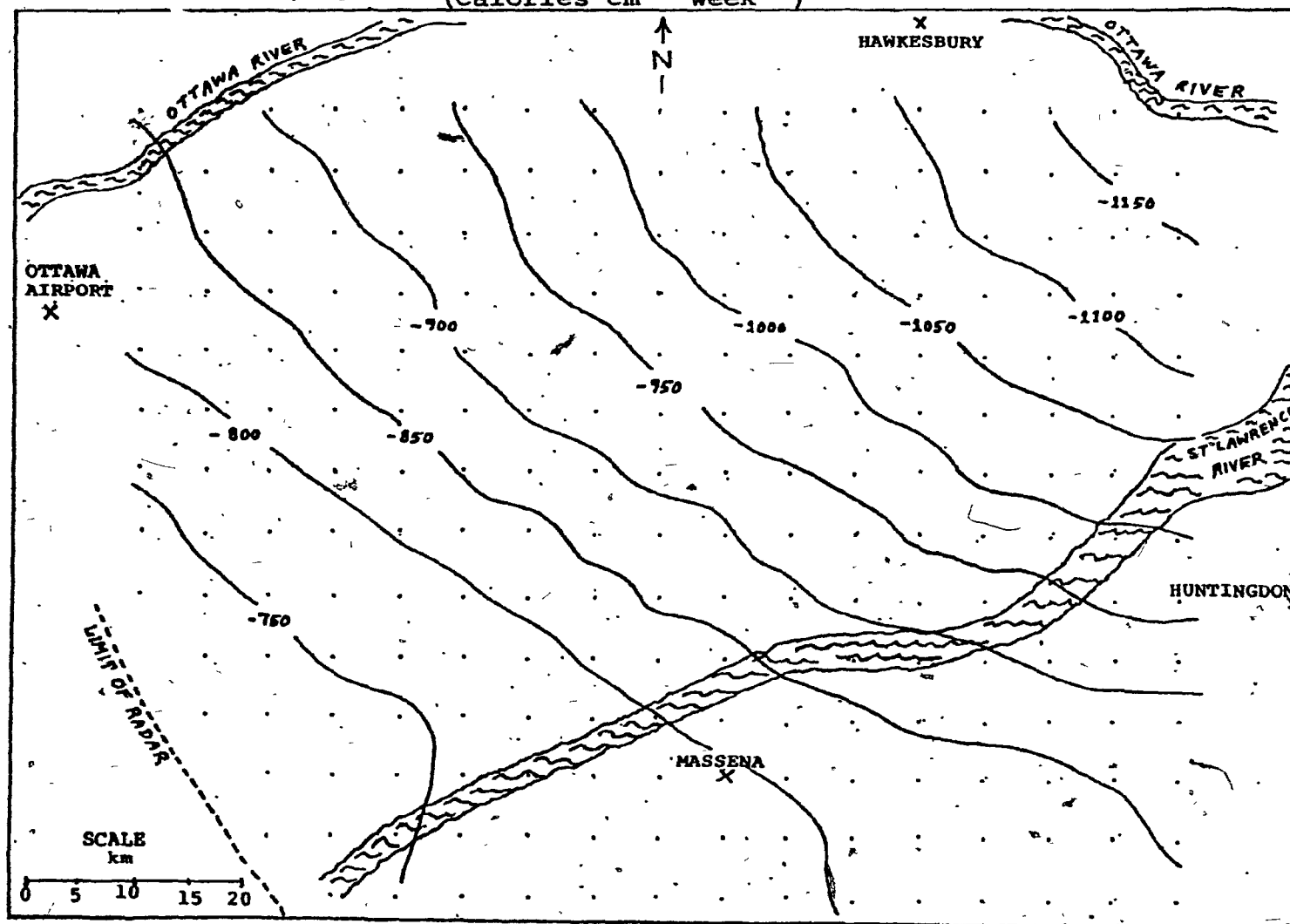
It is seen from Table 18 that the average daytime surface temperature at Ottawa and Montreal vary about .5 degrees, while the dew point is 1.7 degrees higher at Montreal. The wind at Montreal is almost twice that at Ottawa at night. The effect of the dew point and wind is to increase QE and decrease QS towards Montreal, as the results show. The lower temperature at Montreal could not account for the observed effect. From the following, it is clear that the temperature difference is not significant. If the 7-day total QE at a point with an elevation equal to 250 m is compared to one nearby with 60 m elevation, the total QE is nearly identical. This is the case despite the screen level temperature being nearly $2^{\circ}C$ different in the day due to the elevation difference, while the dew point and wind are nearly equal. From this, it must be concluded that the lower dew point and wind at Ottawa in addition to the SGA pattern seen in section IVB6 have caused the large scale variations in QE and QS.

IVC2. Evaporation from Cropland - QE for 7-Day Period

Since these areas were assumed to have no evaporation at the start of the period, the 7-day QE total from such areas will be highly dependent on the time and amount of rainfall. The 7-day QE appears in Figure 26. The results include the effects seen on the potential evaporation from the forest areas. A comparison of two extreme values in Figure 26 shows a variation from 125 calories (where .22 cm of rain fell and evaporated), to 1206 calories (where 2.19 cm of rain fell and infiltrated, of which 2.08 cm evaporated). These two points lie only 30 km apart. This variation of 1000 calories represents

Figure 26.   Latent Heat Flux From Crop, 2-8 July
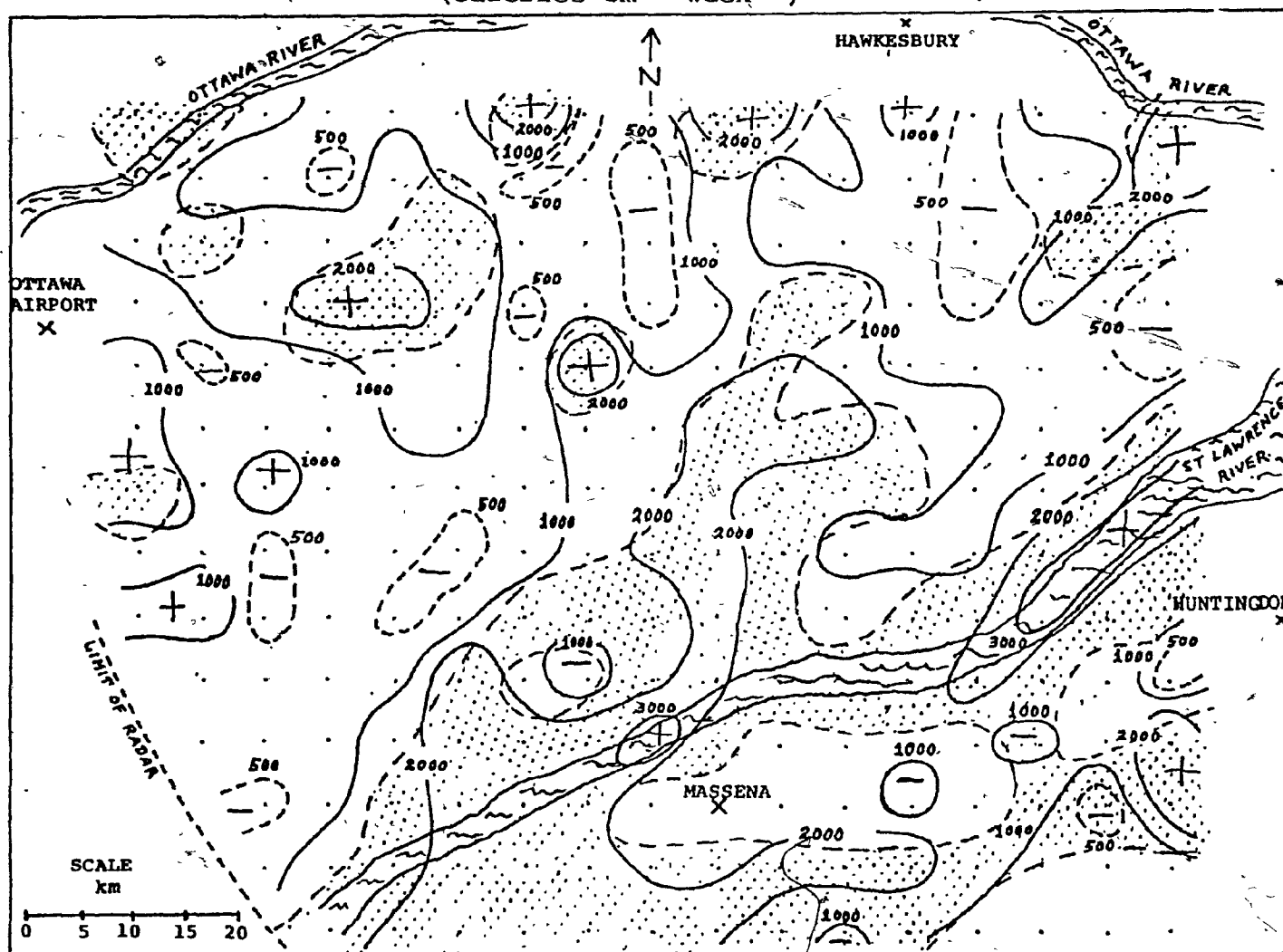(Calories cm^{-2} week^{-1})
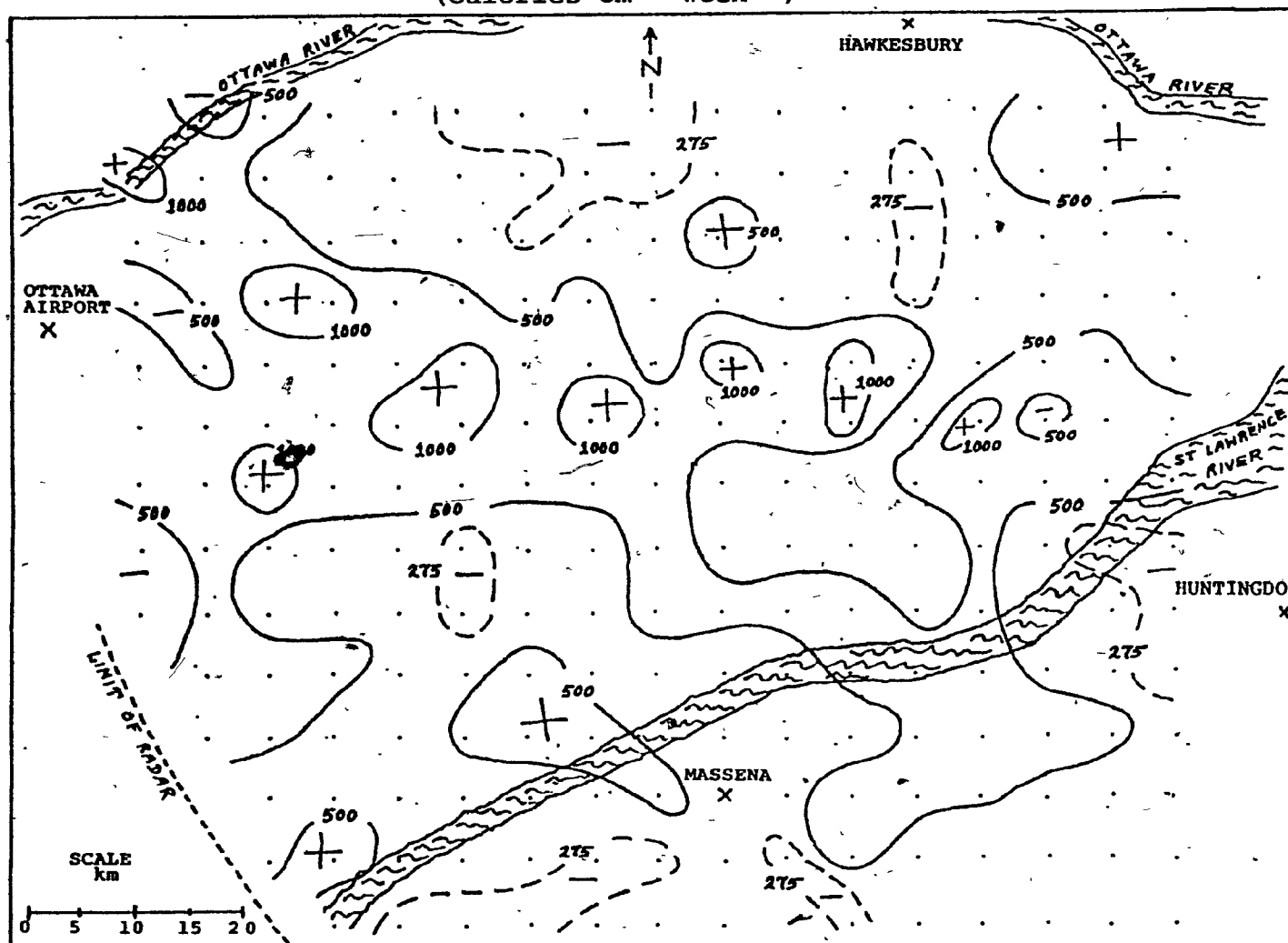
LEGEND

+ Relative Maximum
- Relative Minimum
. Grid Point
X Reference Point

28 % of the average potential transpiration from forest, about three times as great as the variations in QE due to differences in clouds, wind, and dew point between the stations, as seen in IVC1. Also, the variation is not a large scale one, it is related to the scattered nature of the 7-day precipitation shown in Figure 23. The map of QE from cropland shows the most extreme variation which would be expected over a dry area following the passage of scattered convective precipitation.

IVC3.   Average Transpiration from Mixed Crop and Forest

Outside of arid climates, the landscape usually contains some mixture of vegetation types. For simplicity, the energy budget was run with the two extreme land types previously dis- cussed at each grid point. To obtain the variation of the tur- bulent fluxes on the scale desired, the results from the two surface types at each grid point are averaged, with a ratio obtained from the fraction of each grid point area which is forested. The average values of 7-day total QE and QS appear in Figures 27 and 28, respectively. The stipled area represents the portions of the region assumed to contain more than 25% forest. The result is a complex mixture of the two separate land types combined with different ratios at each point, in other words, combined effects of rainfall and land types. For the most part, the higher evaporation values occur on areas of mixed or predominately forested areas. The variation of net QE and QS happens to be even greater than from a region of cropland alone. This is because the region studied contains areas of predominately cropland which happen to have virtually

Figure 27. Net Latent Heat Flux, 2-8 July
(Calories cm^{-2} week^{-1})

Figure 28. Net Sensible Heat Flux, 2-8 July (Calories cm^{-2} week^{-1})
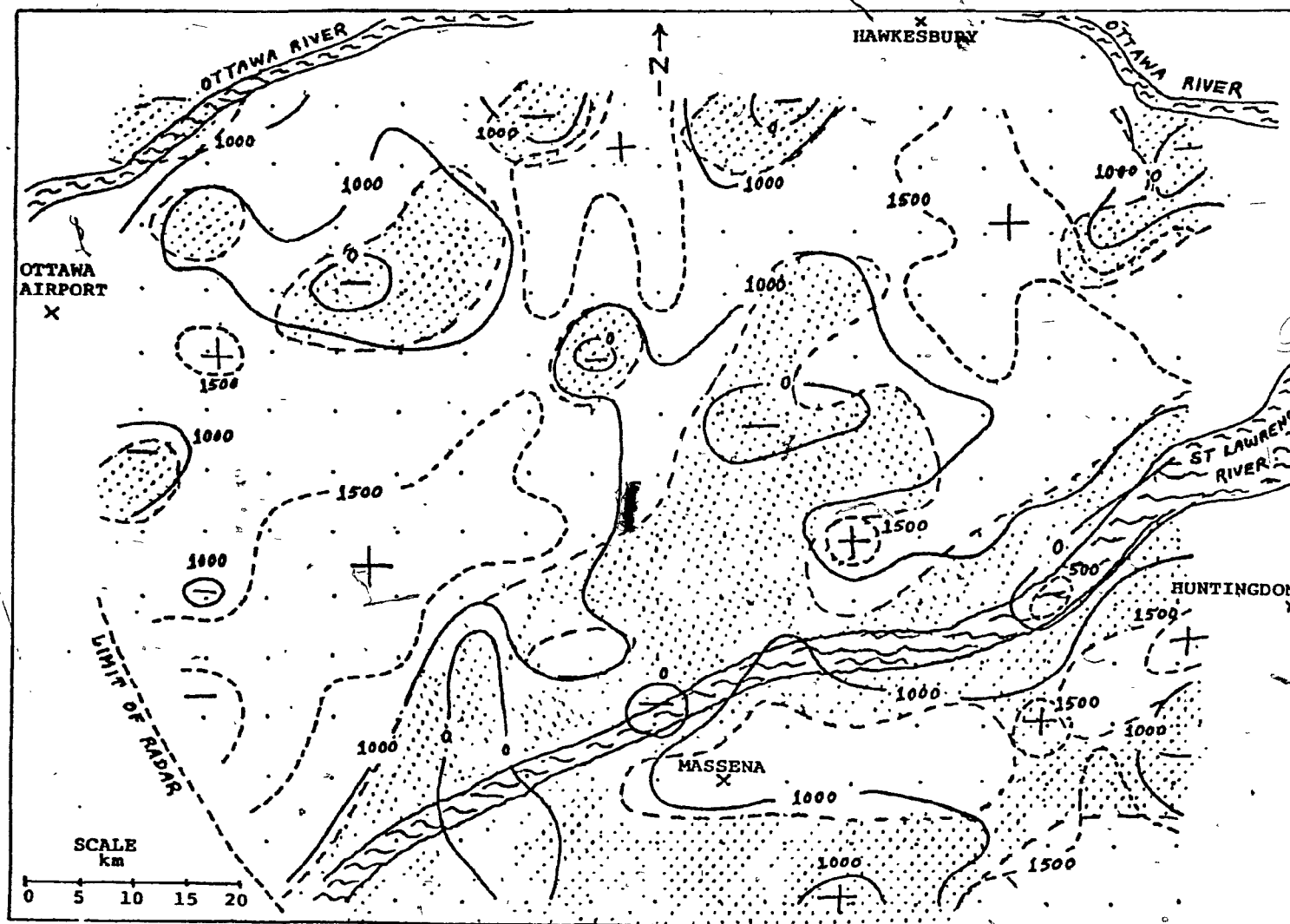
no precipitation. These are therefore near the minimum of Figure 26. The region also contains areas of predominately forest land which happen to have more evaporation than cropland receiving maximum rainfall, the maximum of Figure 26.

IVC4. Representation of Area Average Evaporation by Use of Certain Point Values

Energy budget calculations for very large areas cannot make individual calculations at grid points as closely spaced as in the present study. The usual practice is to choose radiosonde stations as points of calculation. This section will compare the area average evaporation obtained from all 229 grid points to that based on only three points located near the synoptic stations: Montreal, Ottawa, and Massena.

Figure 29 compares the daily evaporation using only three points (dotted line) to that with 229 points of calculation (solid). Rain occurred on the 1st, 6th, and 7th day of the period. The underestimation of area evaporation using only the three point values is noteworthy. Also, the shape of the curve reflects the changes in the real area evaporation. The underestimation first decreases, then increases with time after the first general rainfall. The cumulative error in evaporation from the start of the period is plotted with the dotted line in Fig. 30. The same trend is indicated while the percentages range from -20 to -40 per cent, a formidable error. The fact that the evaporation was underestimated by the three points chosen was by chance. It could be that if three other points were chosen to base the calculations, the evaporation

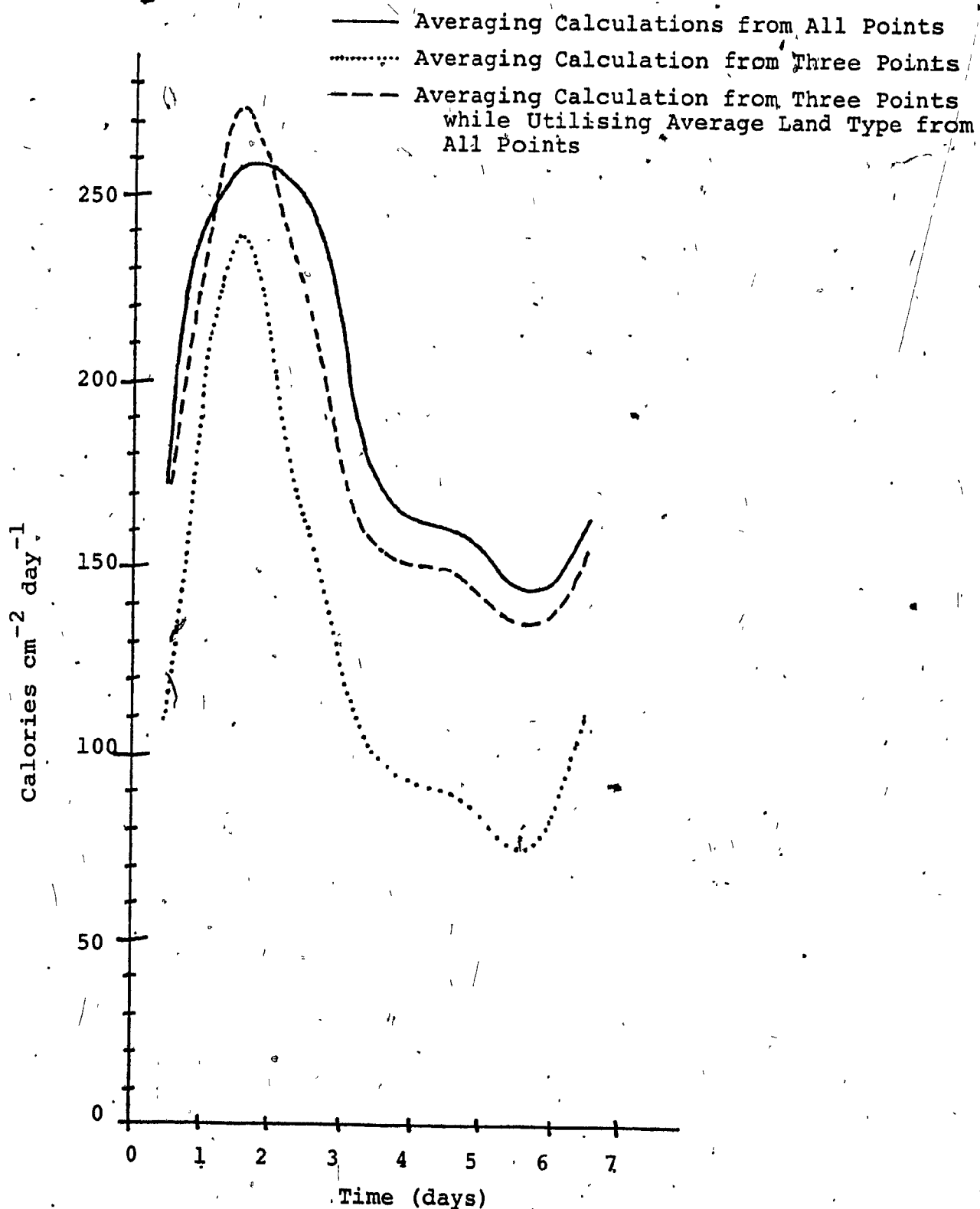Figure 29. Comparison of QE from Area Using Various Methods

——— Averaging Calculations from All Points
·········· Averaging Calculation from Three Points
— — — Averaging Calculation from Three Points while Utilising Average Land Type from All Points

Figure 30. Difference in Methods of Calculating QE
Over Area from that Using All Points

··········· Averaging Calculation From Three Points

– – – Averaging Calculation From Three Points while
Utilizing Average Land Type From All Points

Time (days)
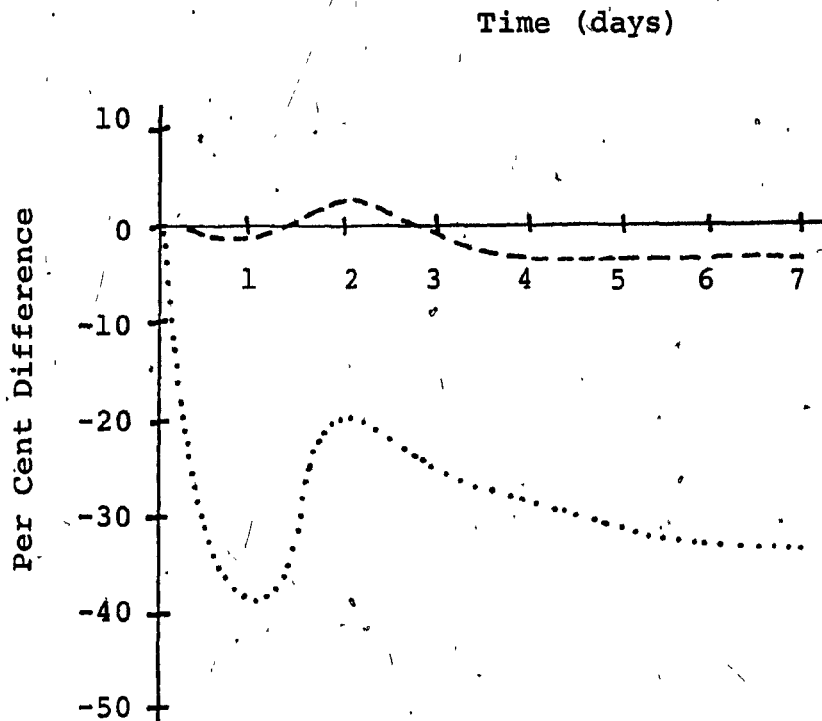
could be overestimated, or even close to the calculation based on all the points. The differences can be caused by these three factors:

1. Precipitation amount and time differ at three points from average using 229 points.

2. Other meteorological parameters such as temperature, dew point, wind, and cloudiness vary at the three points from the average over the grid.

3. Surface types at the three points differ from the area average.

To investigate the second factor, reference is made to the discussion of the 7-day QE from forest over the grid (Fig. 24). Since most of the variation in space was large scale and due to differences in dew point and wind at the three stations, it is reasonable that the average potential evaporation using the three stations should be very close to the average using all the points. However, this omits the consideration of small scale variations in temperature, dew point, wind, and cloud at the grid points. Referring back to the discussion in IIIA, the effects of such variations in temperature and dew point were considered, when scattered areas of wet and dry surfaces are present. If these areas are taken to be in the order of 50 km wide, from Fig. 27, and the average wind of 3 m sec^{-1} is used, then from Figure 18 the error in calculating QE without using the variation of temperature and dew point will not exceed 7/470, or 2%. Since there is no way of knowing the variation of cloudiness at each point, the effect of using the cloudiness from only

three points cannot be determined. The effect of variation of
the wind is presumed small as discussed in   IIIB2.

        Next, a correction for the third factor is made. The
average fraction of forest and crop for the entire area as a
whole is used, rather than the actual fractions which happen .
to be present at the three points. The results appear as
dashed lines in Figures 29 and 30. The difference between the
three point calculation and the calculation using all points
is reduced to at most 3%! The evaporation on day 2 is now an
overestimation. This is probably caused by more precipitation
over the three points used than the area average on day 1.
Thus, the first factor is now considered. From this discussion,
the remaining 3% error must be due at least in part to a diff-
erence in amount and time of precipitation at the three points
sampled and the area average. To test this, the energy budget
would have to be run using the area average of precipitation
each hour. However, it is clear that this error depends on the
initial dryness of an area and the degree of variation of
precipitation in time and space. The precipitation will have
a minimal effect on a totally covered area initially being wet.

        To conclude, the energy budget calculations at a point
can accurately represent an area for a one-week summer period, if
the average surface conditions and average precipitation of the
entire area are used at the point, every time step. There is
no reason to believe that this conclusion will be altered if
a longer period is considered. This is because maximum spatial

variations were considered here. The period included highly convective precipitation, the highest shortwave radiation of the year (and hence the highest turbulent fluxes). Also, the area contained the most extreme differences likely in land characteristics.

IVC5.   Changing the Ratio of Forest to Crop

Man's influence is constantly felt on the earth's surface. Forests are cut down, fields are plowed, crops are grown. This was the first sequence of events which took place on the North American continent since the Europeans arrived over the last three centuries. However, in the last century, the trend has been reversing. There has been a decline in farming and hence the amount of farmland in marginal growing areas has declined drastically (Black River - St. Lawrence Economic Development Commission, 1974). In the area for which the energy budget programme has been calculated, it has been estimated that the amount of farmland has decreased from 12 to 30% in about the last 20 years (Black River - St. Lawrence Economic Development Commission, 1974; Ontario Department of Agriculture, 1969). To assess the effects of this surface change on the climate, it is possible to determine the change in turbulent fluxes which would result. Table 19 includes the present ratio of crop to forest as determined from maps and the ratio about 20 years ago, assuming the two estimated losses in farmland reverted to forest or a forest-type area.

Table 19. Crop and Forest as Fractions of Total Area

	1975	1950 (Assuming Minimum Change)	1950 (Assuming Maximum Change)
CROP	.74	.77	.82
FOREST	.26	.23	.18

These two estimated sets of fractions for 1950 are applied to the area averages of total 7-day QE from crops and forest to obtain estimates of the average evaporation if the changes occurred equally over each grid square. The same is done for QS. The estimations of area averaged turbulent fluxes in 1950 are compared to the average in 1975 (obtained from Figs. 27 and 28). These are shown in Table 20.

Table 20. QE, QS (calories cm^{-2} $week^{-1}$) for 1950 and 1975.

	1975	1950	
		Minimum Change	Maximum Change
QE	1312	1206 (-8%)	1053 (-19%)
QS	1031	1109 (8%)	1239 (20%)

Under the same atmospheric conditions, the evaporation would have been from 106 to 259 calories less two decades ago. This gives from .18 to .43 cm less water evaporated to the atmosphere over a 7-day period. The sensible heat flux would have been from 11 to 30 calories greater each day. If these changes are incorporated into the atmosphere, the maximum surface air temperature would have been about $\frac{1}{2}°C$ higher on a day in 1950. Also,

the dew point would have been nearly $\frac{1}{2}^{\circ}C$ lower. If the additional
sensible heat flux available to the atmosphere in 1950 was used
to warm it below 500 mb (without horizontal divergence of air),
the 500 mb height would have been from 11 to 32 m higher after
one week. These figures imply a formidable effect on the atmo-
sphere following periods of clear dry weather.

The change in land use discussed above has generally
been observed over eastern North America. If there has been no
such change in the western half of the continent, then the high
level flow of air should be different today following periods
of dry weather. The 500 mb height in the east will be lower
than in 1950, while the height in the west will be the same. Thus,
a west to east upper air wind pattern in 1950 should appear more
nearly northwest to southeast today, i.e., there will be a
tendency for the air flow to have a more northerly component
following periods of dry weather than before the land change.
This pattern requires more subsidence of air over central North
America. Hence, the development of precipitation will be
suppressed further in this area. The dry period will be self
enhanced and likely last longer there.

IVC6. Turbulent Flux Patterns Associated with the Appearance
       of Precipitation.

The patterns of convective precipitation which occur
over the area will now be compared to the patterns of hourly QE
and QS. This investigation seeks to probe the conditions of
convection with respect to local variations in air mass (and
hence turbulent fluxes) at specific times when the precipitation

formed or entered the area. Individual cases are thus examined for their own conditions rather than seeking a statistical approach including all cases together. This is done because of the small set of cases available and the danger of combining the results from different physical effects which may occur at different times and places.

Of the 7 days for which the energy budget was calculated, 3 days received precipitation. In all cases, the precipitation appeared convective in nature, and entered or developed in the area during afternoons. The first precipitation day was July 2, when a surface frontal trough and developing 500 mb trough approached and passed the area late at night. A widespread precipitation pattern occurred over the area as a result of large scale lifting near the trough. However, isolated areas of intense convection were imbedded, as evidenced by the non-uniform pattern of rainfall.

July 3, 4, 5 and 6 were free of any precipitation in the region. The troposphere was basically stable during this period as the result of subsidence following the trough passage on the night of the 2nd. However, the fact that these days were stable in no way implies that the quantity of turbulent fluxes were smaller than on days with precipitation. In fact, the mean daily $QE + QS$ from forested areas was 397 calories on non-rain days as compared to 358 calories, 11% less, on rainy days. This is because of more cloudiness on rainy days, yielding less available energy for the turbulent fluxes.

On the afternoon of 7 July, a small area of precipi-
tation developed in the southeast section of the area. On 8
July, an intensifying trough again approached from the west,
but did not pass through until the following day. Isolated
convection first developed, mainly in the north of the area.
This will be the first case to be considered.

1. Case 1 - July 8

To be considered is the precipitation, which first
appeared on radar at about noon on this day. The hourly preci-
pitation at 1200 EST represents the precipitation rate from
1130 EST to 1230 EST and appears in Figure 31. The maps of
hourly QE and QS for the area at 1000 EST are presented in
Figs. 32 and 33, respectively. The area of precipition from
1200 EST is superimposed with shading in these two figures. The
hourly QE and QS at 1100 EST are presented in Figs. 34 and 35,
respectively. It should be noted that sky conditions were
reported as mainly clear at the three reporting stations at
1000, 1100, and 1200 EST. Comparing the turbulent flux maps of
1000 and 1100 EST, one can see little difference between the two
hours. These are nearly the maximum possible fluxes since the
sky is mainly clear and the sun is close to its highest eleva-
tion for the day. Also, this implies that a change in ground
water from the cropland is not noticable from one hour to the
next in the QE, QS patterns. Another point is that an over-
estimation of incoming radiation is very likely between Ottawa
and Montreal just before 1200 EST, because the cloud pattern
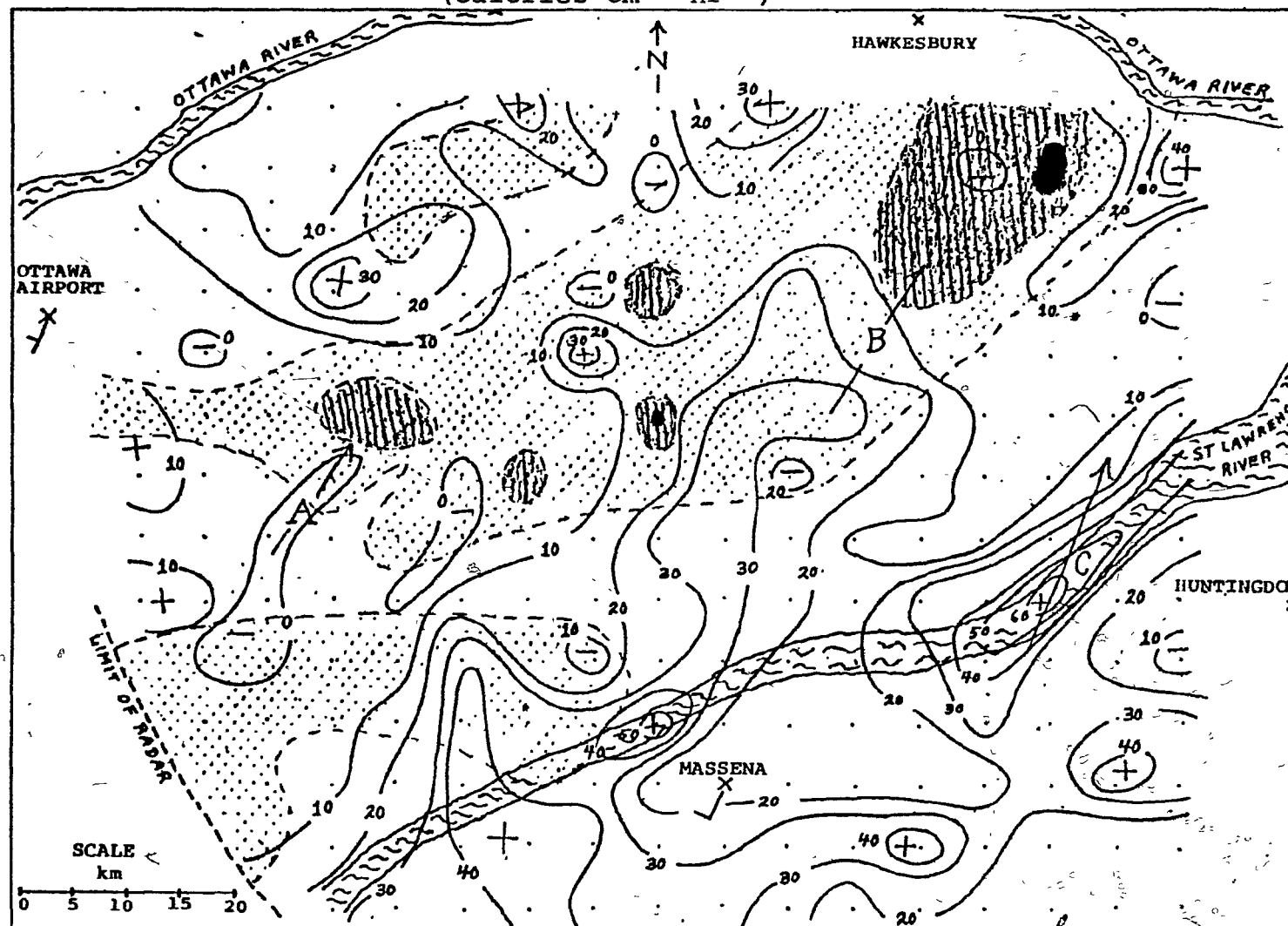associated with the precipitation was likely present at least

Figure 31. Precipitation Rate at 1200 EST, 8 July (cm hr^{-1})
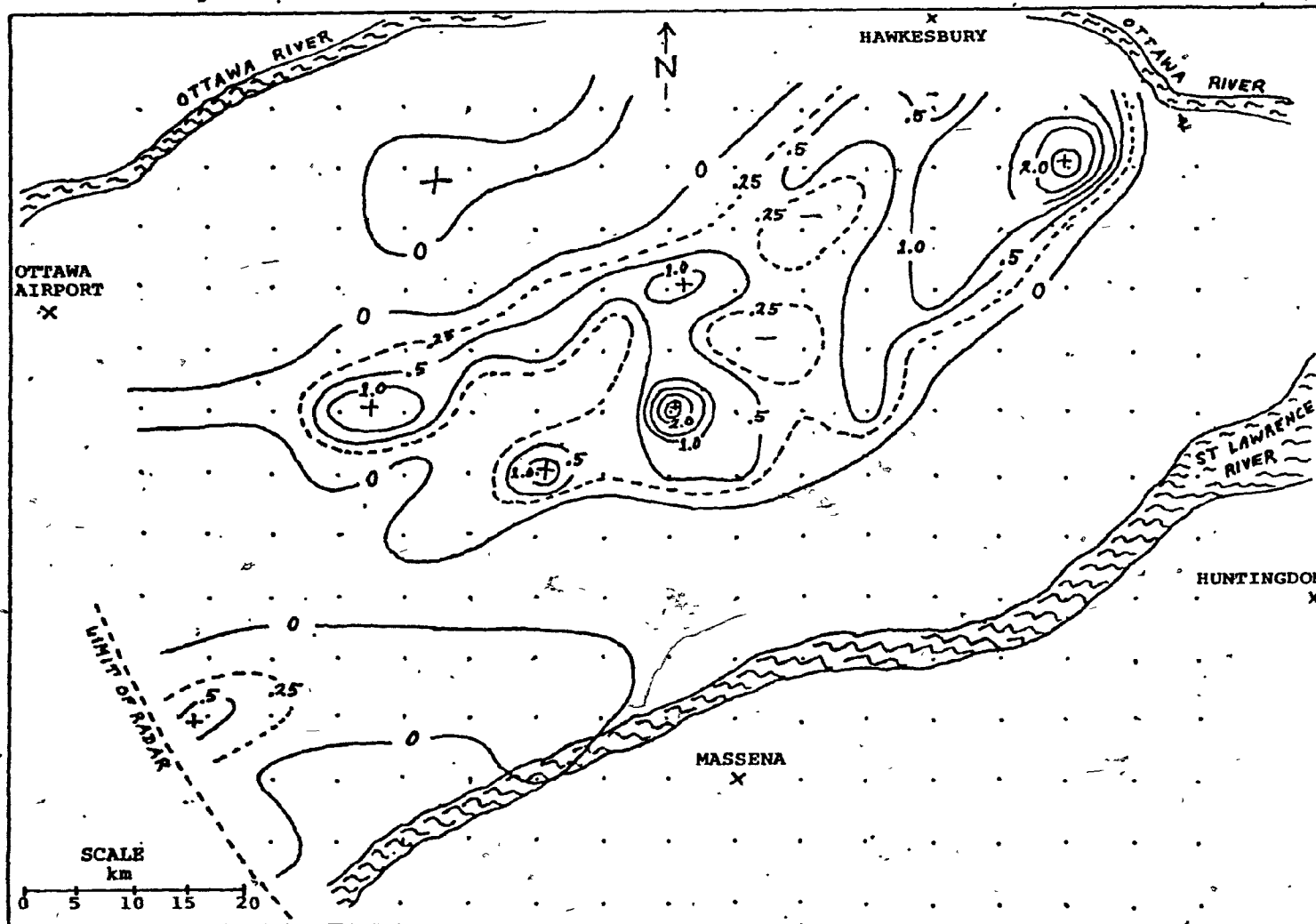
LEGEND

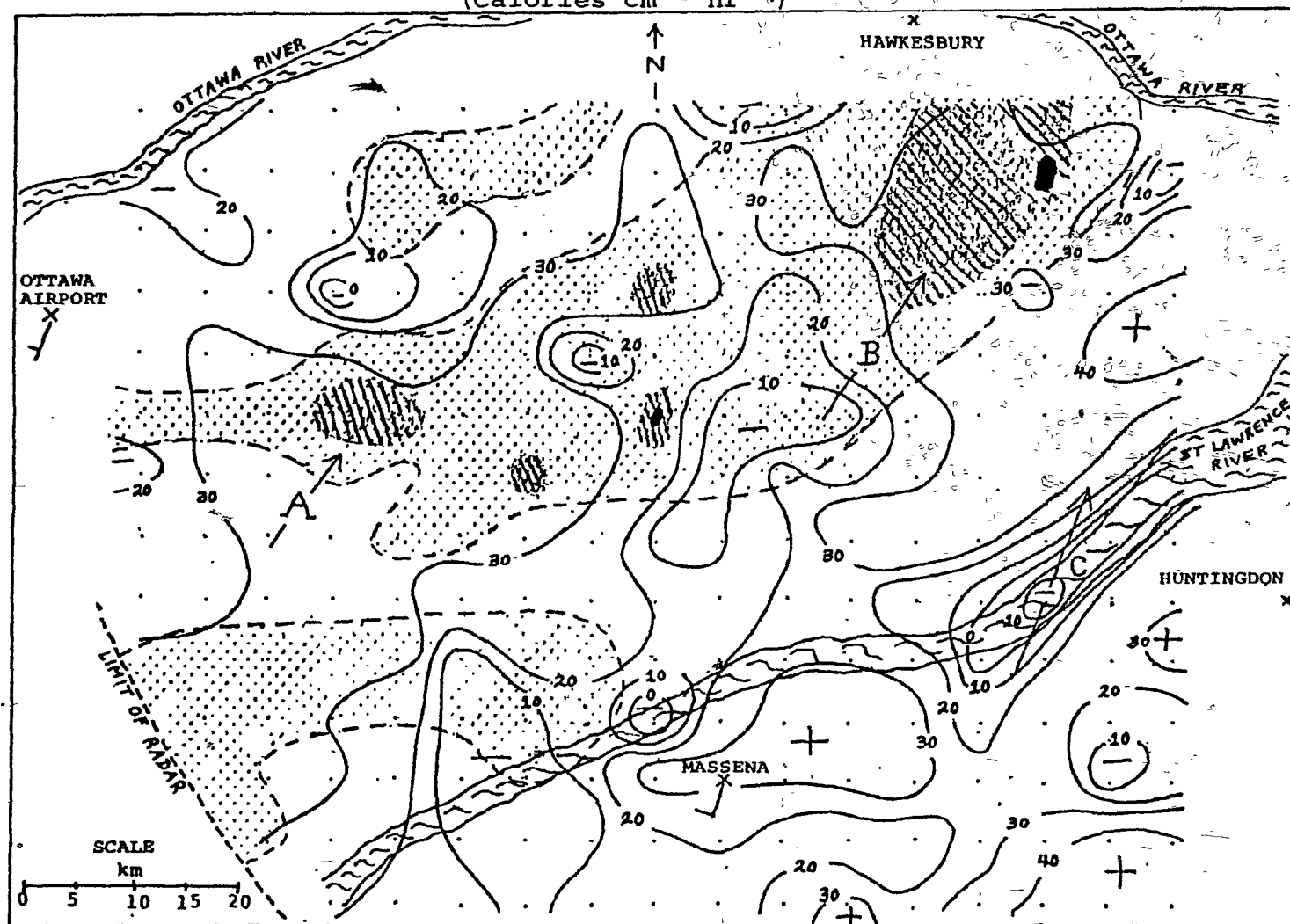+ Relative Maximum
- Relative Minimum
. Grid Point
X Reference Point

Figure 32.   Latent Heat Flux at 1000 EST, 8 July
(Calories cm^{-2} hr^{-1})

Figure 33.   Sensible Heat Flux at 1000 EST, 8 July
(Calories cm^{-2} hr^{-1})

LEGEND

+ Relative Maximum
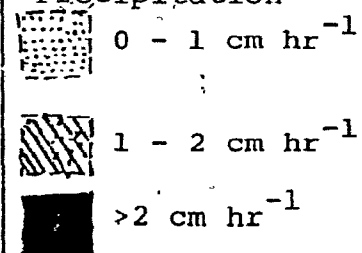- Relative Minimum
. Grid Point
X Reference Point
Precipitation:

0 - 1 cm hr^{-1}

1 - 2 cm hr^{-1}

>2 cm hr^{-1}

Figure 34. Latent Heat Flux at 1100 EST, 8 July
(Calories cm^{-2} hr^{-1})

LEGEND

+ Relative Maximum
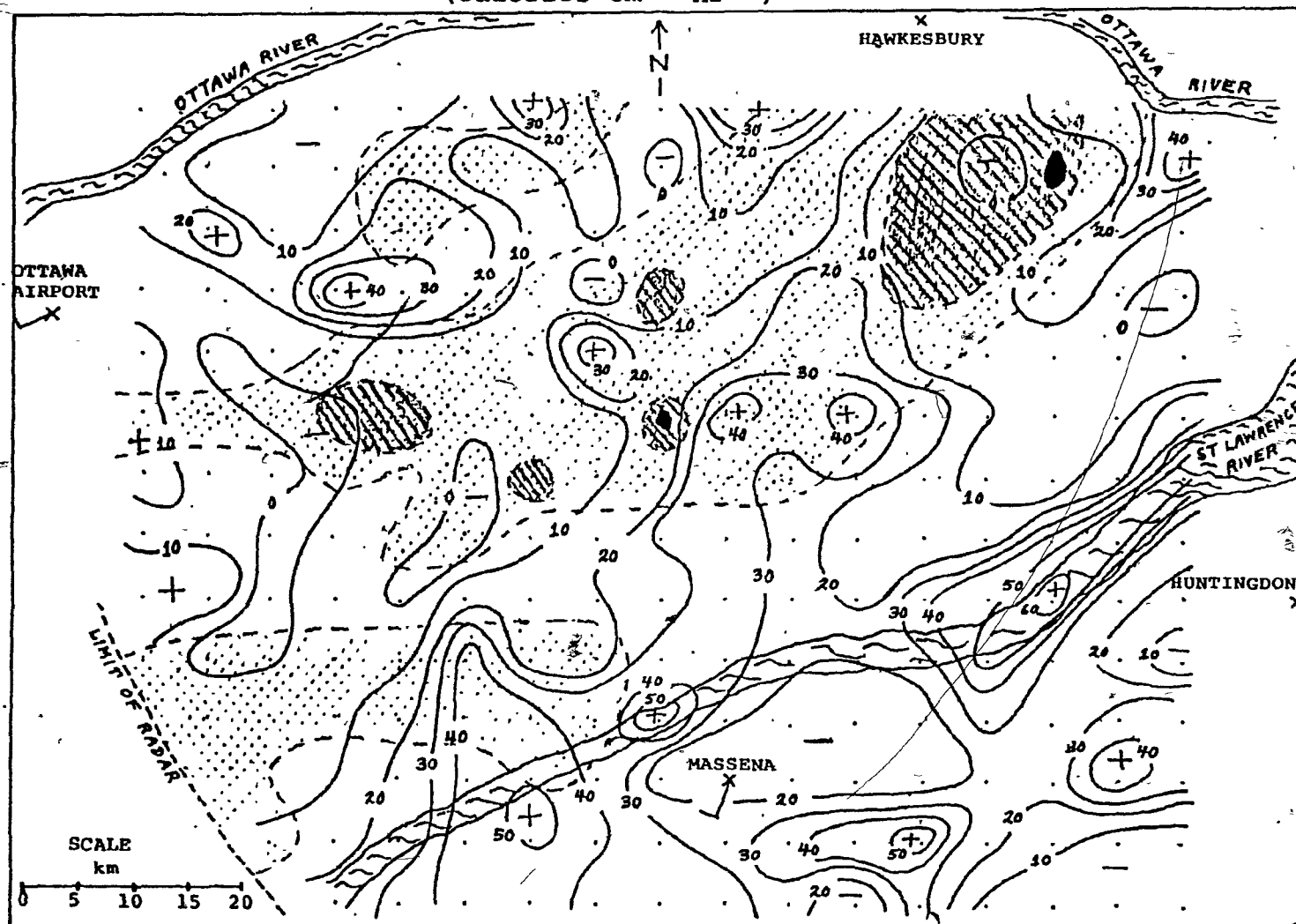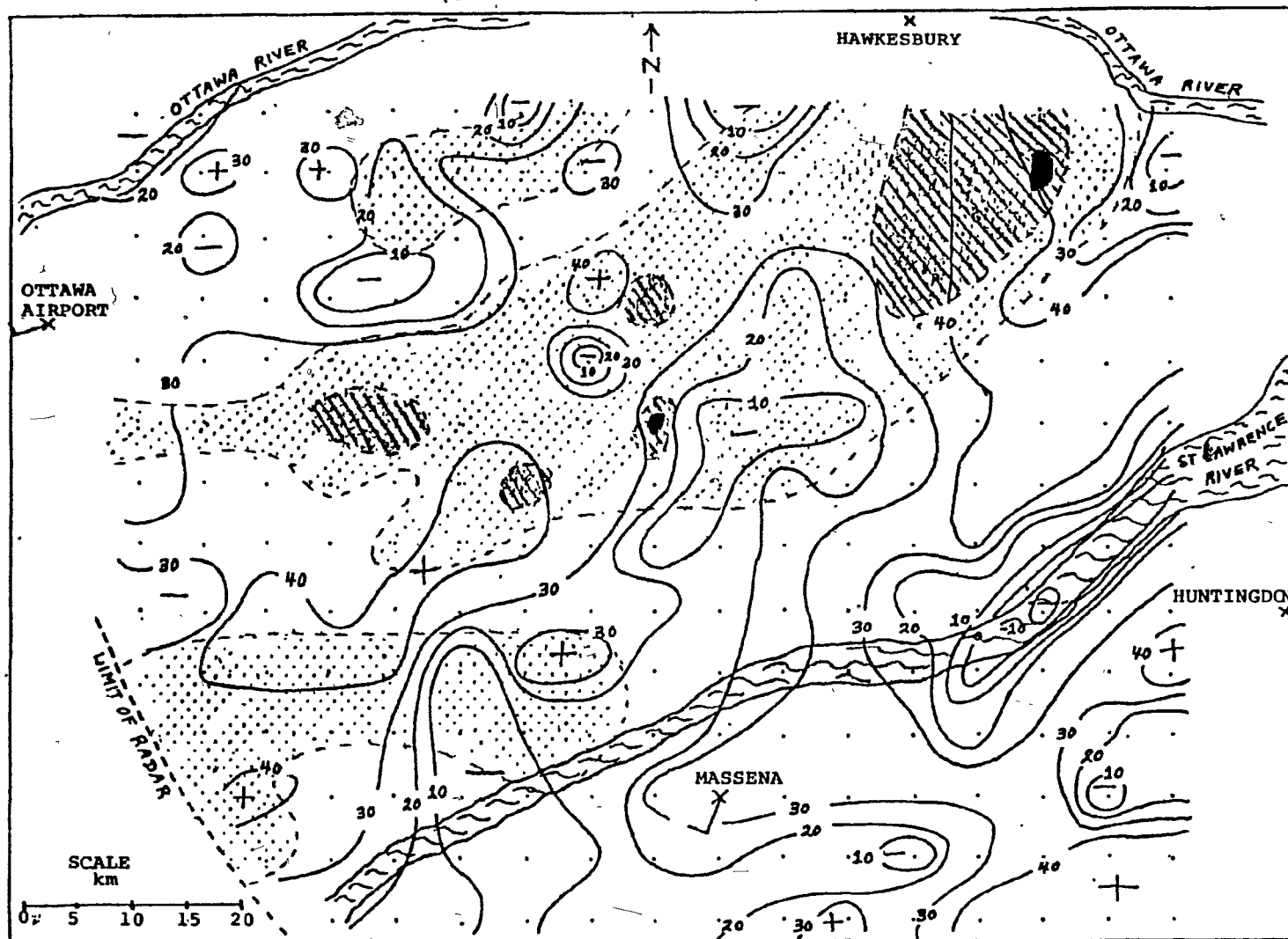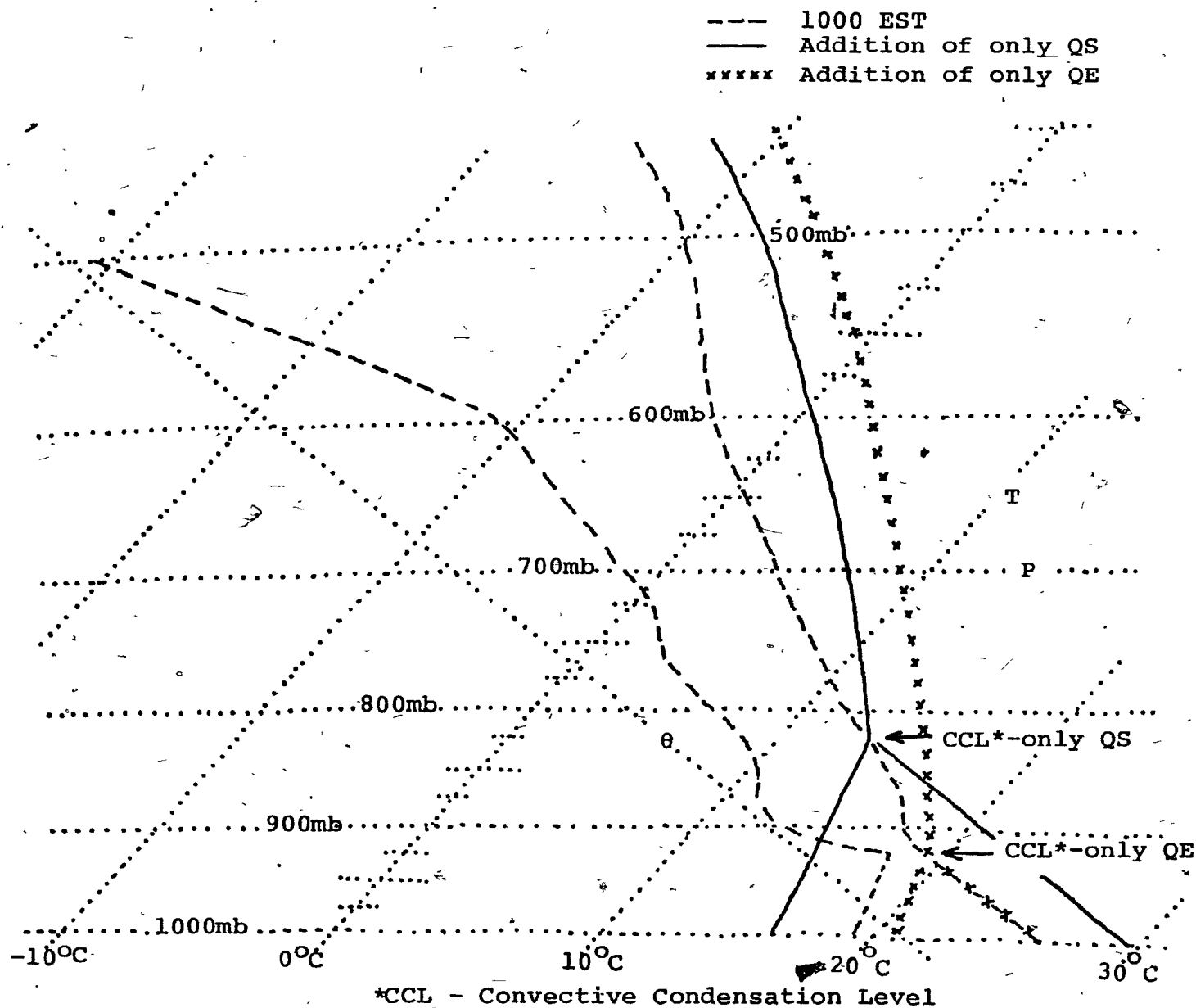- Relative Minimum
. Grid Point
X Reference Point
Precipitation:

0 - 1 cm hr^{-1}

1 - 2 cm hr^{-1}

>2 cm hr^{-1}

Figure 35. Sensible Heat Flux at 1100 EST, 8 July
(Calories cm^{-2} hr^{-1}).

one hour before the outbreak of showers. The cloud pattern
was undetected by the three observing stations when rain was
reported by radar at intermediate points at 1200 EST, so would
it also have been undetected at 1100 EST if present in the same
area. For these reasons, the turbulent fluxes are considered
from 1000 EST to represent those immediately preceding the
development of the precipitation system. Since the input of
energy from the ground is greatest in the lowest part of the
atmosphere, the surface wind is considered to represent the flow
of air parcels being modified prior to convection. Once convec-
tive precipitation develops, it will move with the flow at a
higher level. The surface winds at 1000 EST are plotted near
their points of observation on Figs. 32 and 33, with the
exception of Montreal which actually lies off the map some 30
km to the east. The largest area of precipitation appears down-
wind from a long area of very high QE rates. However, the heavy
precipitation occurs over an area of very high QS values just
northeast of the moist area. Since the available energy (SGA +
DFL) varies only slightly over the grid when the cloud conditions
are the same at all stations, the total of QE + QS is also nearly
equal over the area. Hence, QE is inversely proportional to
QS. Areas of maximum QE are associated with minimum QS, and areas
of minimum QE are associated with maximum QS.

To examine under what conditions convection would be
likely, reference is made to Fig. 36 which contains the radio-
sonde determined at 1000 EST over a point near the area where
heavy precipitation occurred two hours later. Note that the

Figure 36. Atmospheric Sounding, 8 July

```
- - - -   1000 EST
————   Addition of only QS
xxxxx   Addition of only QE
```


500mb

600mb

T

700mb   P

800mb
                θ   CCL*-only QS

900mb   CCL*-only QE

1000mb

-10°C   0°C   10°C   20°C   30°C

*CCL - Convective Condensation Level

layer of convective mixing extends no higher than 925 mb. The lifting condensation level is above this level at 910 mb, but some energy would have to be supplied to overcome a small negative area under the level of free convection at 850 mb. Neglecting frontal or large scale synoptic lifting, it is clear that for convection to occur the air must be heated further, or moistened from the surface.

The addition of water vapour with no addition of sensible heat is first considered, that is, the addition of positive QE but zero QS. The water vapour content must be increased in the layer of convective mixing such that the lifting condensation level is at or below the height of convective mixing, 925 mb. For this to be the case, a large quantity of evaporation is required if the moisture evaporated is distributed evenly through the mixing layer. The dew point curve (x's) represents the addition of water vapour such that the lifting condensation level is brought down to the height of the convective mixing layer so that moist convection will just become possible without large scale vertical motion. An increase of surface dew point of about $2^{o}C$ is required, with the addition of 66 calories of latent heat flux and zero sensible heat flux. However, convection can be prevented if QS is negative and the surface temperature drops; then the lowest layer will become stable. The area of very high QE in the central eastern portion of Fig. 32 is noteworthy. Referring to Fig. 33, the same area is associated with negative QS. This area has a very high fraction of water due to the St. Lawrence river. As mentioned earlier, water

areas are parameterized as if they were forest. If water were considered, QS would be even more negative since changes in water temperature lag those of ground surface temperature. It is noteworthy that no precipitation formed downwind from these areas.

Now the addition of sensible heat flux is considered with no latent heat flux, i.e., the addition of positive QS with QE equal to zero. In this case, the increased thickness of the layer of convective mixing is shown in Fig. 36 by solid lines. To increase the layer to 820 mb, the surface temperature must be raised about $2^\circ C$ and the addition of 134 calories is required. Since it is assumed that water vapour is evenly distributed with height in the mixing layer, the mean mixing ratio of the thicker layer is less because the lower moist air was mixed with dryer air above. Hence, the surface dew point drops and the increase of the convective mixing zone without evaporation also increases the height of the lifting condensation level, from 910 to 820 mb. Thus, the mixing level must be raised beyond the original level of free convection because of the effect of vertical mixing of water vapour. Moist convection can begin only at a higher level and the total positive energy of convection will be less. Therefore, convection is likely to be somewhat less intense than in the case of moistening. This could explain the small areas of heavy precipitation which occurred downwind of a large area of high QS in the southwest part of the area.

Finally, the addition of both latent and sensible heat together is considered as it would occur with the passage of air over areas of positive QE and QS. For example, the addition of QE can compensate for the increased lifting condensation level associated with the addition of QS. The height of convective mixing is thereby raised without changing the lifting condensation level. Table 21 summarises the preceding discussion. It contains the turbulent fluxes required to obtain moist convection as a function of height of base of the convection.

Table 21. Various Combinations of QE and QS (calories cm^{-2}) Necessary for Convection, 8 July, 1000 EST

BASE OF CONVECTION	QE	QS	QE+QS	REPRESENTATION IN FIG. 36
820 mb	0	134	134	Solid Lines
850 mb	45	67	112	None
900 mb	48	34	82	None
925 mb	66	0	66	Lines of X's
No Convection	--	<0	--	None

The vertical stratification of temperature and dew point on this day were such that the total amount of energy derived from turbulent fluxes necessary to start convection decreased with a shift of energy from QS to QE. This type of stratification will be referred to as a moist sounding. It follows that convection should occur earliest over areas of highest QE where QS is not less than zero. The three paths indicated on Figs. 32 and 33 (derived from the surface wind field) are used to

follow the motion of surface air for a period of two hours (0930 EST - 1130 EST). The turbulent fluxes added in each case are presented in Table 22.

Table 22. QE and QS (calories cm^{-2} two hours^{-1}) for Various Air Trajectories

PATH	A	B	C
QE	12	70	108
QS	57	8	- 3
QE+QS	70	78	105

Conditions for convection will be met after these two hours only for path B, over the moist areas. It is not met for path A or C. Indeed, the largest and most intense precipitation was first reported 1 hour later downwind from path B (the time necessary for the growth of an echo from a cumulus cloud is in the order of 1/3 hour). Moreover, the area is of the same scale as the width of the moist land area of high QE flux parallel to the wind. The more spotty precipitation downwind of the large dry area with high QS is evidence that convection is on the verge of developing. It is reasonable that once convective cells develop, they may be advected with the higher level flow and also set up their own dynamic vertical motion field. For example, subsidence and/or increased cloudiness surrounding the first area of convection may influence the possible later development in surrounding areas. For these reasons, later times were not investigated.

2. Case 2 - July 2

As mentioned earlier, the precipitation pattern was widespread as it was advected eastwards in the afternoon. Hence, cloudiness was also widespread in the vicinity of the large precipitation area. However, the pattern on this day is still worth examining since only a high overcast was present at the stations an hour or two before precipitation entered the western portion of the area, yielding 70 to 80 per cent of their maximum values under clear skies for a given hour.
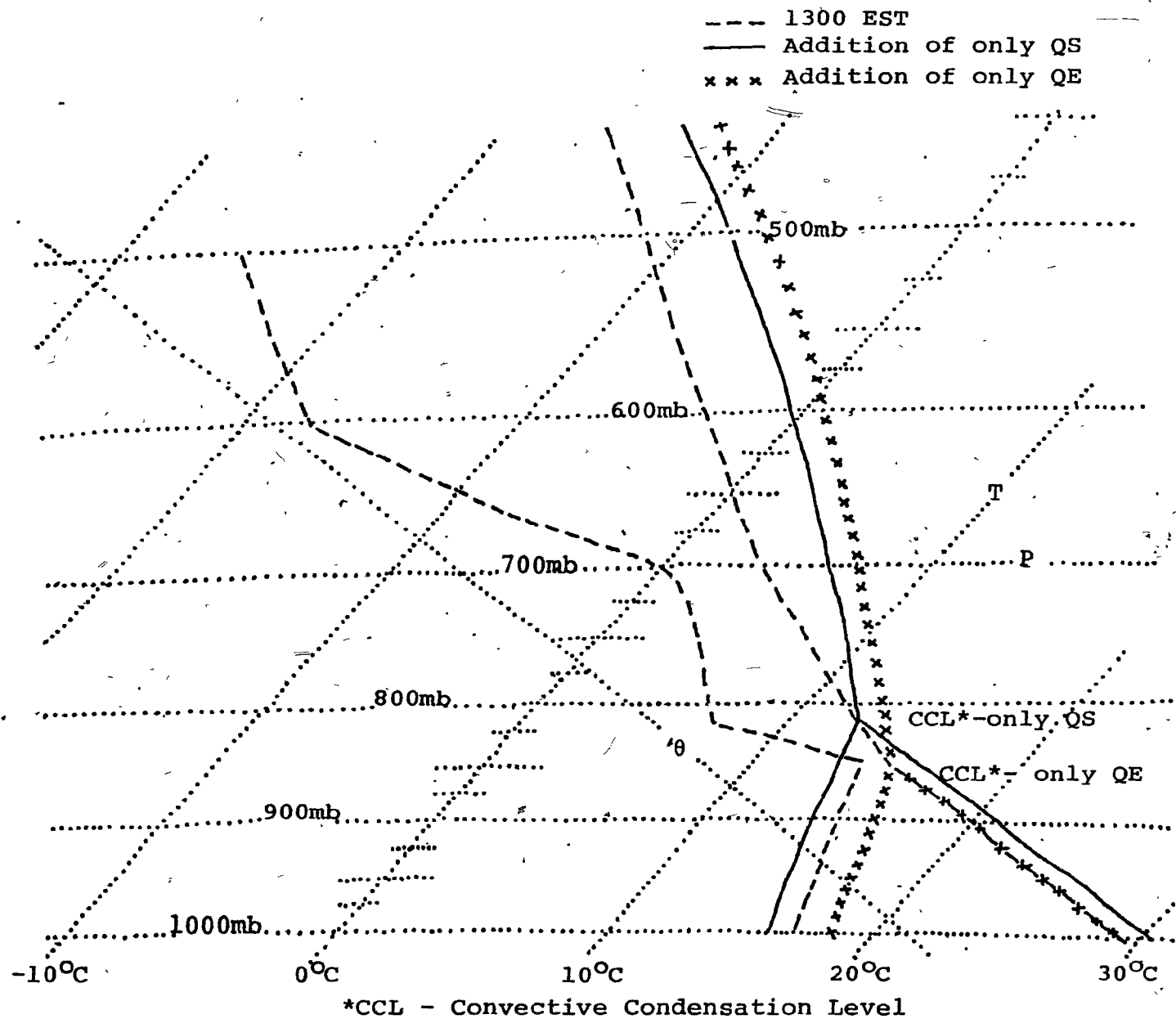
If the radiosonde at 1300 EST is considered, from Fig. 37, the stratification is rather unstable but dry. Thus, a small amount of QS relative to QE is necessary to start moist convection. In contrast to the moist sounding on July 8, this sounding will be referred to as dry. If the same analysis of turbulent flux combinations necessary for moist convection is done, the results are obtained and presented in Table 23.

Table 23. Various Combinations of QE and QS (calories cm^{-2}) Necessary for Convection, 2 July, 1300 EST

BASE OF CONVECTION	QE	QS	QE+QS
820 mb	0	44	44
835 mb	36	22	58
850 mb	90	0	90

Less total turbulent flux energy is required for moist convection as more energy is partitioned to QS, which is the opposite effect as that on July 8.

Figure 37. Atmospheric Sounding, 2 July

--- 1300 EST
— Addition of only QS
x x x Addition of only QE

500mb

600mb

T

700mb

P

800mb

CCL*-only QS

θ

CCL*- only QE

900mb

1000mb

-10°C   0°C   10°C   20°C   30°C

*CCL - Convective Condensation Level

Figures 38 and 39 show the precipitation patterns for 1500 EST and 1600 EST, respectively, on July 2. The precipitation should first develop in areas of highest QS rates. On the first day's calculations, the highest rates will be over those grid squares with the highest fractions of crop land. The area with more than 75% crop is unshaded in Figures 38 and 39. The shaded area is mixed forest and crop with less than 50% crop common. The turbulent fluxes preceding precipitation at points representative of the shaded and non-shaded areas are presented in Table 24.

Table 24. Representative QE, QS (calories cm^{-2} two hours^{-1}) at 1230 EST - 1430 EST, 2 July

	CROP		FOREST	
Crop Fraction	1.00	0.75	0.50	0.00
QE	0	30	59	118
QS	79	52	26	-27
QE+QS	79	82	85	91

The amount of QS+QE from most areas is enough to start convection by itself without lifting of air from another source. However, the areas of highest QS require the least energy, and should initiate precipitation first. At 1500 EST, the heaviest, and in fact, most of the precipitation occurred in the crop area as the system moved in from the west. By 1600 EST, the precipitation fell over nearly all areas. The bands of heaviest precipitation generally correspond to the
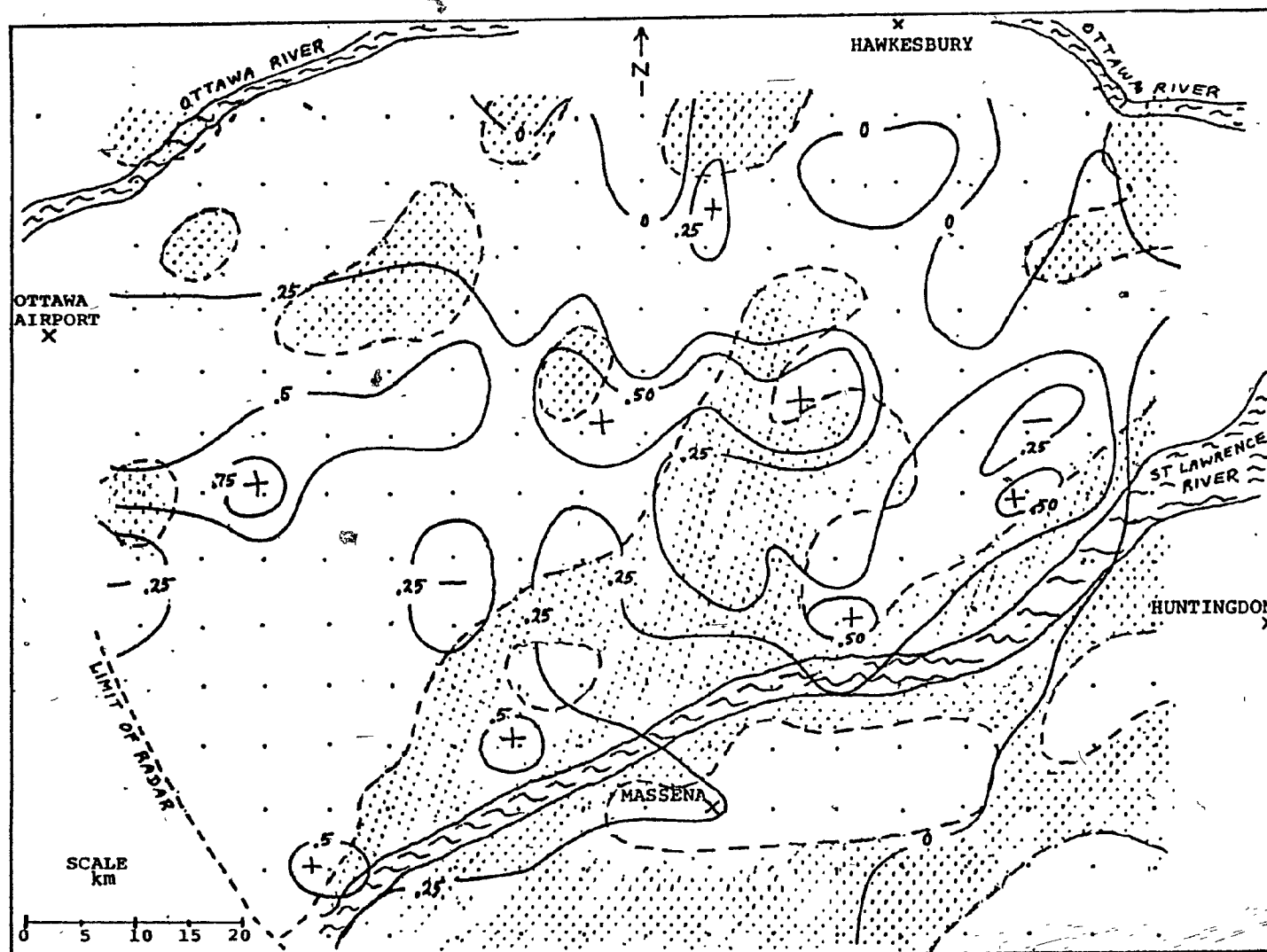
Figure 38.   Precipitation Rate at 1500 EST, 2 July (cm hr^{-1})
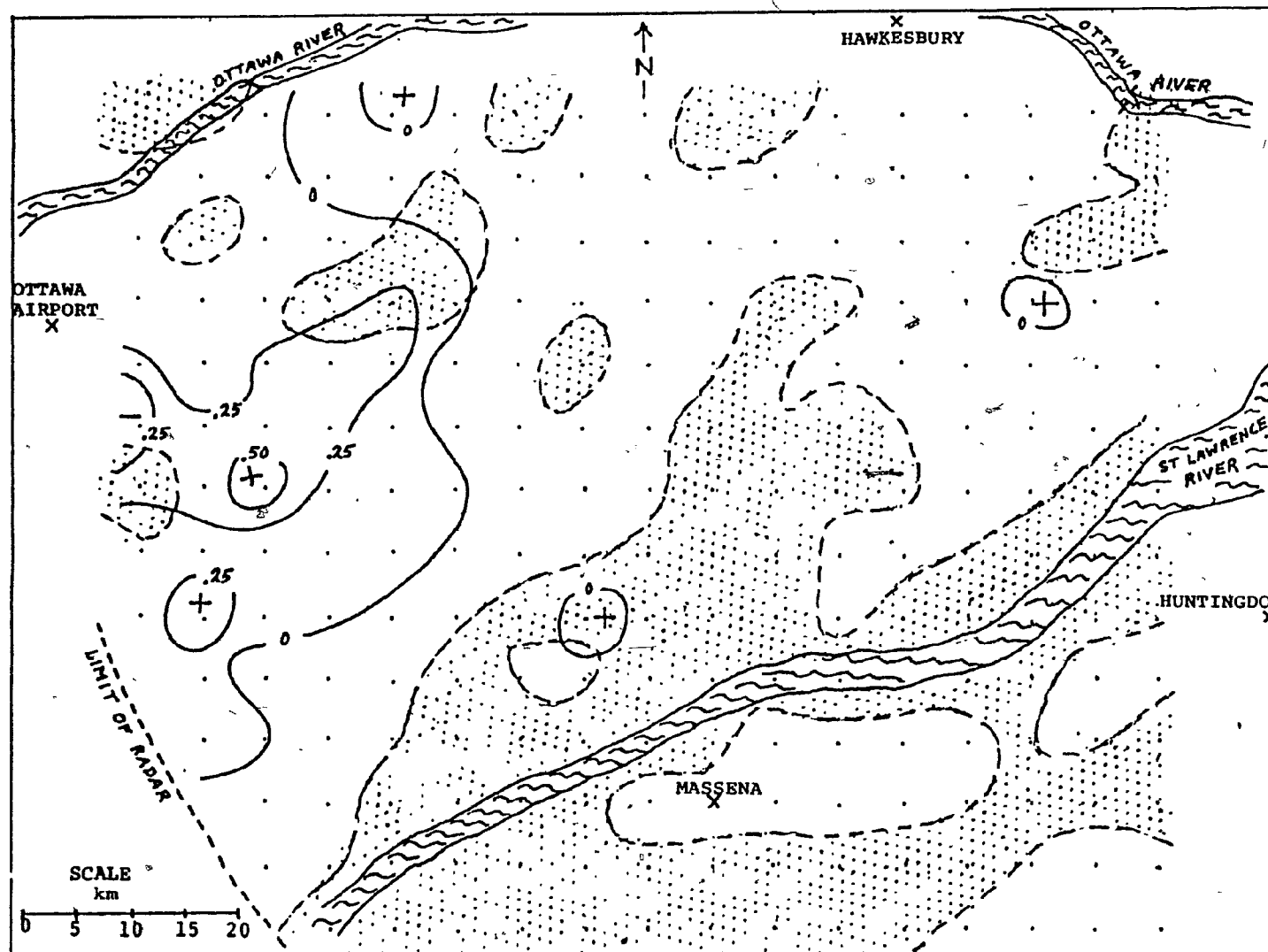
Figure 39. Precipitation Rate at 1600 EST, 2 July (cm hr^{-1})

LEGEND

+ Relative Maximum
− Relative Minimum
. Grid Point
X Reference Point

≥25% Forest

areas of high QS. However, advection of predeveloped precipi-
tation makes the analysis more difficult. This, and the importance
of larger scale lifting over sensible heat flux variations, make
the effect of the surface less noticeable in the present case
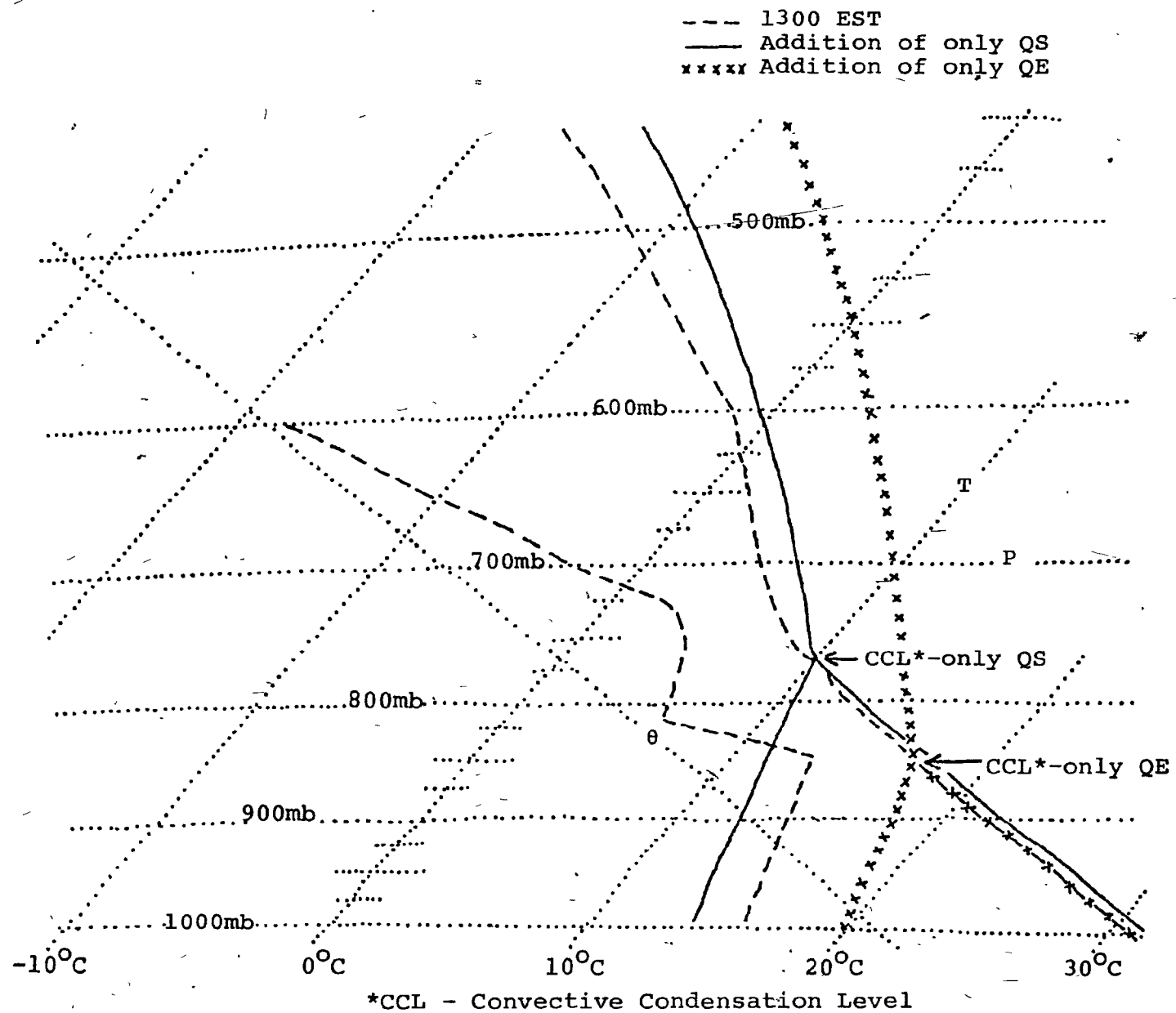than in the first.

3. Case 3 - July 7

The third and final case is the precipitation of July 7.
The sounding used at 1300 EST is presented in Fig. 40. Similar
to case number 2, this sounding is classified as dry. Table
25 contains the results of an analysis of turbulent fluxes nec-
essary to initiate moist convection at various heights:

Table 25. Various Combinations of QE, QS (calories cm^{-2})
Necessary for Convection, 7 July, 1300 EST

BASE OF CONVECTION	QE	QS	QE+QS
775 mb	0	27	27
800 mb	120	24	144
820 mb	216	21	237
850 mb	297	0	297

As in case 2, partitioning of energy to QS would facilitate
convection. The sounding is more dry and unstable, so that the
time difference between initiation of moist convection between
dry and moist surfaces should be much greater than the previous
case, making the effect of the surface more noticeable.

Figure 40. Atmospheric Sounding, 7 July

--- 1300 EST
—— Addition of only QS
xxxxx Addition of only QE

500mb

600mb

T

700mb

P

CCL*-only QS

800mb

θ

CCL*-only QE

900mb

1000mb

-10°C   0°C   10°C   20°C   30°C

*CCL – Convective Condensation Level

However, the sounding generated one hour later at 1400 EST actually indicates that moist convection would take place, yet no precipitation was reported until 1500 EST. Only a small area of precipitation, which was not very intense, developed in the southeast corner and is shown in Figure 41. If the constructed radiosonde is accurate, then subsidence must have suppressed convection over most of the area. Indeed, the comparison of the 0700 EST and 1900 EST observed radiosondes showed subsidence warming of up to 2-3°C near 700 mb at both Manawaki and Albany, the two nearest measuring locations. Assuming that all this warming was due to subsidence, downward large scale motion of the order of 1 cm sec^{-1} was occurring at this time.

The comparison of the precipitation to the QE and QS patterns one hour earlier at 1400 EST are shown in Figures 42 and 43, respectively. Again, precipitation should begin noticeably earlier in areas of highest QS. The western portion of the precipitation developed over an area of high QS, nearly 30 calories cm^{-2}. However, the eastern portion was over an area of near zero QS, and 25 calories cm^{-2} of QE. Moreover, extensive areas in the north and west had relatively large amounts of QS, approaching 30 calories, yet no precipitation occurred there. Thus, the occurrence of precipitation in this case is not noticeably affected by surface variations. The precipitation seems to occur downwind from the Adirondack Mountains. The topography of this area is known to have an effect on rainfall. This appears to have been the case on the 7th, as more precipitation also fell over the mountains to the south and east of the area considered.
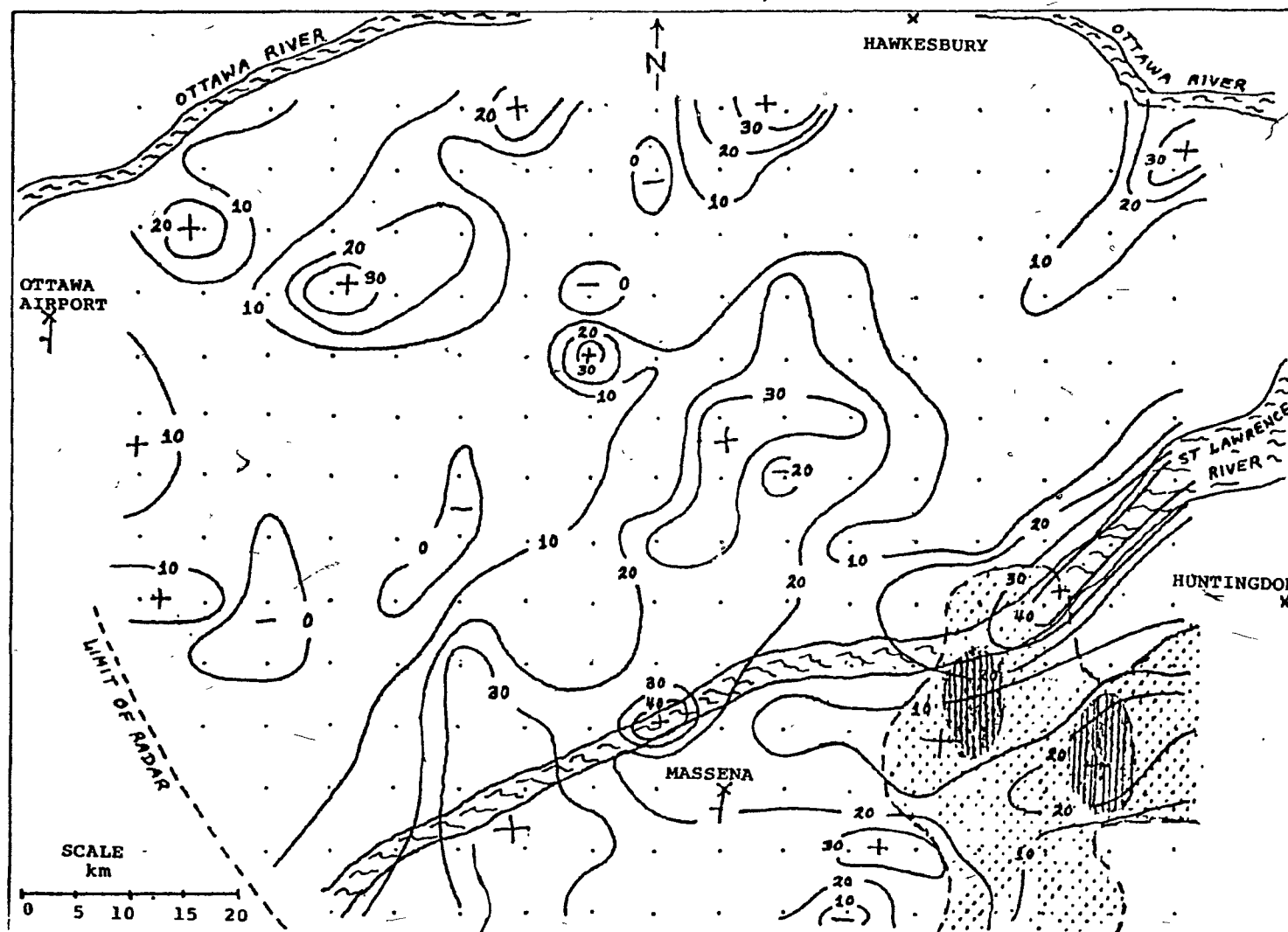
Figure 41. Precipitation Rate at 1500 EST, 7 July (cm hr^{-1})
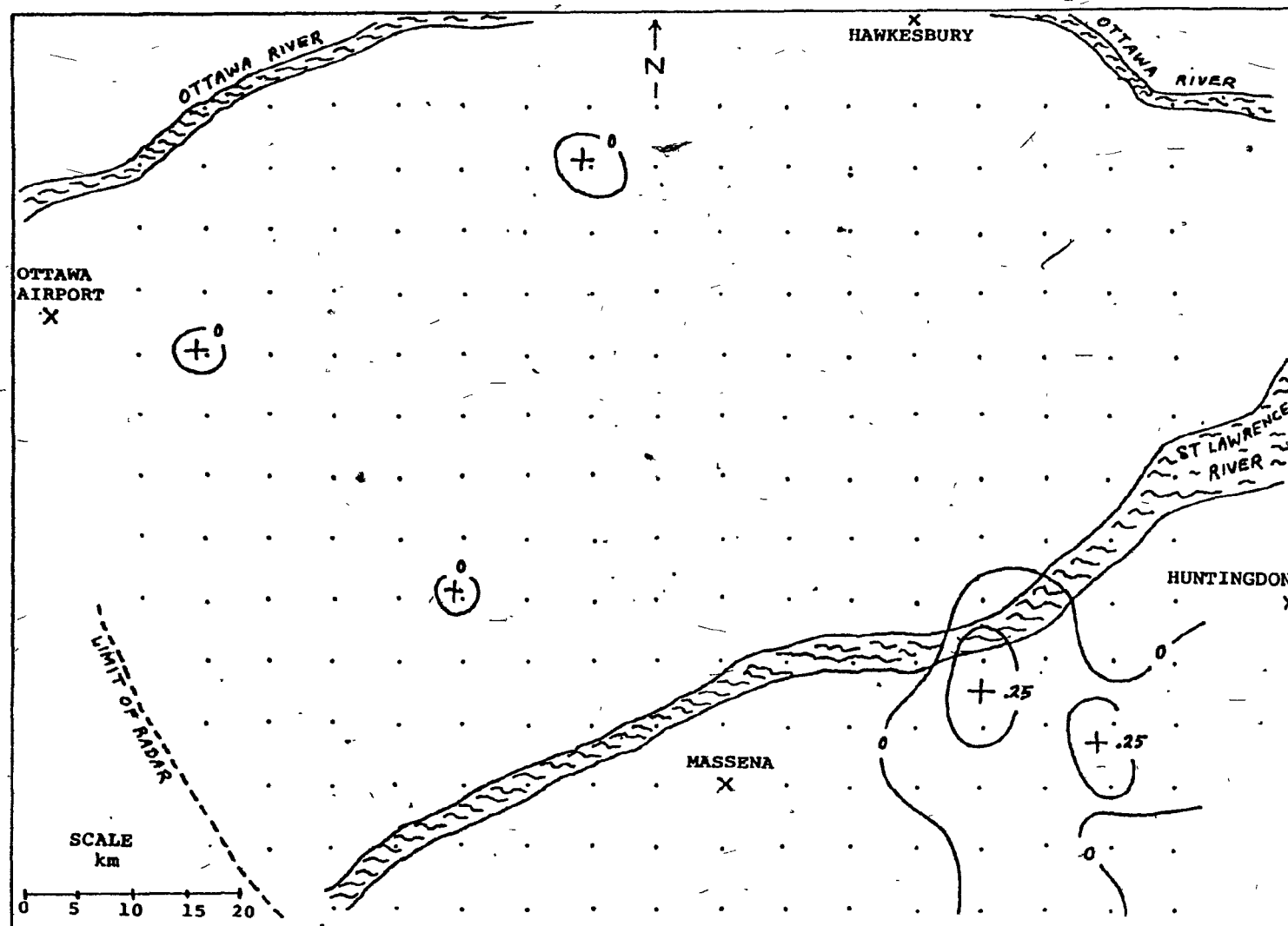
LEGEND

+ Relative Maximum
- Relative Minimum
. Grid Point
X Reference Point

Figure 42. Latent Heat Flux at 1400 EST, 7 July
(Calories $cm^{-2} hr^{-1}$)

Figure 43. Sensible Heat Flux at 1400 EST, 7 July
(Calories cm^{-2} hr^{-1})
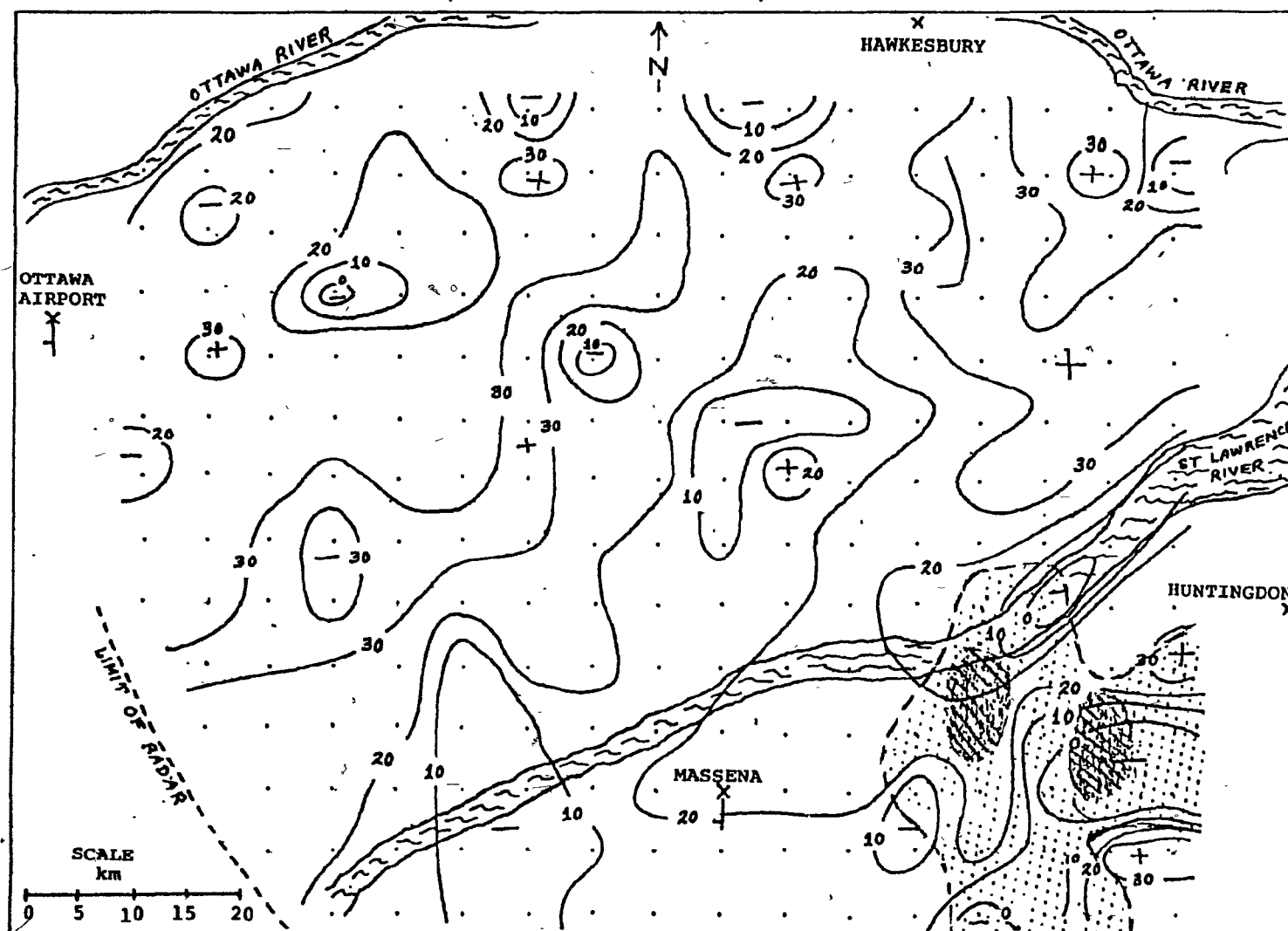
4. Conclusions

From three cases considered, it is seen that the surface has an influence on the time of development of convective precipitation by means of turbulent flux patterns. However, this influence is only evident at certain times. The manner in which the influence is manifested depends on the nature of the atmospheric stratification of heat and moisture. The addition of QS will favor convection if the lower troposphere is unstable and dry, while an addition of QE will favor convection if the sounding is moist in the lower levels. The spatial variations of the turbulent fluxes found over an area of varied land use can at a given time be sufficient to influence convection in cases where vertical motion is not dominant. However, variation in precipitation on the small scale cannot be totally due to evaporation and sensible heat variations over an area.

A spatial distribution of precipitation, of the scale considered here, can only be maintained over a longer period of time if the same distribution repeats itself due to the effect of stationary surface characteristics. Since variations in surface characteristics do not always have an effect, one would expect the spatial variation in precipitation, as a fraction of average total precipitation over an area, to decrease as the period of time considered is lengthened.

CHAPTER V

SUMMARY AND CONCLUSIONS

The surface energy budget of a land area has been studied during a summer period containing convective precipitation. This was done by using an existing numerical model with measured meteorological parameters as input. Calculations were done at closely spaced points between synoptic stations.

It was found that spatial variations in turbulent fluxes due to differences in ground water can be quite significant. A minimum dry period required for depletion of soil water was found as a function of root depth. If rooting depth is constant over an area, variations in turbulent fluxes can only arise if scattered precipitation occurs after such a dry period. However, variations in rooting depth between forest and crop areas can account for large spatial variations in turbulent fluxes after the minimum dry period for the rooting depth of crops. The addition of a varied precipitation pattern was secondary in affecting the spatial variation of turbulent fluxes.

The spatial variations in dew point and temperature resulting from the differences in ground water are insufficient to require the use of closely spaced points of observation to determine the evaporation over an area. However, the spatial average in precipitation and vegetation types in the area must be accounted for when using the calculation of the energy budget at a single point to represent that for an area.

The decrease in farmland over the last two decades could account for significantly higher evaporation after prolonged dry periods, if forest-like areas have replaced the abandoned land.

Finally, the spatial variation in turbulent fluxes which arise after a dry period in summer can have an influence on the pattern of convective precipitation, if large scale vertical motion is weak. The type of surface over which convection will first develop depends on the moisture and temperature stratification of the troposphere.

BIBLIOGRAPHY

Aase, J.K., Id, S.B., 1975: "Solar Radiation Interactions with
Mixed Prairie Rangland in Natural and Denuded Conditions".
Archiv Fur Meteorologie, Geophysik, und Bioklimatologie,
Ser. B, Vol. 23, pp. 255-264.

Bailey, D.T., 1965: "A Study of Solar Radiation, Barrow,
Alaska, 1962". M.Sc. Thesis, McGill University, Montreal,
80 pp.

Black River - St. Lawrence Economic Development Commission, 1974:
"Overall Economic Development Program, 1974". Black
River - St. Lawrence Econ. Dev. Comm. Publication,
Canton, N.Y., 82 pp.

Canada Department of Agriculture, Soil Research Institute,
1966: Soil Capability for Agriculture Map, The Queen's
Printer, Ottawa.

Canada Department of Energy, Mines and Resources, Surveys and
Mapping Branch, 1974: Topographical Maps 31B and 31G,
Series A501, Edition 3, The Queen's Printer, Ottawa.

Changnon Jr., S.A., 1976: "Effects of Urban Areas and Echo
Merging on Radar Echo Behavior". Journal of Applied
Meteorology, Vol. 15, pp. 561-570.

Fujita, T., 1955: "Results of Detailed Synoptic Studies of
Squall Lines". Tellus, Vol. 7, pp. 405-436.

Geiger, R., 1950: The Climate Near the Ground. (Translation by
M. N. Stewart, et.al.), Harvard Press, Cambridge,
Mass., 482 pp.

Harnick, R.P., Landsberg, H.E., 1973: "Selected Cases of
Convective Precipitation Caused by the Metropolitan
Area of Washington, D.C.". Journal of Applied Meteorology,
Vol. 14, pp. 1050-1060.

Haurwitz, B., 1945: "Insolation in Relation to Cloudiness and
Cloud Density". Journal of Meteorology, Vol. 2, pp. 154-
166.

-123-

Holmes, R.M., 1969: "Airborne Techniques in Climatology: Oasis Effects Above Prairie Surface Features". Inland Waters Branch, Department of Energy, Mines and Resources, Technical Bulletin, No. 19, Ottawa, 28 pp.

Kramer, P.J., 1949: Plant and Soil Water Relationships, McGraw-Hill, New York, 347 pp.

Kung, E.C., Bryson, R.A., Lenshow, D.H., 1964: "Study of a Continental Surface Albedo on the Basis of Flight Measurements and Structure of the Earth's Surface Cover Over North America". Monthly Weather Review, Vol. 92, No. 12, pp. 543-563.

Lee, R.J., 1972: "Relations Between Surface Energy and Water Budgets". M.Sc. Thesis, McGill University, Montreal, 128 pp.

Malkus, J.S., 1962: "Large-Scale Interactions". The Sea, Interscience Press, New York, pp. 88-294.

Marshall, J.S., Palmer, W. McK., 1948: "The Distribution of Raindrops with Size". Journal of Meteorology, Vol. 5, pp. 165-166.

Morin, P.L.J., 1973: "Air Mass Modification Over the Gulf of St. Lawrence". M.Sc. Thesis, McGill University, Montreal, 79 pp.

Myrop, L.O., 1969: "A Numerical Model of the Urban Heat Island". Journal of Atmospheric Science, Vol. 8, pp. 908-918.

Ninomiya, K., 1968: "Heat and Water Budget Over the Japan Sea and the Japan Islands in the Winter Season". Journal of the Meteorological Society of Japan, Vol. 46, pp. 343-372.

Ontario Department of Agriculture, Farm Economics, Co-operatives and Statistic Branch, 1969: "Changes in Improved Acreage". In Economic Atlas of Ontario, (Edited by W. G. Dean), University of Toronto, Toronto, Plate 68.

Pugsley, W.I., 1970: "The Surface Energy Budget of Central Canada". M.Sc. Thesis, McGill University, Montreal, 182 pp.

Schaefer, J., 1975: "Moisture Stratification in the 'Well-Mixed' Boundary Layer". _Preprints of the Ninth Conference on Severe Local Storms_, American Meteorological Society, Boston, pp. 45-50.

Sellers, W.D., 1965: _Physical Climatology_. University of Chicago Press, Chicago, 272 pp.

Thomas, J.E., 1975: "An Energy Budget Model of the Coniferous Forest Biome for Determining the Hydrologic Impact of Logging". _Publications in Meteorology_, No. 115, McGill University, Montreal, 150 pp.

Thornthwaite, C.W., Mather, J.R., 1957: "Instructions and Tables for Computing Potential Evaporation and the Water Balance". _Technical Publications in Climatology_, Vol. 10, No. 3, Drexel Institute of Technology, Centerton, New Jersey.

Veihmeyer, F.J., 1927: "Some Factors Affecting the Irrigation Requirements of Deciduous Orchards". _Hilgardia_, Vol. 2, pp. 125-284.

Vowinckel, E., 1965: "The Energy Budget Over the North Atlantic-January, 1963". _Publications in Meteorology_, No. 78, McGill University, Montreal, 38 pp.

Vowinckel, E., Orvig, S., 1972: "EBBA, An Energy Budget Programme". _Publications in Meteorology_, No. 105, McGill University, Montreal, 50 pp.

United States Department of Agriculture, 1958: "Soil Survey of Franklin County, New York". _U.S. Dept. Agr. Soil Survey Report_, Series 1952, No. 1, U.S. Government Printing Office, Washington, 75 pp. and Maps.